The Distant Cluster Population from the Atacama Cosmology Telescope

(see Menanteau et al. 2012, [ApJ, 748,7]; Sifon, Menanteau et al. 2012 [arXiv:1201.0991], Menanteau et al. 2010, [ApJ, 723,1523]; Marriage et al. 2011, [Apj, 731,61]; Sehgal et al. 2011 [ApJ.732,44])

Felipe Menanteau (Rutgers)

and the ACT Collaboration

Outline

- The SZ Cluster Selection.
- The first SZ-selected clusters sample from ACT.
- “El Gordo,” the most massive cluster at z>0.6
- First Cosmological Constraints from SZ-clusters
- SZ-mass calibration from follow-up observations.
- New Results from 2009-2010 observations on celestial equator.

SZE Signature (Observable)

(Sunyaev & Zel'dovich 1972)

Hot electron gas imposes a unique spectral signature

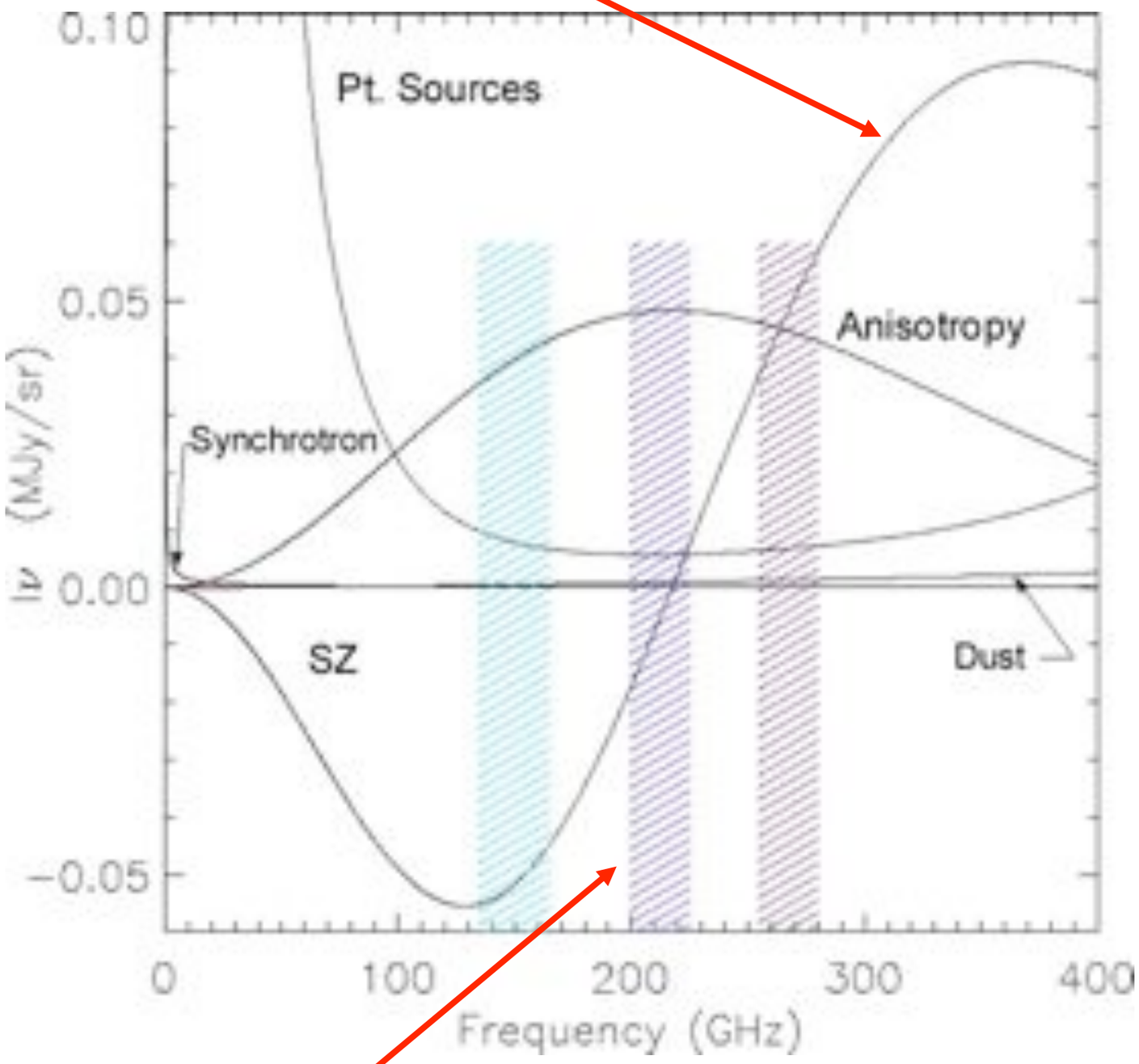

(Credit: Neelima Sehgal) 1.4°x 1.4°

148 GHz ~ 2.0mm (decrement)
220 GHz ~ 1.4mm (null)
270 GHz ~ 1.1mm (increment)

NO SZ Contribution in Central Band

SZE Signature (Observable)

(Sunyaev & Zel'dovich 1972)

Hot electron gas imposes a unique spectral signature

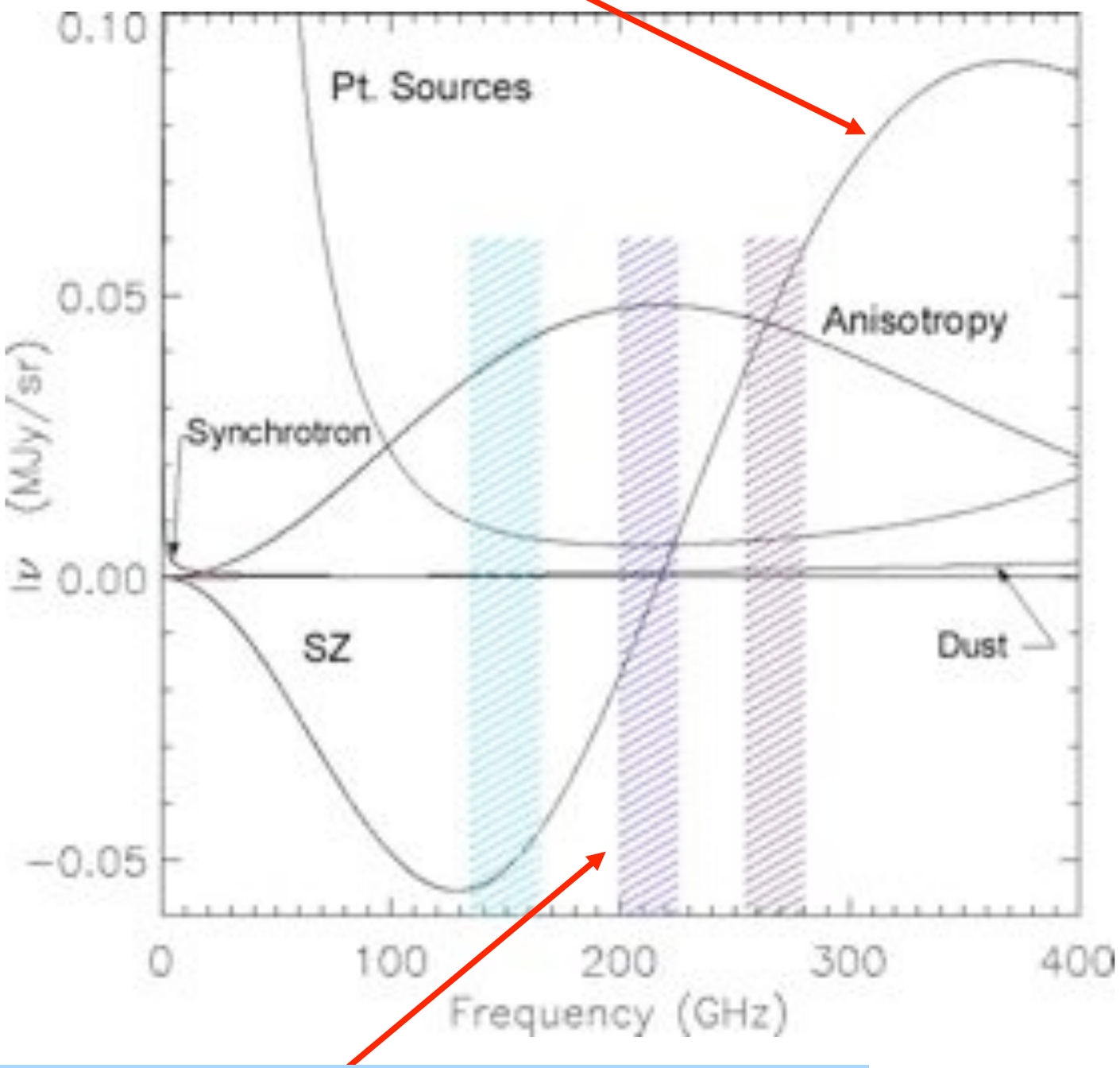

(Credit: Neelima Sehgal) 1.4°x 1.4°

148 GHz ~ 2.0mm (decrement)
220 GHz ~ 1.4mm (null)
270 GHz ~ 1.1mm (increment)

NO SZ Contribution in Central Band

SZE Signature (Observable)

(Sunyaev & Zel'dovich 1972)

Hot electron gas imposes a unique spectral signature

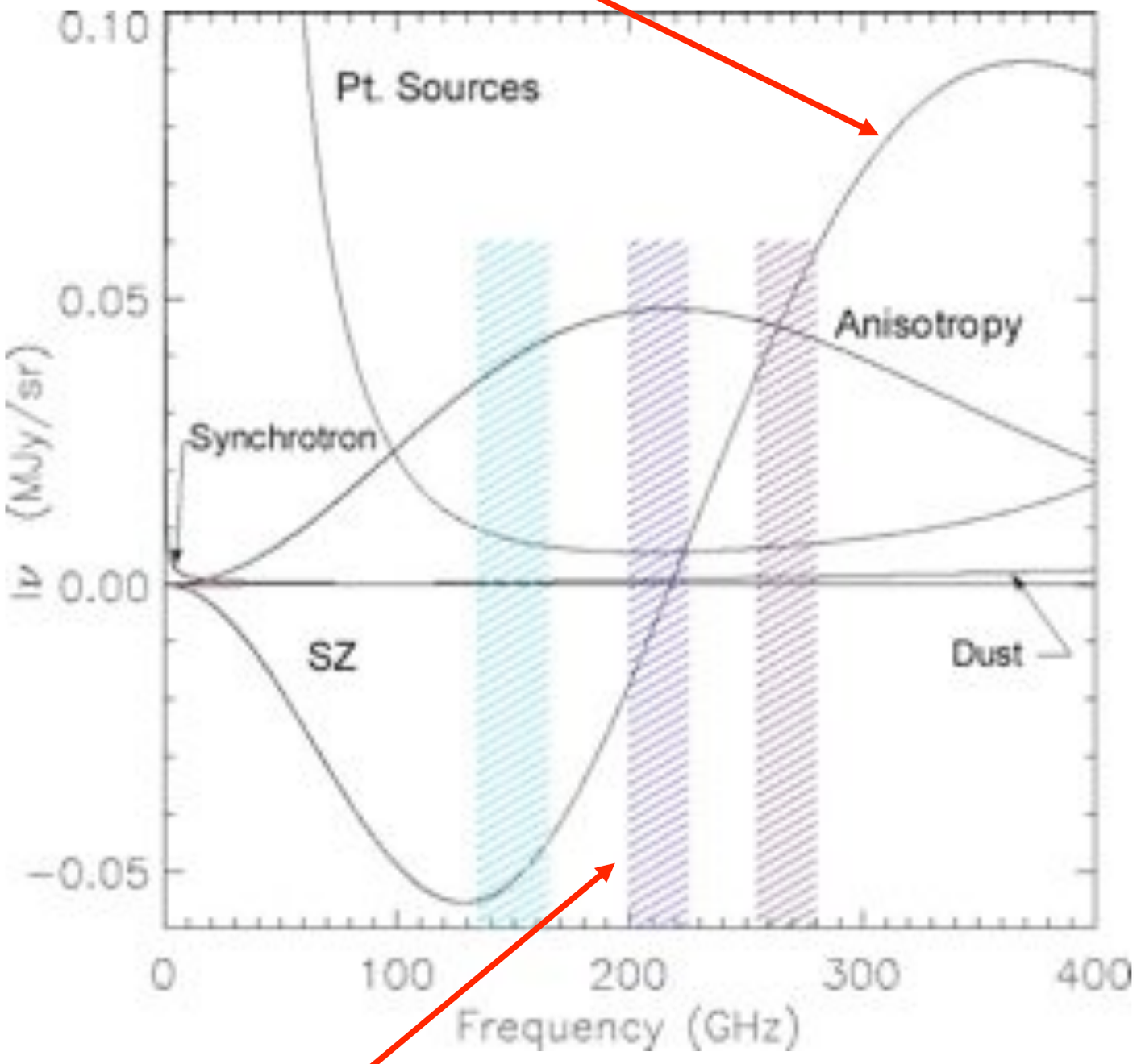

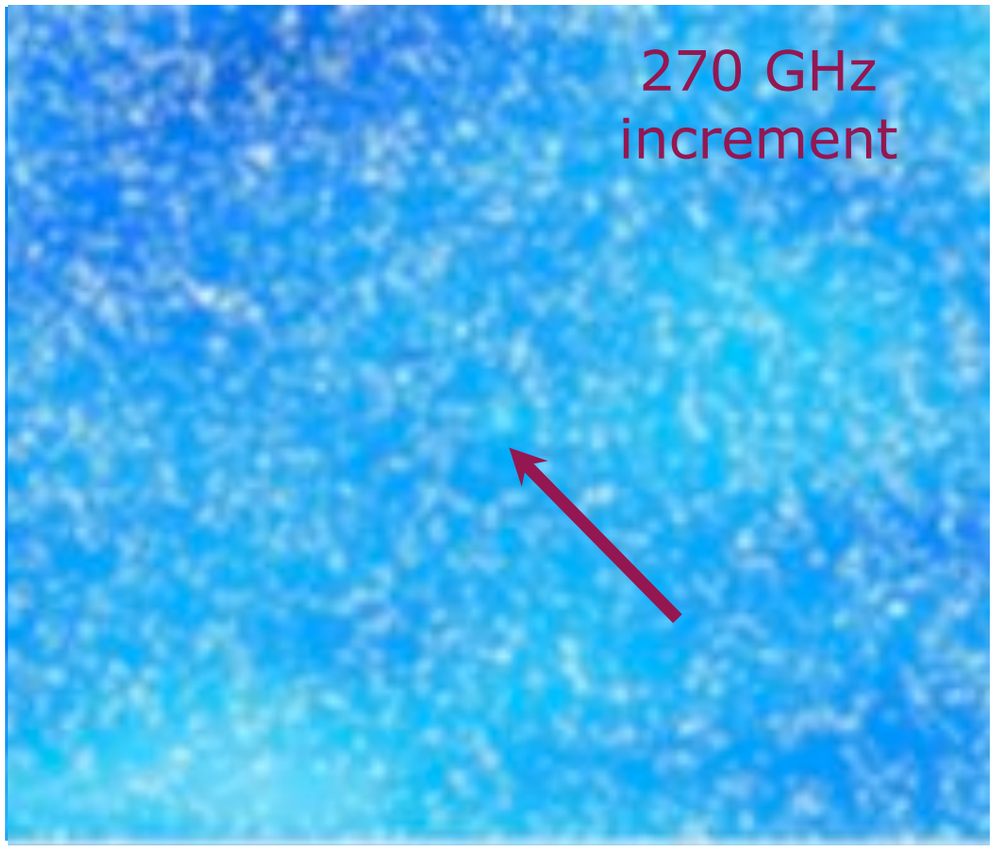

(Credit: Neelima Sehgal) 1.4°x 1.4°

148 GHz ~ 2.0mm (decrement)
220 GHz ~ 1.4mm (null)
270 GHz ~ 1.1mm (increment)

NO SZ Contribution in Central Band

New View of the CMB

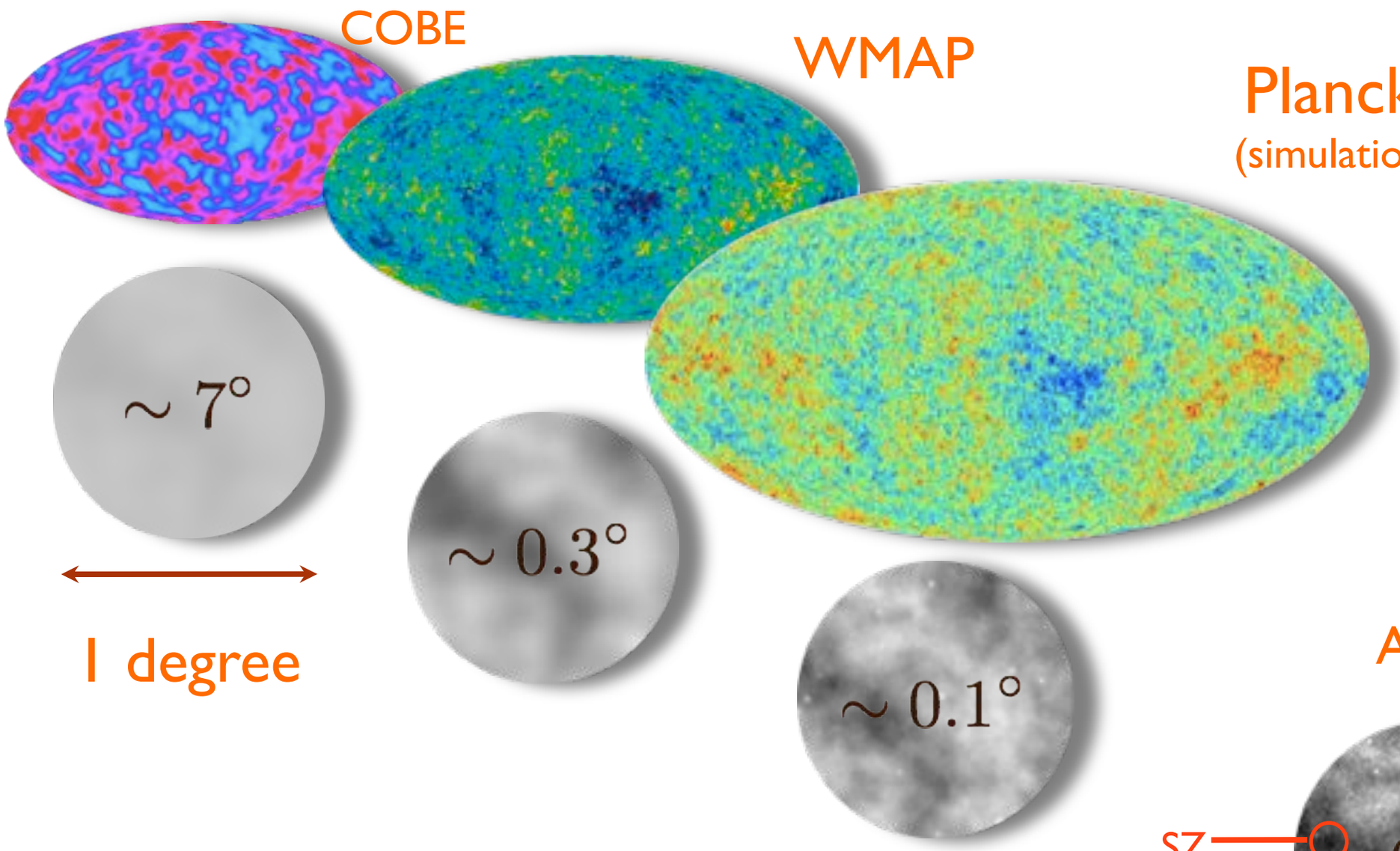

At arcminute scales, secondary anisotropies become important and bring us in contact with astrophysics.

The Era of SZ Surveys has arrived

Planck

ACT: The Atacama Cosmology Telescope

- PI: Lyman Page (Princeton University)
- 5200 meters (17,000 ft)
- "High and dry": 0.49 mm median Precipitable Water Vapor (PWV).
- 6 m primary mirror. Off-axis Gregorian telescope
- ~1 arcmin resolution
- 148, 218, 277 GHz channels (~ 2.0, 1.4 and 1.1 mm)
- **ACTPol (2013-2016) deep/wide survey**
- **a few x1000 deg^2 of equatorial observations**

ACT Sky Coverage

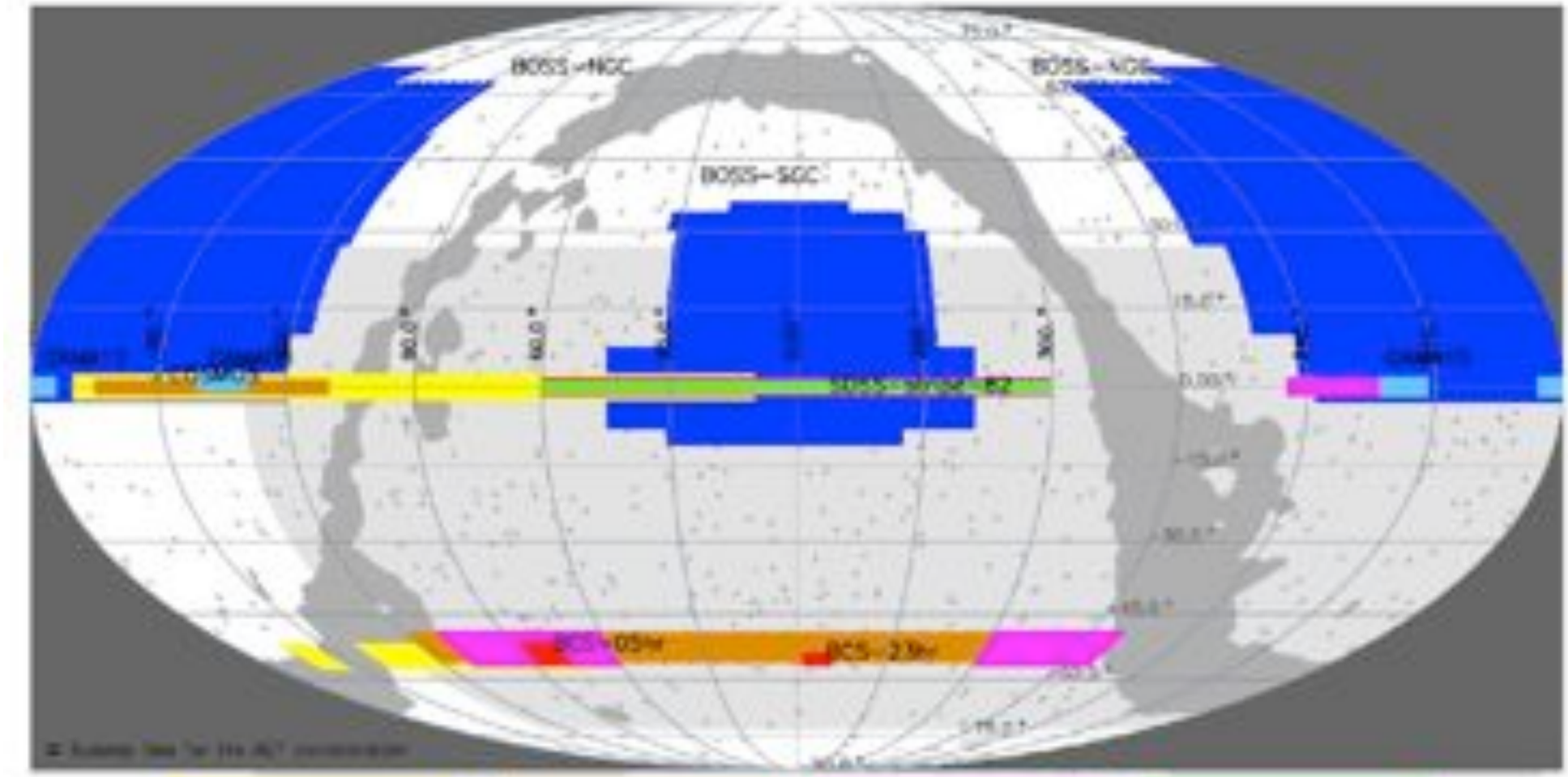

2008 ACT Stripe from Marriage et al. (2011)

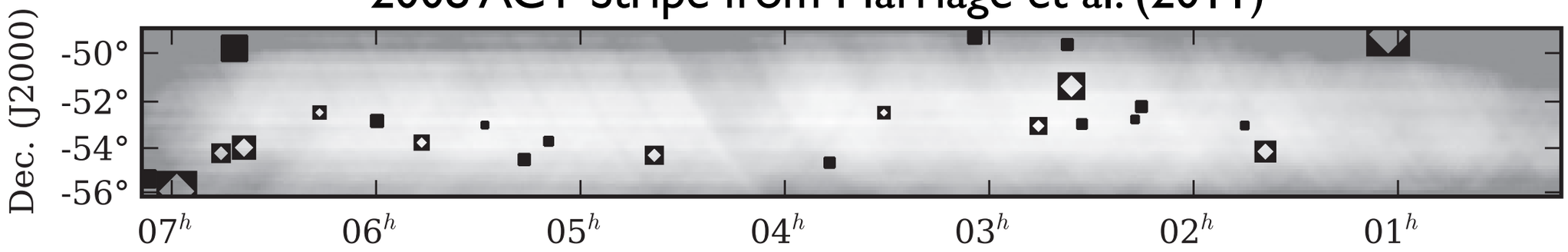

ACT Sky Coverage

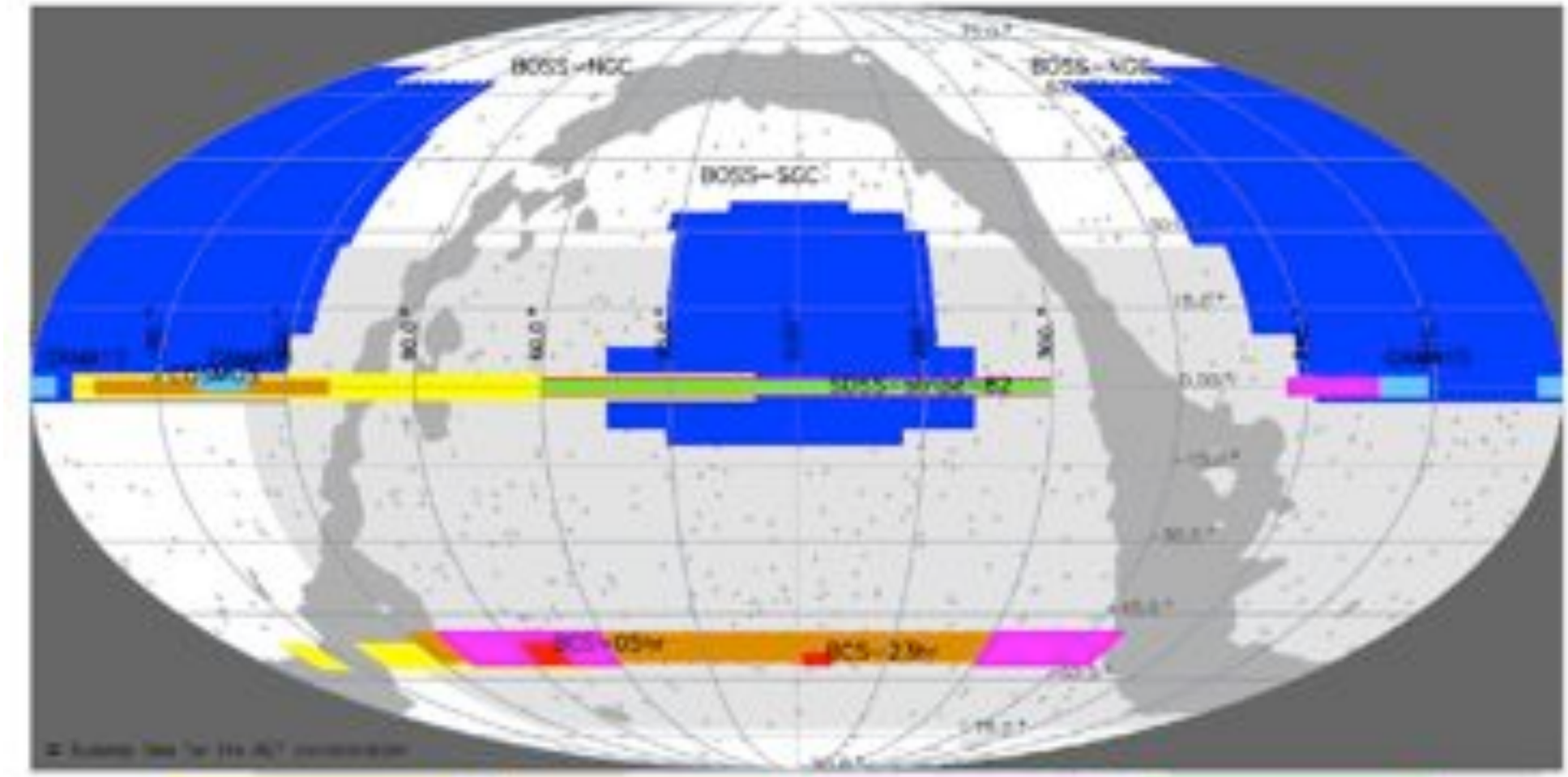

2007 | 2008 | 2009+2010 | Stripe 82

BCS | BOSS | GAMA | ACT Range | Mask

2008 ACT Stripe from Marriage et al. (2011)

El Gordo

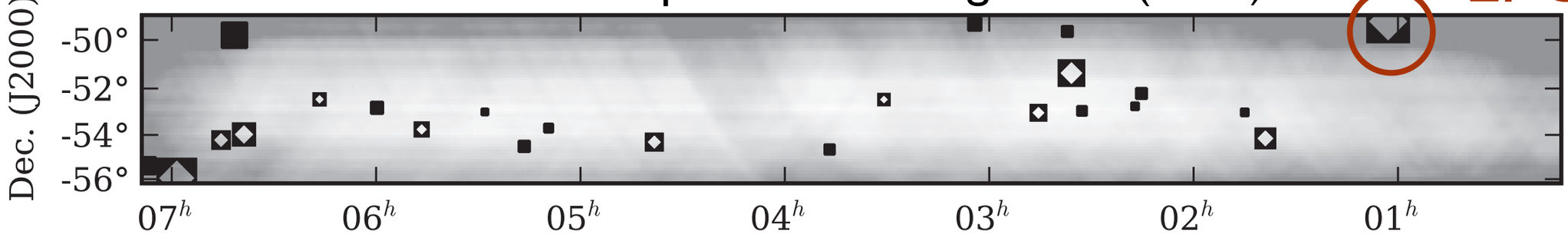

Detecting SZ clusters and point sources

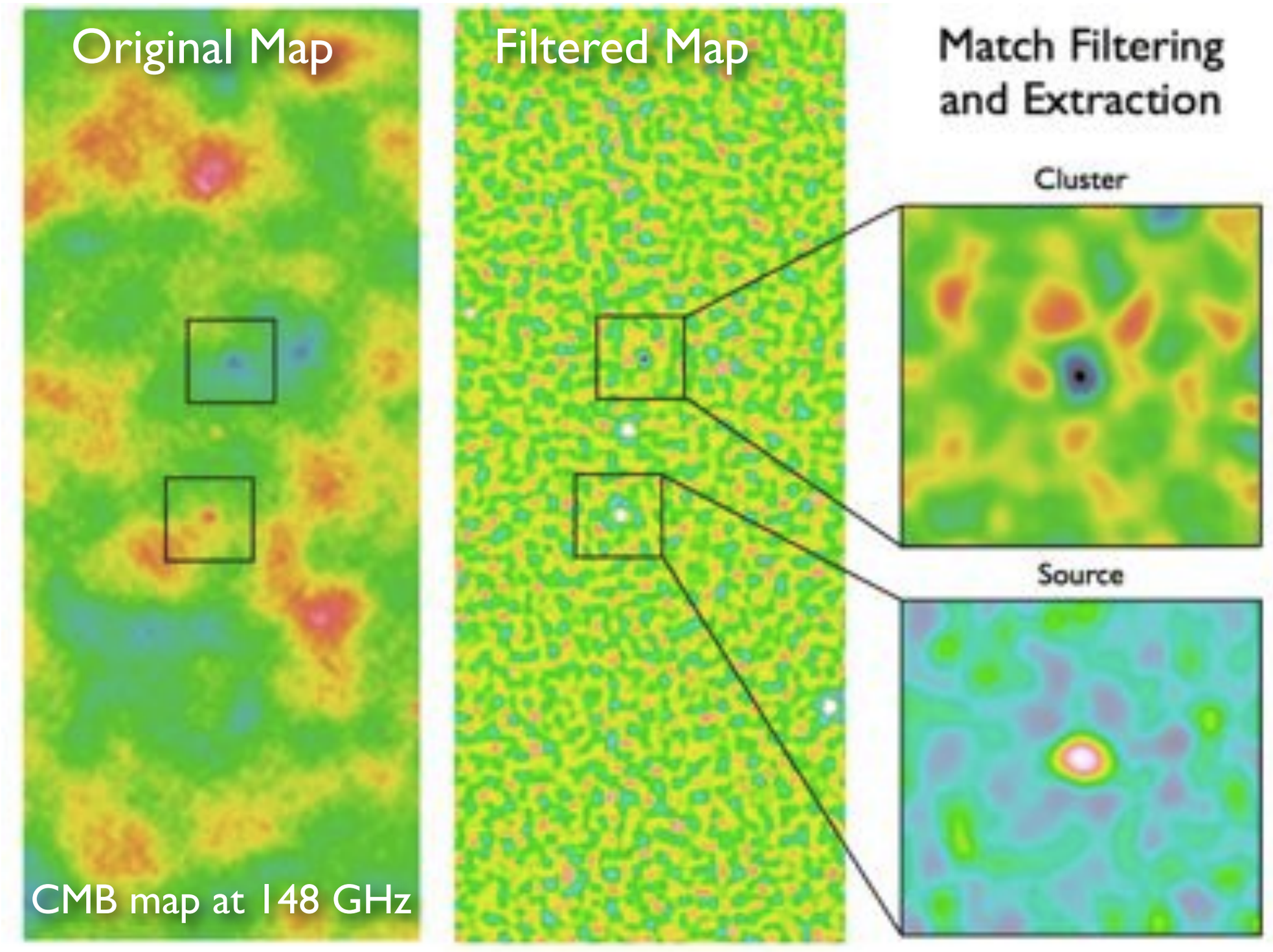

Optical Cluster Identification

Expected cluster distribution

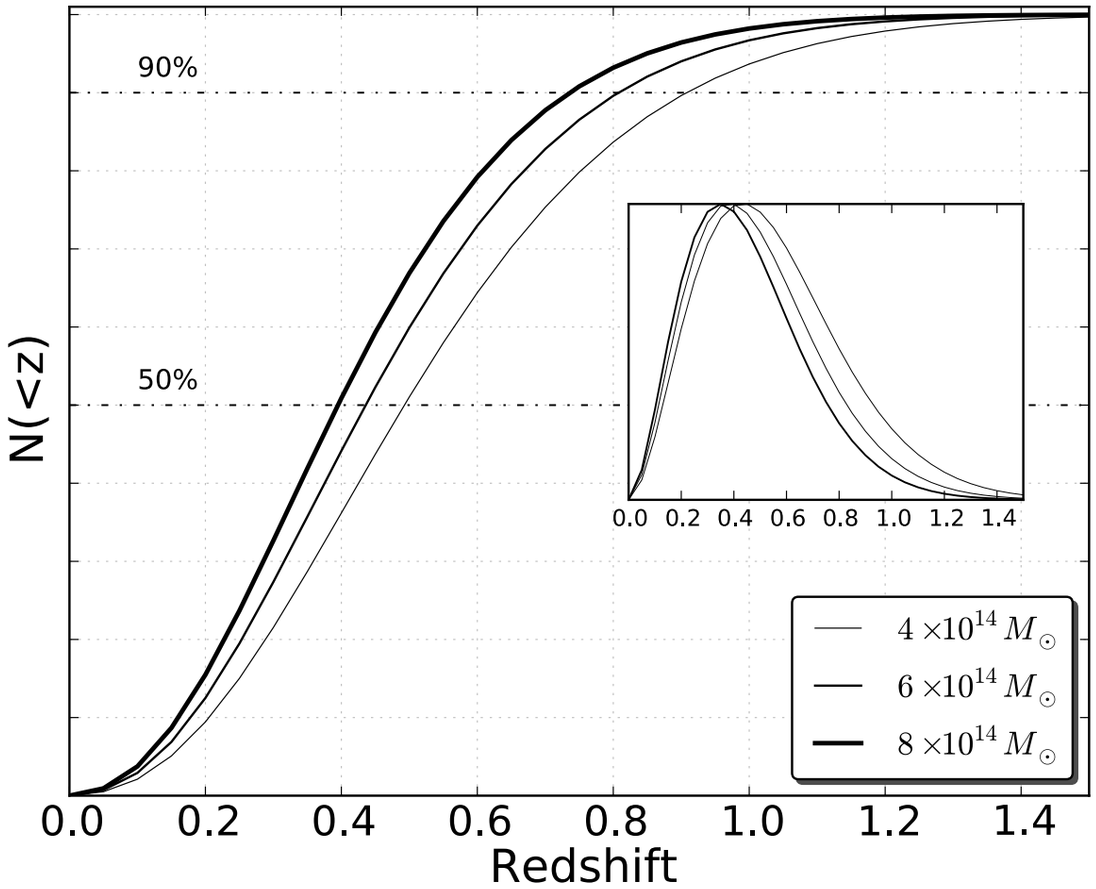

ΛCDM, Tinker et al (2008) mass function

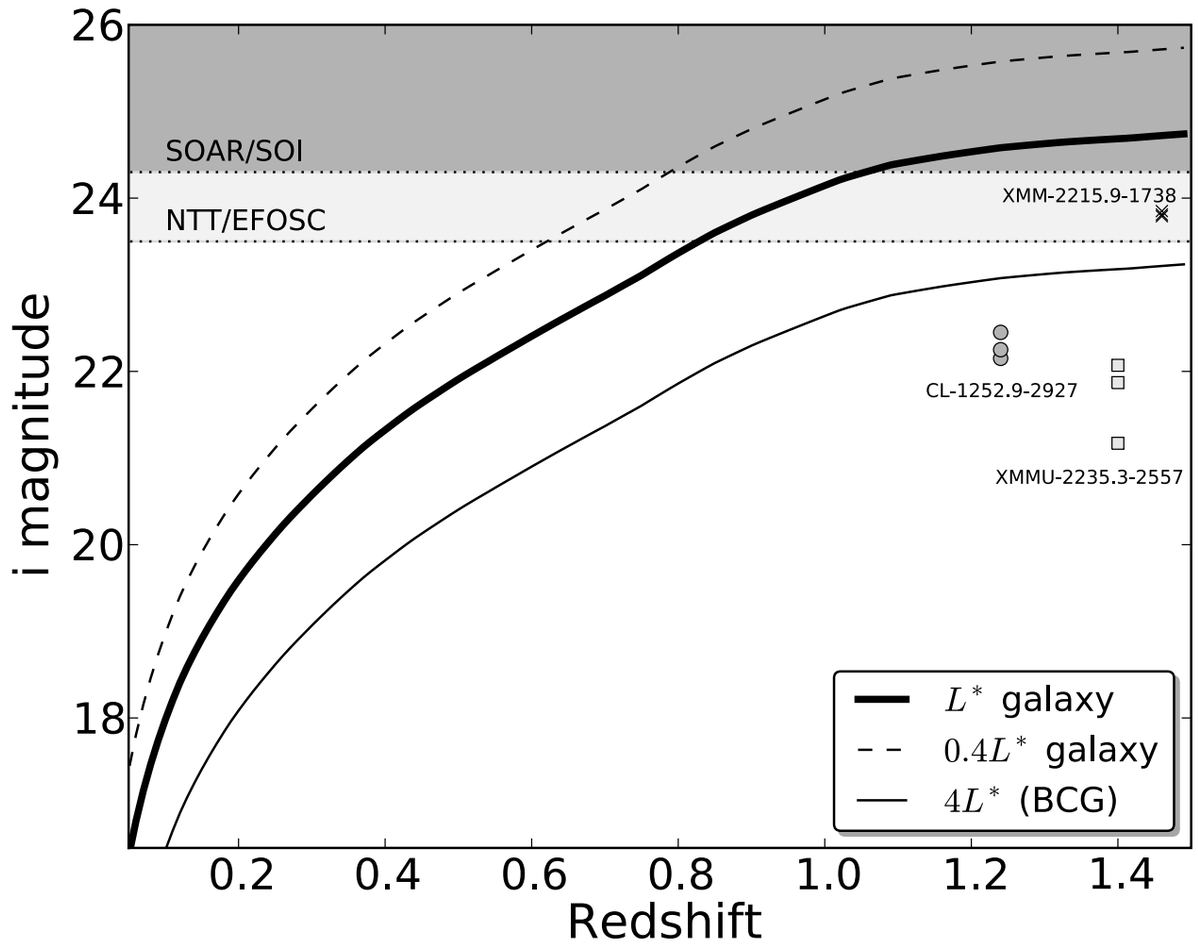

Galaxy *i*-band apparent magnitude as function of redshift (includes passive evolutions)

The Southern ACT-SZ cluster sample

(455 sq-degree area)

Table 2
ACT 2008 clusters

ACT Descriptor	R.A. (J2000)	Dec. (J2000)	Redshift	SNR	Alt Name
ACT-CL J0145-5301	01:45:03.6	-53:01:23.4	0.118 [a]	4.7 (4.0)	Abell 2941
ACT-CL J0641-4949	06:41:37.8	-49:46:55.0	0.146 [b]	4.9 (4.9)	Abell 3402
ACT-CL J0645-5413	06:45:29.5	-54:13:37.0	0.167 [a]	7.1 (7.1)	Abell 3404
ACT-CL J0638-5358	06:38:49.4	-53:58:40.8	0.222 [a]	10.6 (10.0)	Abell S0592
ACT-CL J0516-5430	05:16:37.4	-54:30:01.5	0.294 [c]	5.2 (4.7)	Abell S0520/SPT-CL J0516-5430
ACT-CL J0658-5557	06:58:33.1	-55:57:07.2	0.296 [d]	11.6 (11.5)	1E0657-56 (Bullet)
ACT-CL J0245-5302	02:45:35.8	-53:02:16.8	0.300 [e]	8.3 (9.1)	Abell S0295
ACT-CL J0217-5245	02:17:12.6	-52:44:49.0	0.343 [f]	4.5 (4.1)	RXC J0217.2-5244
ACT-CL J0237-4939	02:37:01.7	-49:38:10.0	0.40 ± 0.05	4.9 (3.9)	
ACT-CL J0707-5522	07:07:04.7	-55:23:08.5	0.43 ± 0.06	4.2 (...)	
ACT-CL J0235-5121	02:35:45.3	-51:21:05.2	0.43 ± 0.07	5.7 (6.2)	
ACT-CL J0330-5227	03:30:56.8	-52:28:13.7	0.440 [g]	7.4 (6.1)	Abell 3128(NE)
ACT-CL J0509-5341	05:09:21.4	-53:42:12.3	0.461 [h]	4.4 (4.8)	SPT-CL J0509-5342
ACT-CL J0304-4921	03:04:16.0	-49:21:26.3	0.47 ± 0.05	5.0 (3.9)	
ACT-CL J0215-5212	02:15:12.3	-52:12:25.3	0.51 ± 0.05	4.8 (4.9)	
ACT-CL J0438-5419	04:38:17.7	-54:19:20.7	0.54 ± 0.05	8.8 (8.0)	
ACT-CL J0346-5438	03:46:55.5	-54:38:54.8	0.55 ± 0.05	4.4 (4.4)	
ACT-CL J0232-5257	02:32:46.2	-52:57:50.0	0.59 ± 0.07	5.2 (4.7)	
ACT-CL J0559-5249	05:59:43.2	-52:49:27.1	0.611 [i]	5.1 (5.1)	SPT-CL J0559-5249
ACT-CL J0616-5227	06:16:34.2	-52:27:13.3	0.71 ± 0.10	6.3 (5.9)	
ACT-CL J0102-4915	01:02:52.5	-49:14:58.0	0.75 ± 0.04	8.8 (9.0)	
ACT-CL J0528-5259	05:28:05.3	-52:59:52.8	0.768 [h]	4.7 (...)	SPT-CL J0528-5300
ACT-CL J0546-5345	05:46:37.7	-53:45:31.1	1.066 [h]	7.2 (6.5)	SPT-CL J0546-5345

from Menanteau et al. (2010), ApJ, 723,1523

The Southern ACT-SZ cluster sample

(455 sq-degree area)

Table 2
ACT 2008 clusters

ACT Descriptor	R.A. (J2000)	Dec. (J2000)	Redshift	SNR	Alt Name
ACT-CL J0145-5301	01:45:03.6	-53:01:23.4	0.118 [a]	4.7 (4.0)	Abell 2941
ACT-CL J0641-4949	06:41:37.8	-49:46:55.0	0.146 [b]	4.9 (4.9)	Abell 3402
ACT-CL J0645-5413	06:45:29.5	-54:13:37.0	0.167 [a]	7.1 (7.1)	Abell 3404
ACT-CL J0638-5358	06:38:49.4	-53:58:40.8	0.222 [a]	10.6 (10.0)	Abell S0592
ACT-CL J0516-5430	05:16:37.4	-54:30:01.5	0.294 [c]	5.2 (4.7)	Abell S0520/SPT-CL J0516-5430
ACT-CL J0658-5557	06:58:33.1	-55:57:07.2	0.296 [d]	11.6 (11.5)	1E0657-56 (Bullet)
ACT-CL J0245-5302	02:45:35.8	-53:02:16.8	0.300 [e]	8.3 (9.1)	Abell S0295
ACT-CL J0217-5245	02:17:12.6	-52:44:49.0	0.343 [f]	4.5 (4.1)	RXC J0217.2-5244
ACT-CL J0237-4939	02:37:01.7	-49:38:10.0	0.40 ± 0.05	4.9 (3.9)	
ACT-CL J0707-5522	07:07:04.7	-55:23:08.5	0.43 ± 0.06	4.2 (...)	
ACT-CL J0235-5121	02:35:45.3	-51:21:05.2	0.43 ± 0.07	5.7 (6.2)	
ACT-CL J0330-5227	03:30:56.8	-52:28:13.7	0.440 [g]	7.4 (6.1)	Abell 3128(NE)
ACT-CL J0509-5341	05:09:21.4	-53:42:12.3	0.461 [h]	4.4 (4.8)	SPT-CL J0509-5342
ACT-CL J0304-4921	03:04:16.0	-49:21:26.3	0.47 ± 0.05	5.0 (3.9)	
ACT-CL J0215-5212	02:15:12.3	-52:12:25.3	0.51 ± 0.05	4.8 (4.9)	
ACT-CL J0438-5419	04:38:17.7	-54:19:20.7	0.54 ± 0.05	8.8 (8.0)	
ACT-CL J0346-5438	03:46:55.5	-54:38:54.8	0.55 ± 0.05	4.4 (4.4)	
ACT-CL J0232-5257	02:32:46.2	-52:57:50.0	0.59 ± 0.07	5.2 (4.7)	
ACT-CL J0559-5249	05:59:43.2	-52:49:27.1	0.611 [i]	5.1 (5.1)	SPT-CL J0559-5249
ACT-CL J0616-5227	06:16:34.2	-52:27:13.3	0.71 ± 0.10	6.3 (5.9)	
ACT-CL J0102-4915	01:02:52.5	-49:14:58.0	0.75 ± 0.04	8.8 (9.0)	
ACT-CL J0528-5259	05:28:05.3	-52:59:52.8	0.768 [h]	4.7 (...)	SPT-CL J0528-5300
ACT-CL J0546-5345	05:46:37.7	-53:45:31.1	1.066 [h]	7.2 (6.5)	SPT-CL J0546-5345

(9) known

from Menanteau et al. (2010), ApJ, 723,1523

The Southern ACT-SZ cluster sample

(455 sq-degree area)

Table 2
ACT 2008 clusters

ACT Descriptor	R.A. (J2000)	Dec. (J2000)	Redshift	SNR	Alt Name
ACT-CL J0145-5301	01:45:03.6	-53:01:23.4	0.118 [a]	4.7 (4.0)	Abell 2941
ACT-CL J0641-4949	06:41:37.8	-49:46:55.0	0.146 [b]	4.9 (4.9)	Abell 3402
ACT-CL J0645-5413	06:45:29.5	-54:13:37.0	0.167 [a]	7.1 (7.1)	Abell 3404
ACT-CL J0638-5358	06:38:49.4	-53:58:40.8	0.222 [a]	10.6 (10.0)	Abell S0592
ACT-CL J0516-5430	05:16:37.4	-54:30:01.5	0.294 [c]	5.2 (4.7)	Abell S0520/SPT-CL J0516-5430
ACT-CL J0658-5557	06:58:33.1	-55:57:07.2	0.296 [d]	11.6 (11.5)	1E0657-56 (Bullet)
ACT-CL J0245-5302	02:45:35.8	-53:02:16.8	0.300 [e]	8.3 (9.1)	Abell S0295
ACT-CL J0217-5245	02:17:12.6	-52:44:49.0	0.343 [f]	4.5 (4.1)	RXC J0217.2-5244
ACT-CL J0237-4939	02:37:01.7	-49:38:10.0	0.40 ± 0.05	4.9 (3.9)	
ACT-CL J0707-5522	07:07:04.7	-55:23:08.5	0.43 ± 0.06	4.2 (...)	
ACT-CL J0235-5121	02:35:45.3	-51:21:05.2	0.43 ± 0.07	5.7 (6.2)	
ACT-CL J0330-5227	03:30:56.8	-52:28:13.7	0.440 [g]	7.4 (6.1)	Abell 3128(NE)
ACT-CL J0509-5341	05:09:21.4	-53:42:12.3	0.461 [h]	4.4 (4.8)	SPT-CL J0509-5342
ACT-CL J0304-4921	03:04:16.0	-49:21:26.3	0.47 ± 0.05	5.0 (3.9)	
ACT-CL J0215-5212	02:15:12.3	-52:12:25.3	0.51 ± 0.05	4.8 (4.9)	
ACT-CL J0438-5419	04:38:17.7	-54:19:20.7	0.54 ± 0.05	8.8 (8.0)	
ACT-CL J0346-5438	03:46:55.5	-54:38:54.8	0.55 ± 0.05	4.4 (4.4)	
ACT-CL J0232-5257	02:32:46.2	-52:57:50.0	0.59 ± 0.07	5.2 (4.7)	
ACT-CL J0559-5249	05:59:43.2	-52:49:27.1	0.611 [i]	5.1 (5.1)	SPT-CL J0559-5249
ACT-CL J0616-5227	06:16:34.2	-52:27:13.3	0.71 ± 0.10	6.3 (5.9)	
ACT-CL J0102-4915	01:02:52.5	-49:14:58.0	0.75 ± 0.04	8.8 (9.0)	
ACT-CL J0528-5259	05:28:05.3	-52:59:52.8	0.768 [h]	4.7 (...)	SPT-CL J0528-5300
ACT-CL J0546-5345	05:46:37.7	-53:45:31.1	1.066 [h]	7.2 (6.5)	SPT-CL J0546-5345

(9) known

(10) new

from Menanteau et al. (2010), ApJ, 723,1523

The Southern ACT-SZ cluster sample

(455 sq-degree area)

Table 2
ACT 2008 clusters

ACT Descriptor	R.A. (J2000)	Dec. (J2000)	Redshift	SNR	Alt Name
ACT-CL J0145-5301	01:45:03.6	-53:01:23.4	0.118 [a]	4.7 (4.0)	Abell 2941
ACT-CL J0641-4949	06:41:37.8	-49:46:55.0	0.146 [b]	4.9 (4.9)	Abell 3402
ACT-CL J0645-5413	06:45:29.5	-54:13:37.0	0.167 [a]	7.1 (7.1)	Abell 3404
ACT-CL J0638-5358	06:38:49.4	-53:58:40.8	0.222 [a]	10.6 (10.0)	Abell S0592
ACT-CL J0516-5430	05:16:37.4	-54:30:01.5	0.294 [c]	5.2 (4.7)	Abell S0520/SPT-CL J0516-5430
ACT-CL J0658-5557	06:58:33.1	-55:57:07.2	0.296 [d]	11.6 (11.5)	1E0657-56 (Bullet)
ACT-CL J0245-5302	02:45:35.8	-53:02:16.8	0.300 [e]	8.3 (9.1)	Abell S0295
ACT-CL J0217-5245	02:17:12.6	-52:44:49.0	0.343 [f]	4.5 (4.1)	RXC J0217.2-5244
ACT-CL J0237-4939	02:37:01.7	-49:38:10.0	0.40 ± 0.05	4.9 (3.9)	
ACT-CL J0707-5522	07:07:04.7	-55:23:08.5	0.43 ± 0.06	4.2 (...)	
ACT-CL J0235-5121	02:35:45.3	-51:21:05.2	0.43 ± 0.07	5.7 (6.2)	
ACT-CL J0330-5227	03:30:56.8	-52:28:13.7	0.440 [g]	7.4 (6.1)	Abell 3128(NE)
ACT-CL J0509-5341	05:09:21.4	-53:42:12.3	0.461 [h]	4.4 (4.8)	SPT-CL J0509-5342
ACT-CL J0304-4921	03:04:16.0	-49:21:26.3	0.47 ± 0.05	5.0 (3.9)	
ACT-CL J0215-5212	02:15:12.3	-52:12:25.3	0.51 ± 0.05	4.8 (4.9)	
ACT-CL J0438-5419	04:38:17.7	-54:19:20.7	0.54 ± 0.05	8.8 (8.0)	
ACT-CL J0346-5438	03:46:55.5	-54:38:54.8	0.55 ± 0.05	4.4 (4.4)	
ACT-CL J0232-5257	02:32:46.2	-52:57:50.0	0.59 ± 0.07	5.2 (4.7)	
ACT-CL J0559-5249	05:59:43.2	-52:49:27.1	0.611 [i]	5.1 (5.1)	SPT-CL J0559-5249
ACT-CL J0616-5227	06:16:34.2	-52:27:13.3	0.71 ± 0.10	6.3 (5.9)	
ACT-CL J0102-4915	01:02:52.5	-49:14:58.0	0.75 ± 0.04	8.8 (9.0)	
ACT-CL J0528-5259	05:28:05.3	-52:59:52.8	0.768 [h]	4.7 (...)	SPT-CL J0528-5300
ACT-CL J0546-5345	05:46:37.7	-53:45:31.1	1.066 [h]	7.2 (6.5)	SPT-CL J0546-5345

(9) known

(14) SZ discovered

from Menanteau et al. (2010), ApJ, 723,1523

Some Previously Known Clusters

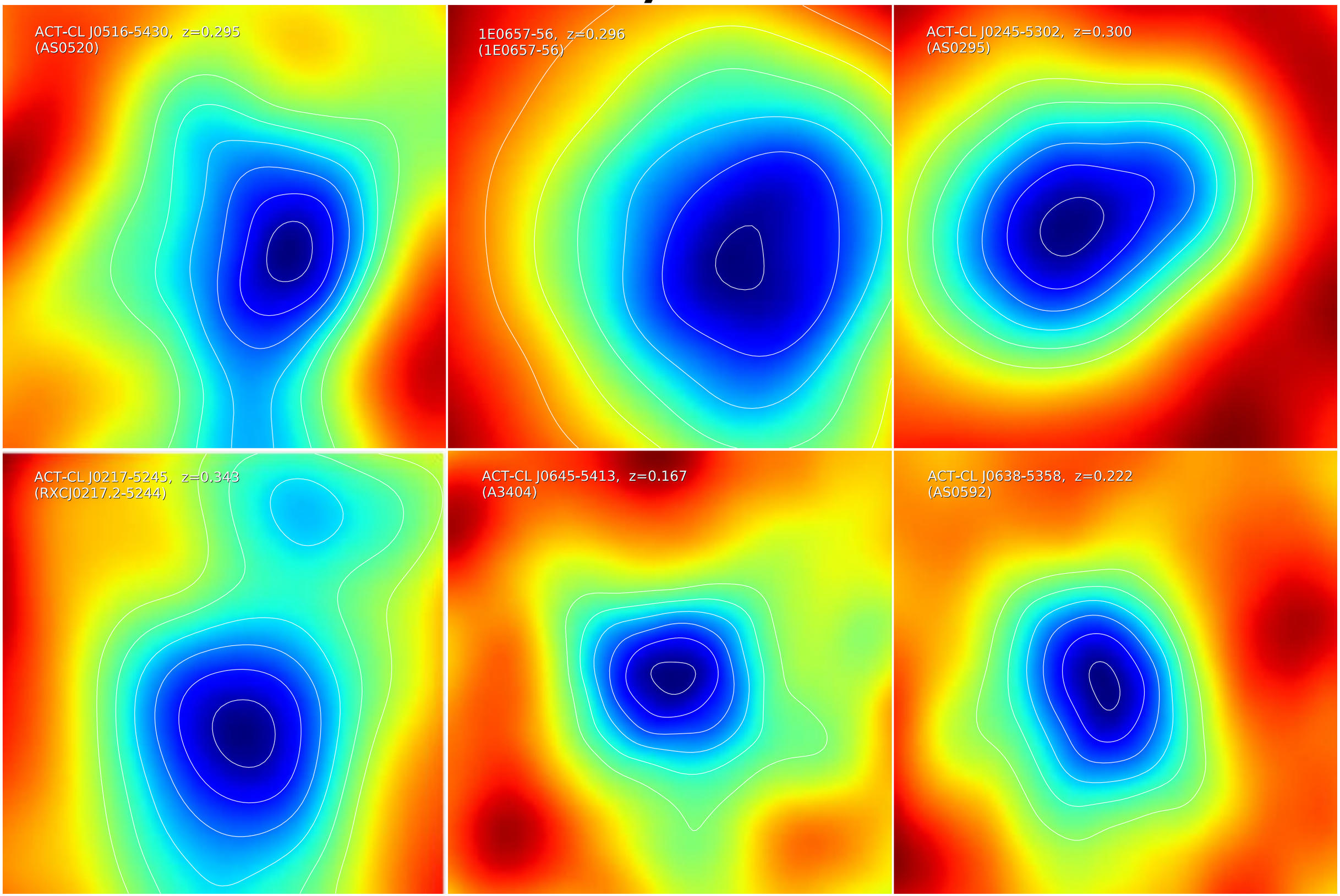

Menanteau et al. (2010), ApJ, 723,1523

Some Previously Known Clusters

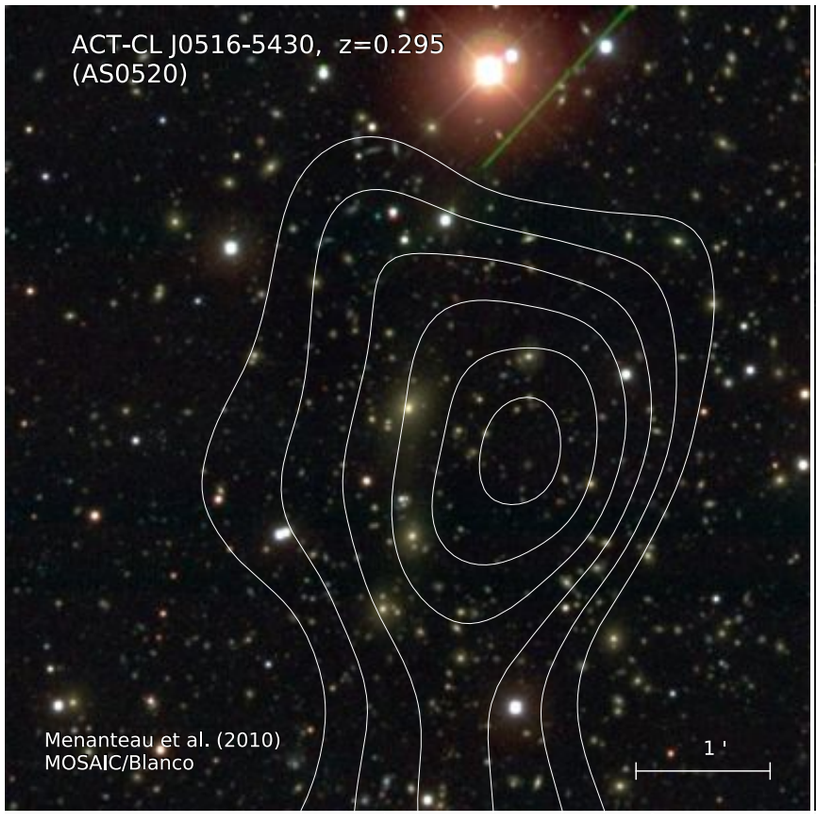

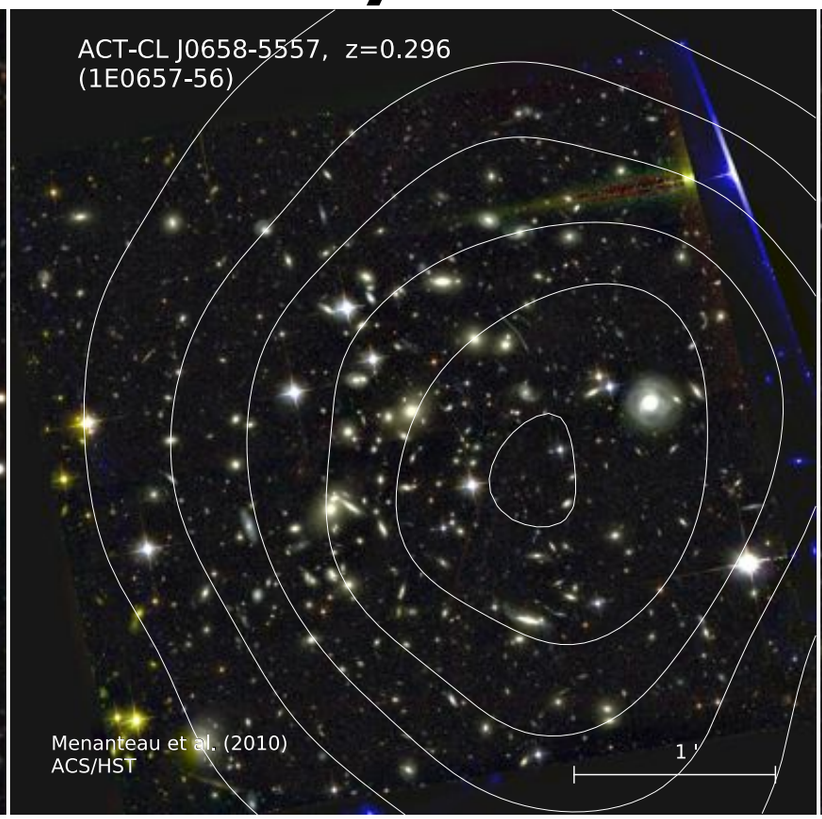

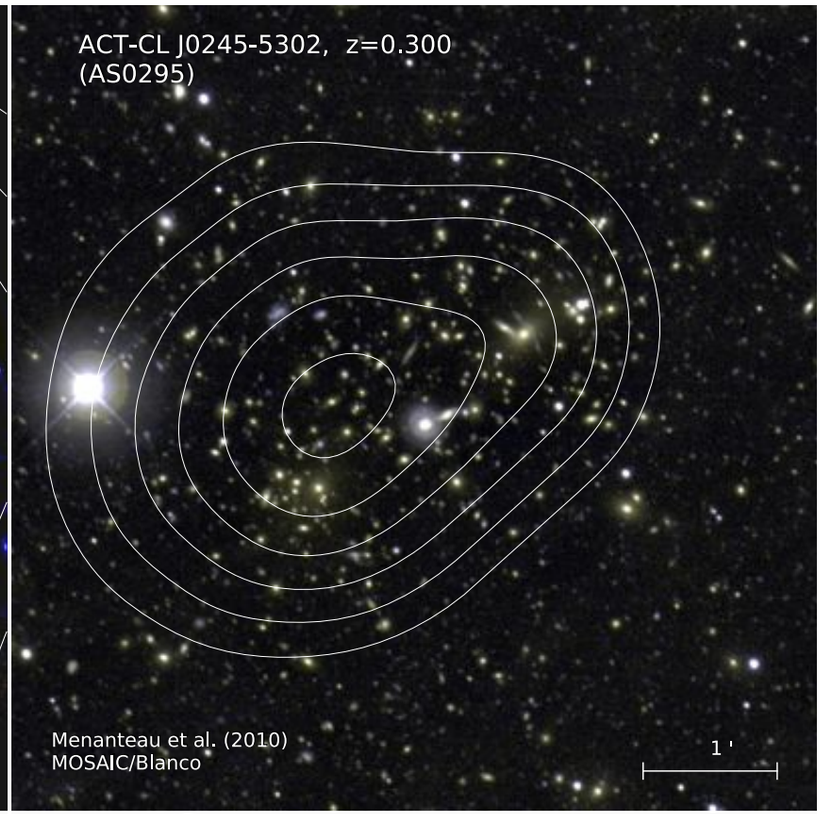

Menanteau et al. (2010), ApJ, 723,1523

Some 2008 ACT SZ-discovered Clusters

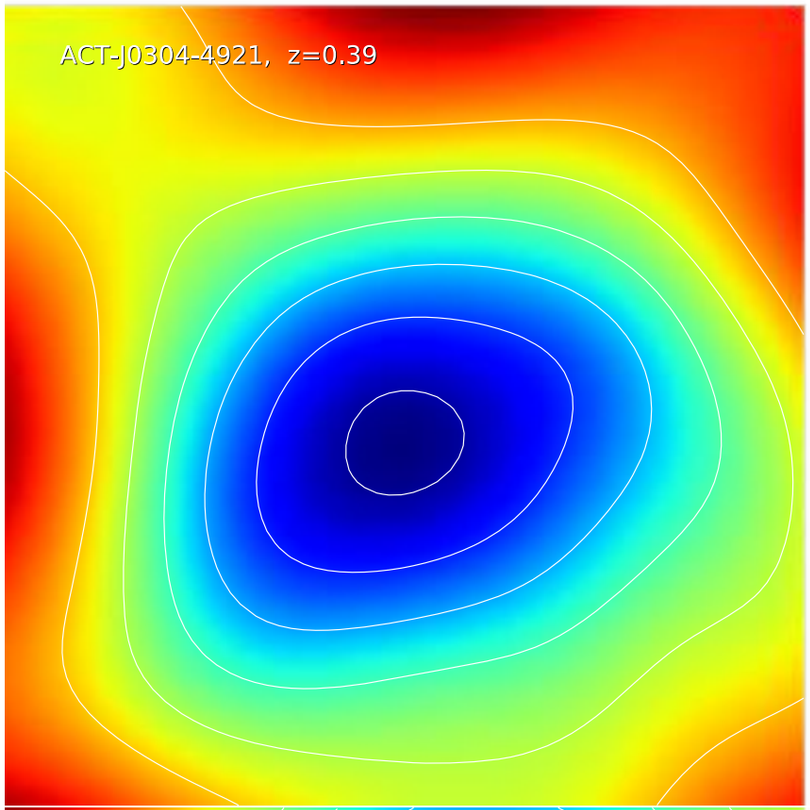

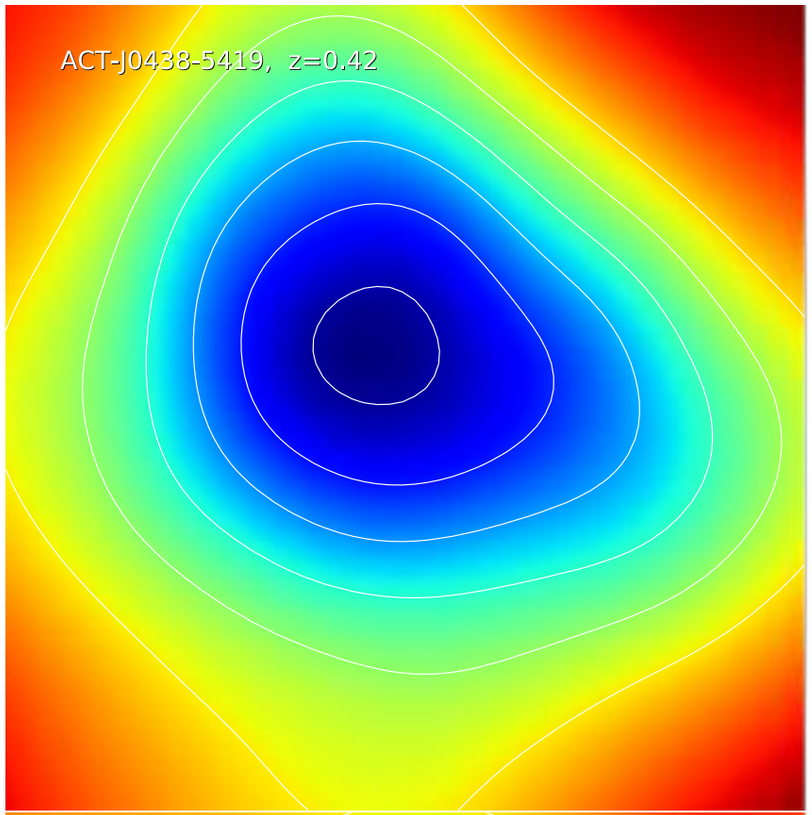

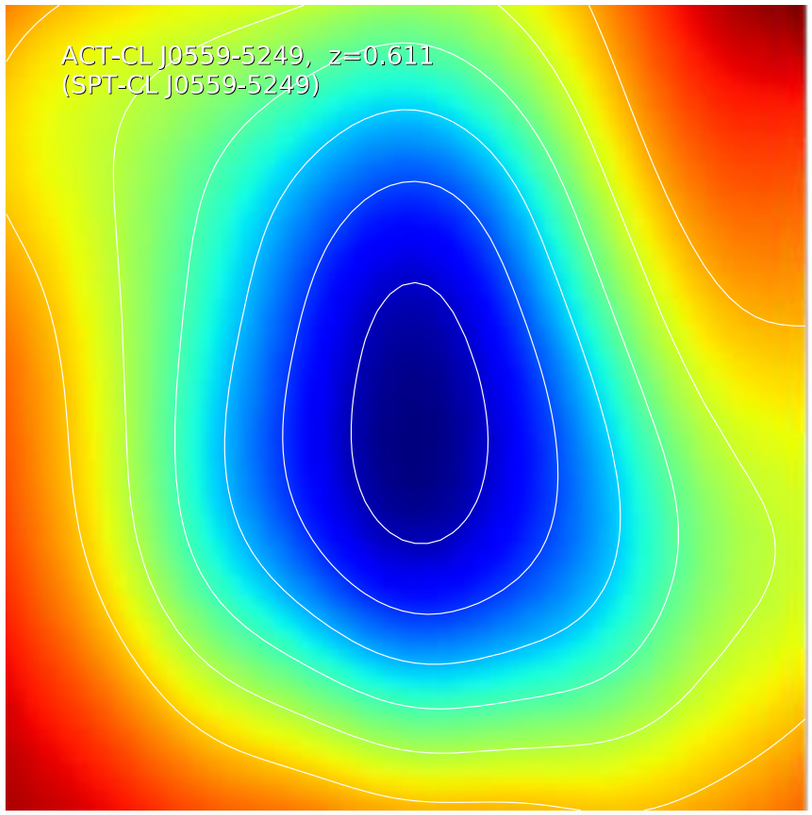

Menanteau et al. (2010), ApJ, 723,1523

Some 2008 ACT SZ-discovered Clusters

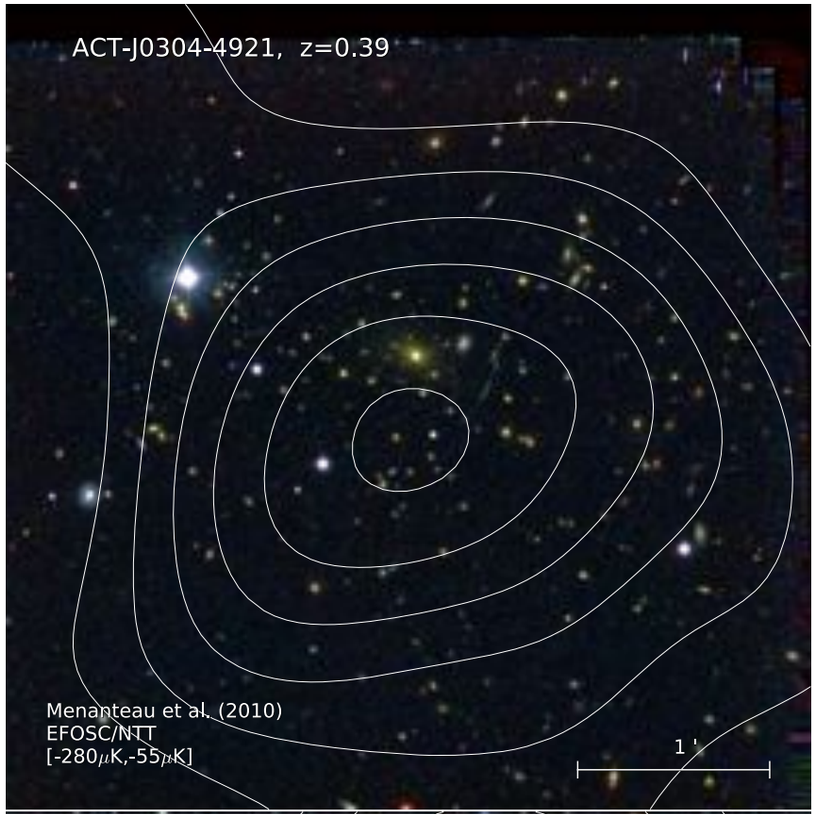

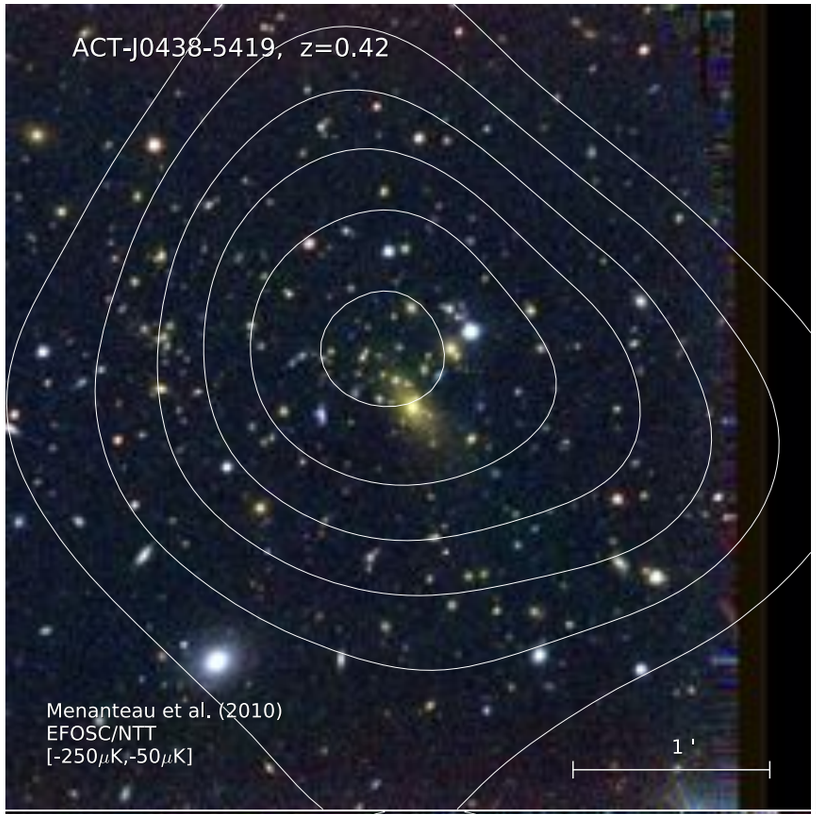

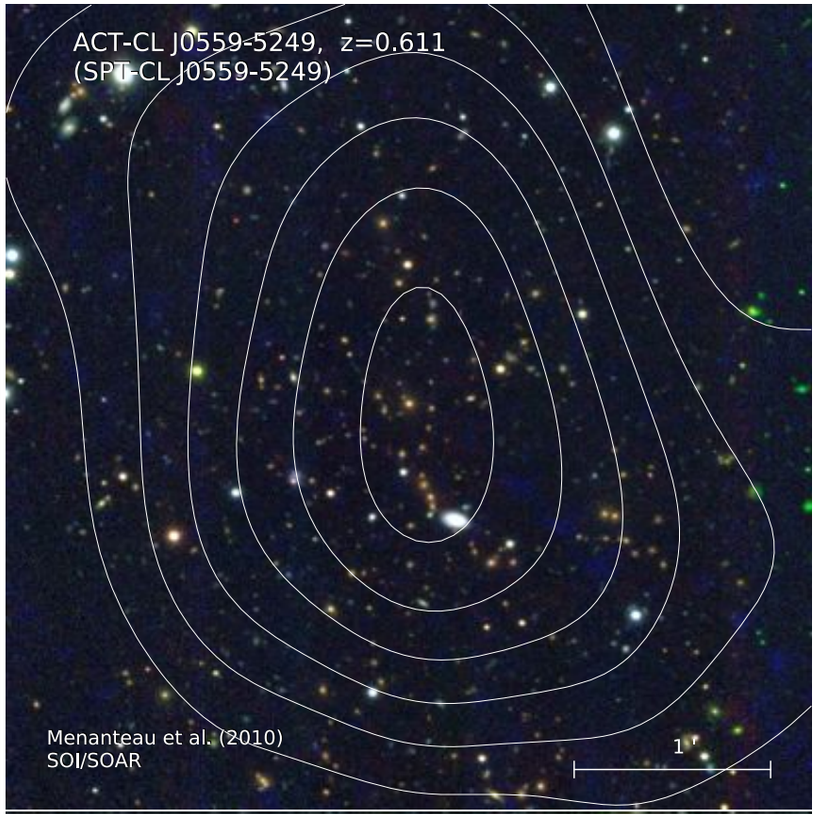

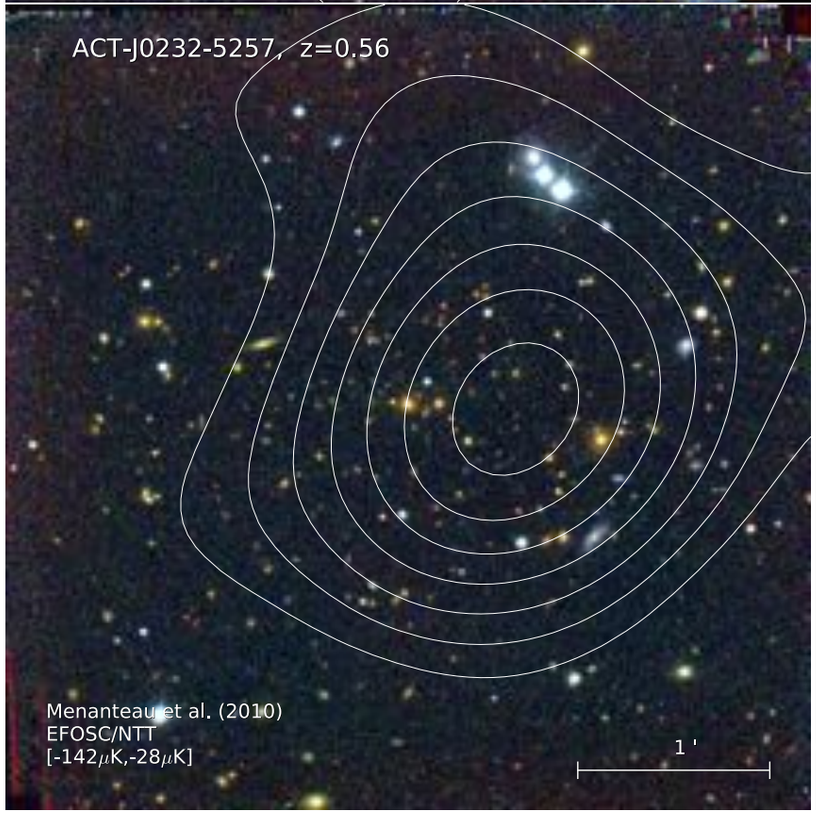

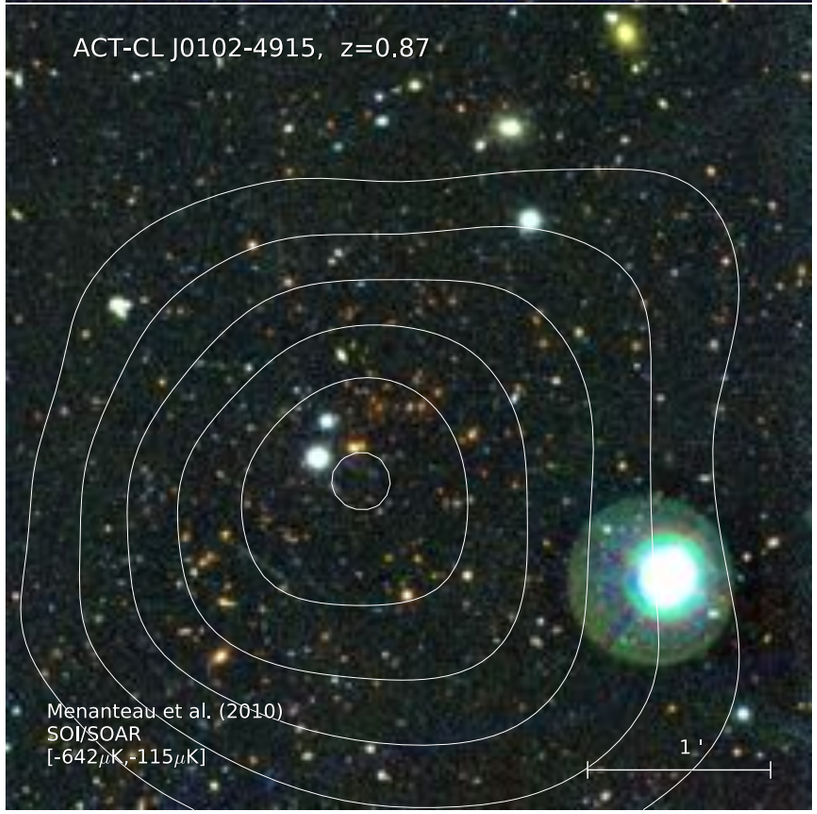

Menanteau et al. (2010), ApJ, 723,1523

Some 2008 ACT SZ-discovered Clusters

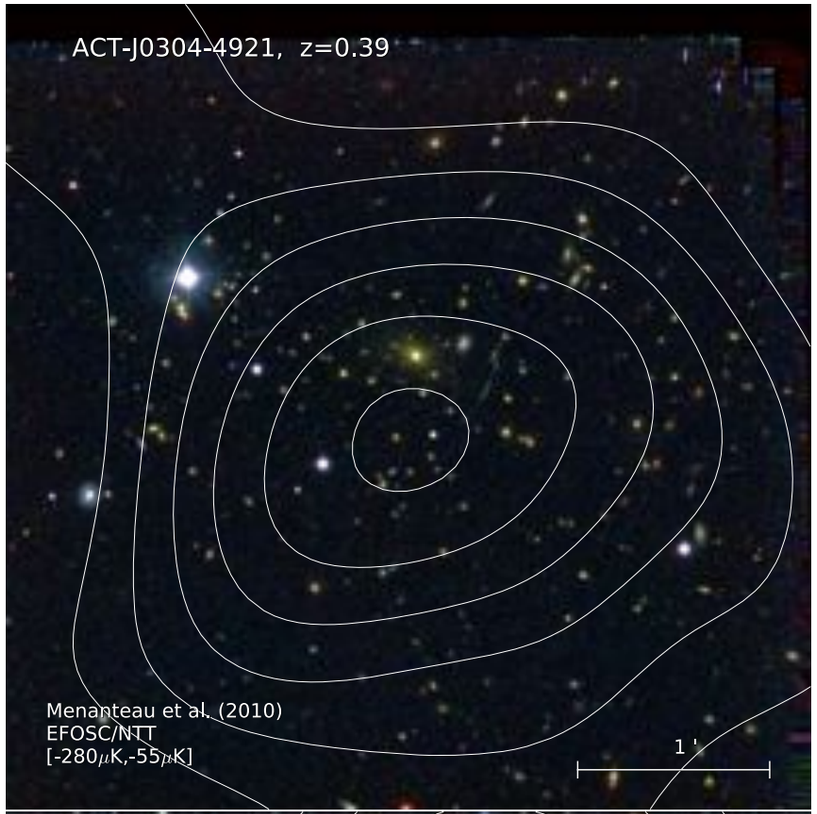

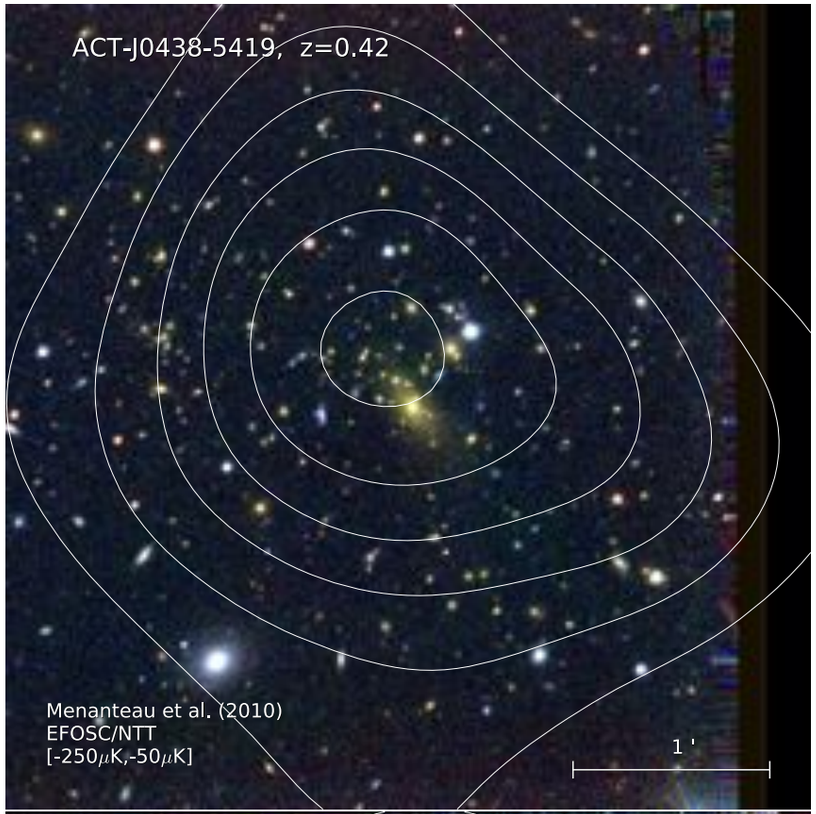

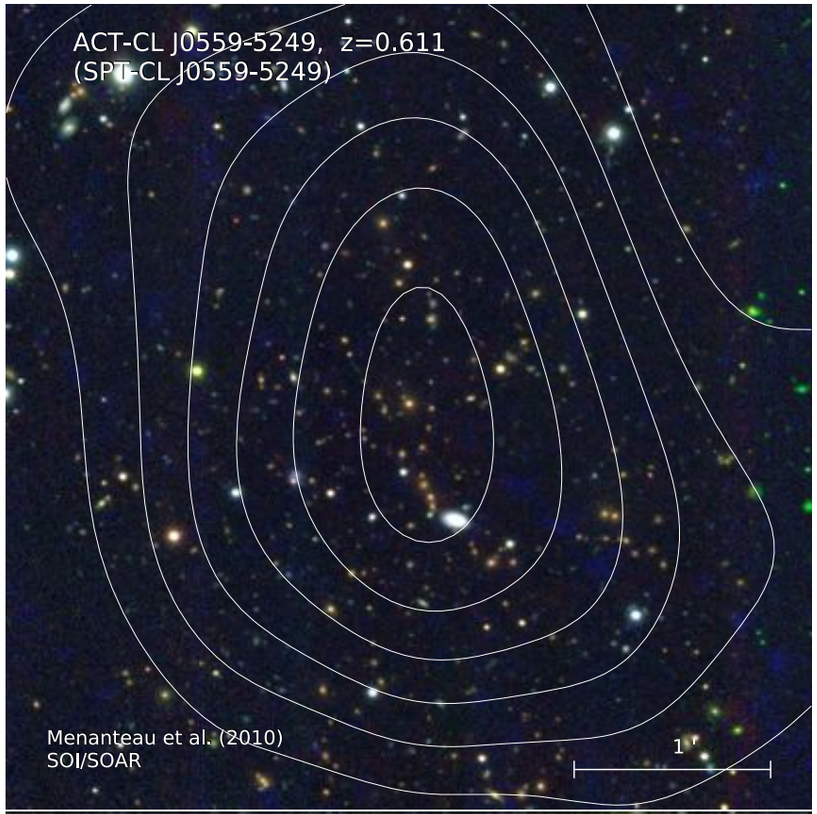

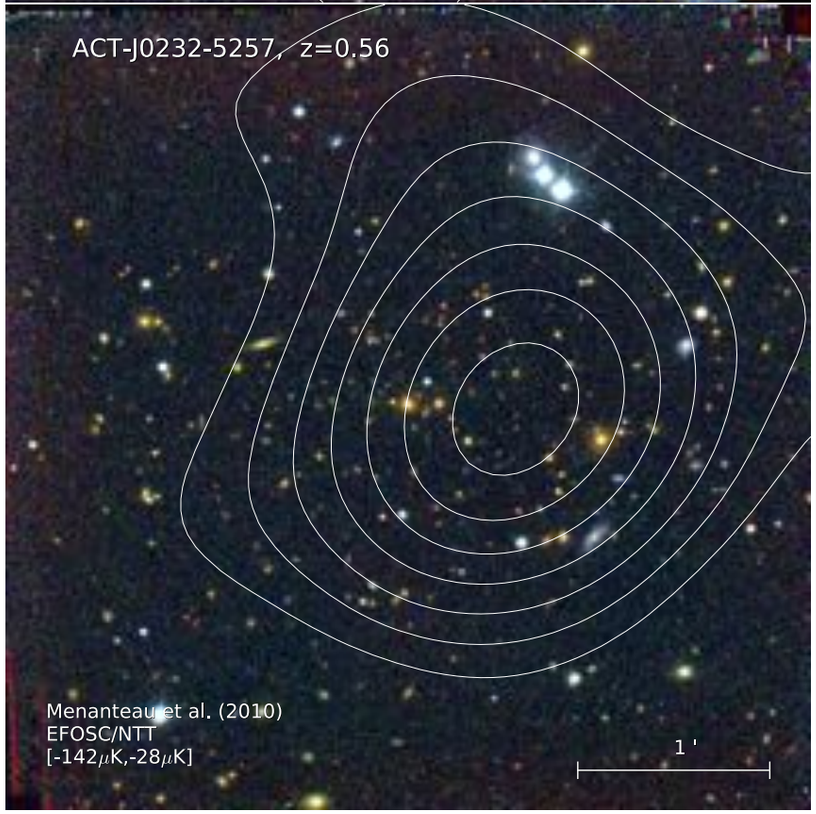

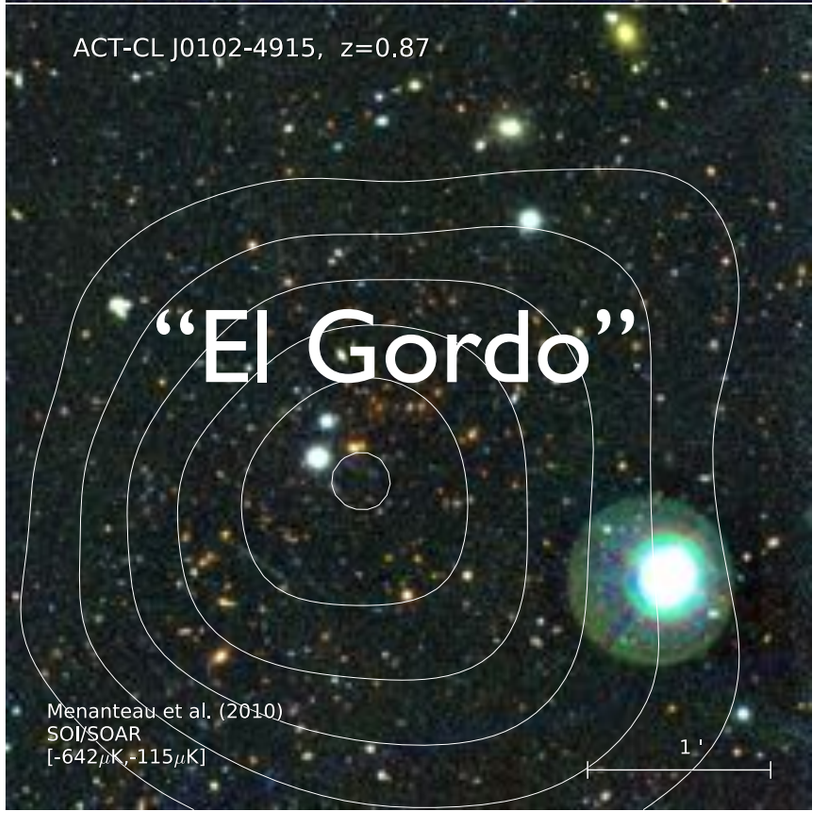

Menanteau et al. (2010), ApJ, 723,1523

Strong Lensing (examples)

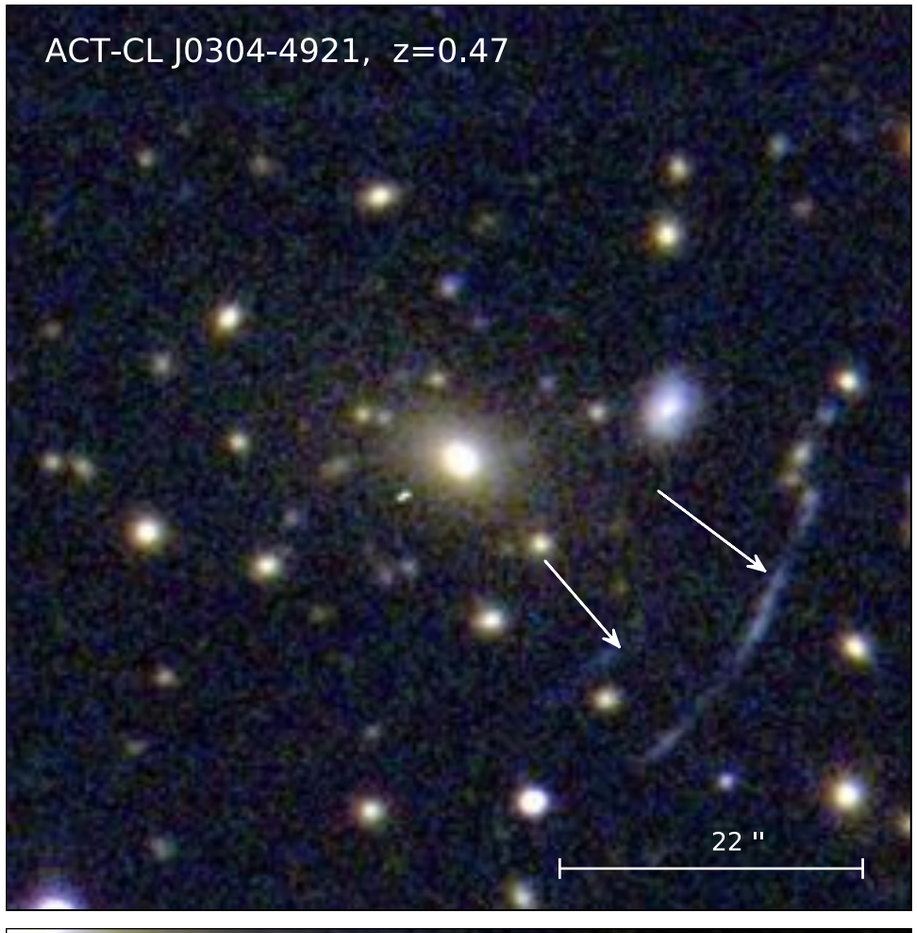

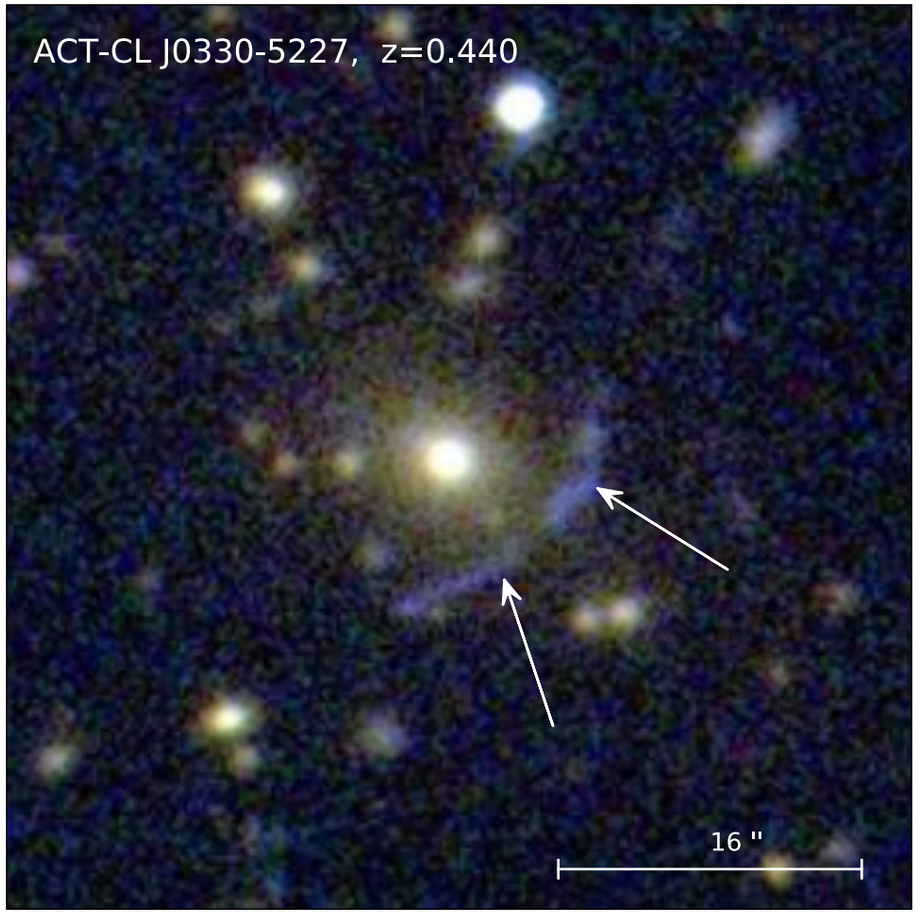

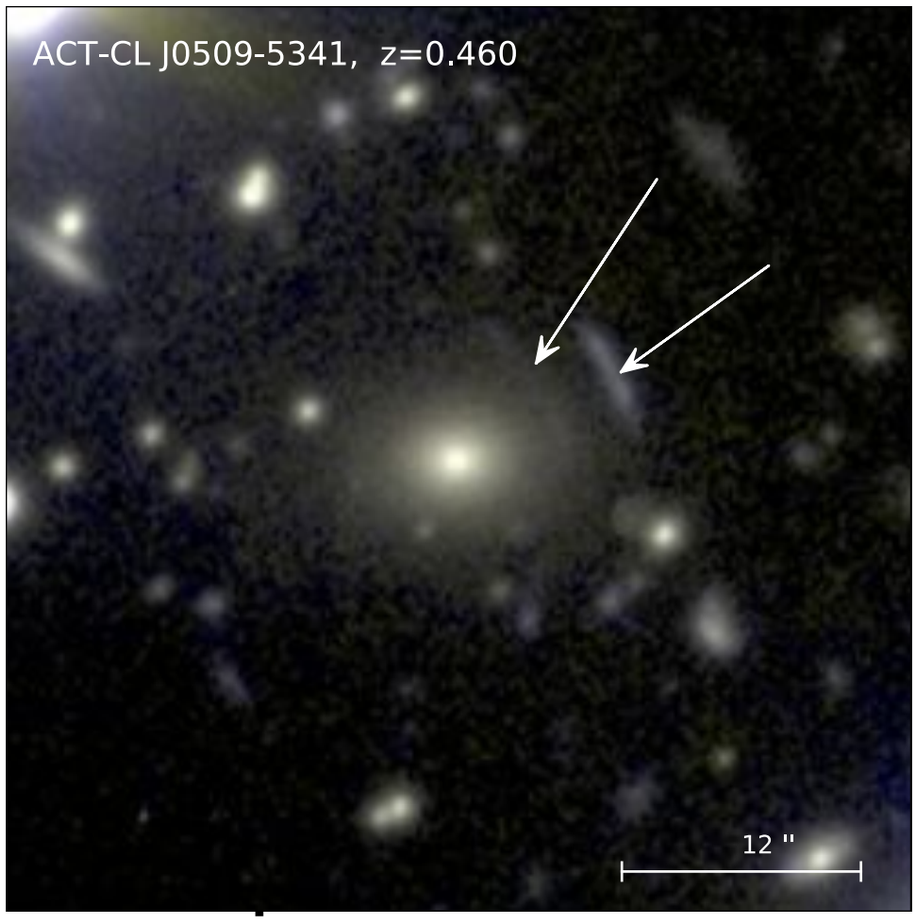

- 7/23 clusters show strong lensing arcs
- 3 of these have already reported

Menanteau et al. (2010), ApJ, 723,1523

Strong Lensing (examples)

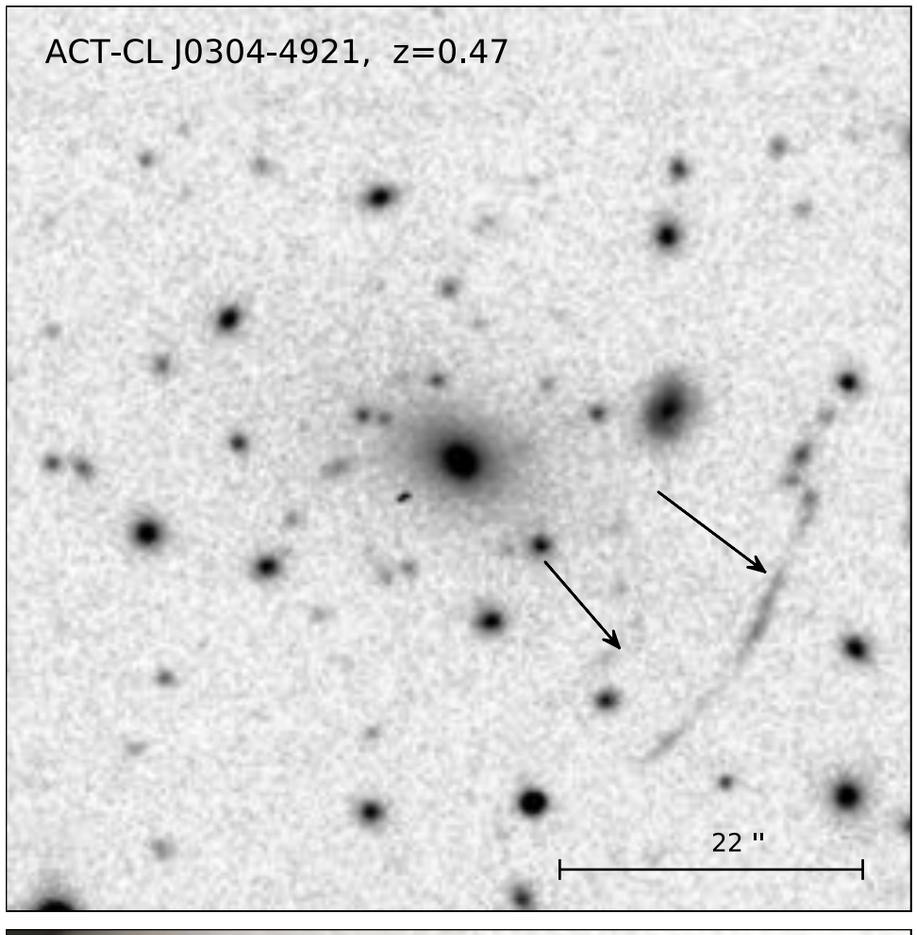

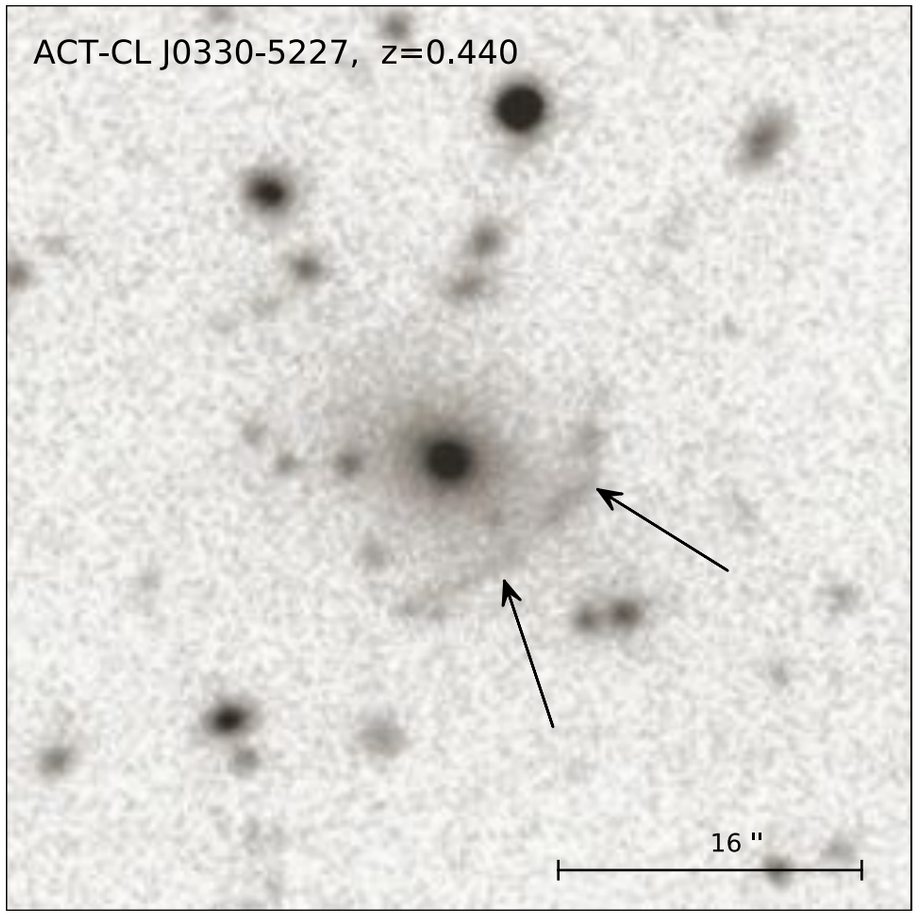

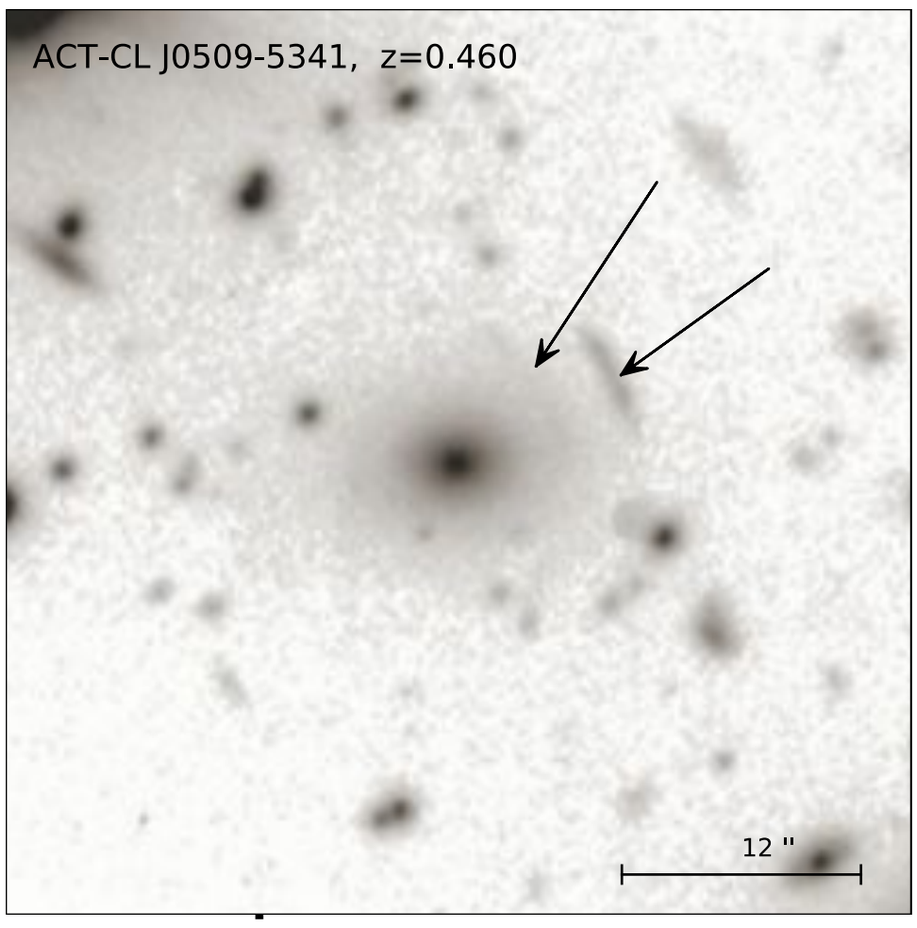

- 7/23 clusters show strong lensing arcs
- 3 of these have already reported

Menanteau et al. (2010), ApJ, 723,1523

"El Gordo," Multi-wavelength Observations

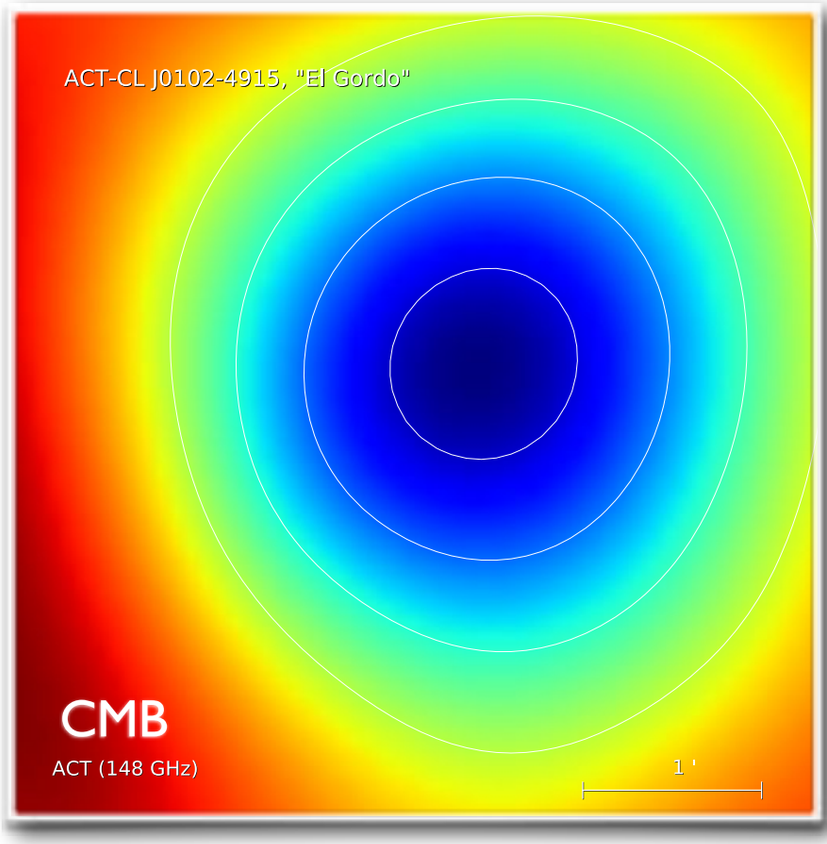

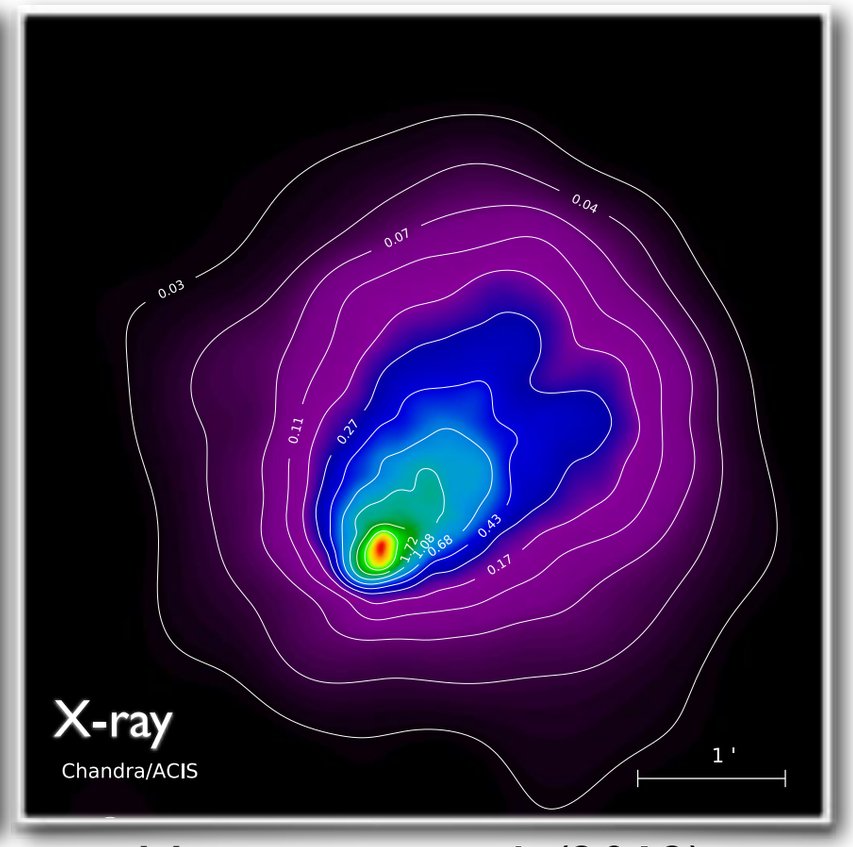

Menanteau et al. (2012)

- Detected in 2008 ACT maps of Southern Strip (Menanteau et al. 2010, Marriage et al. 2011)
  - Strongest SZ decrement over 755 deg^2 (South + Equator)
- Optical follow-up: **89 redshifts!**
  - Imaged (*griz*) at SOAR/SOI (9-12 Dec 2009)
  - VLT/FORS2 MOS (10-hrs) + Imaging (2 hrs) in Jan 2011

- *Chandra* X-ray Observations
  - ACIS-I, 60 ks, observed 27 Jan 2011
- Spitzer IRAC warm-phase follow-up
  - Imaged at 3.6 μm and 4.5 μm

The well-known Bullet Cluster

Clowe et al.(2006)

The well-known Bullet Cluster

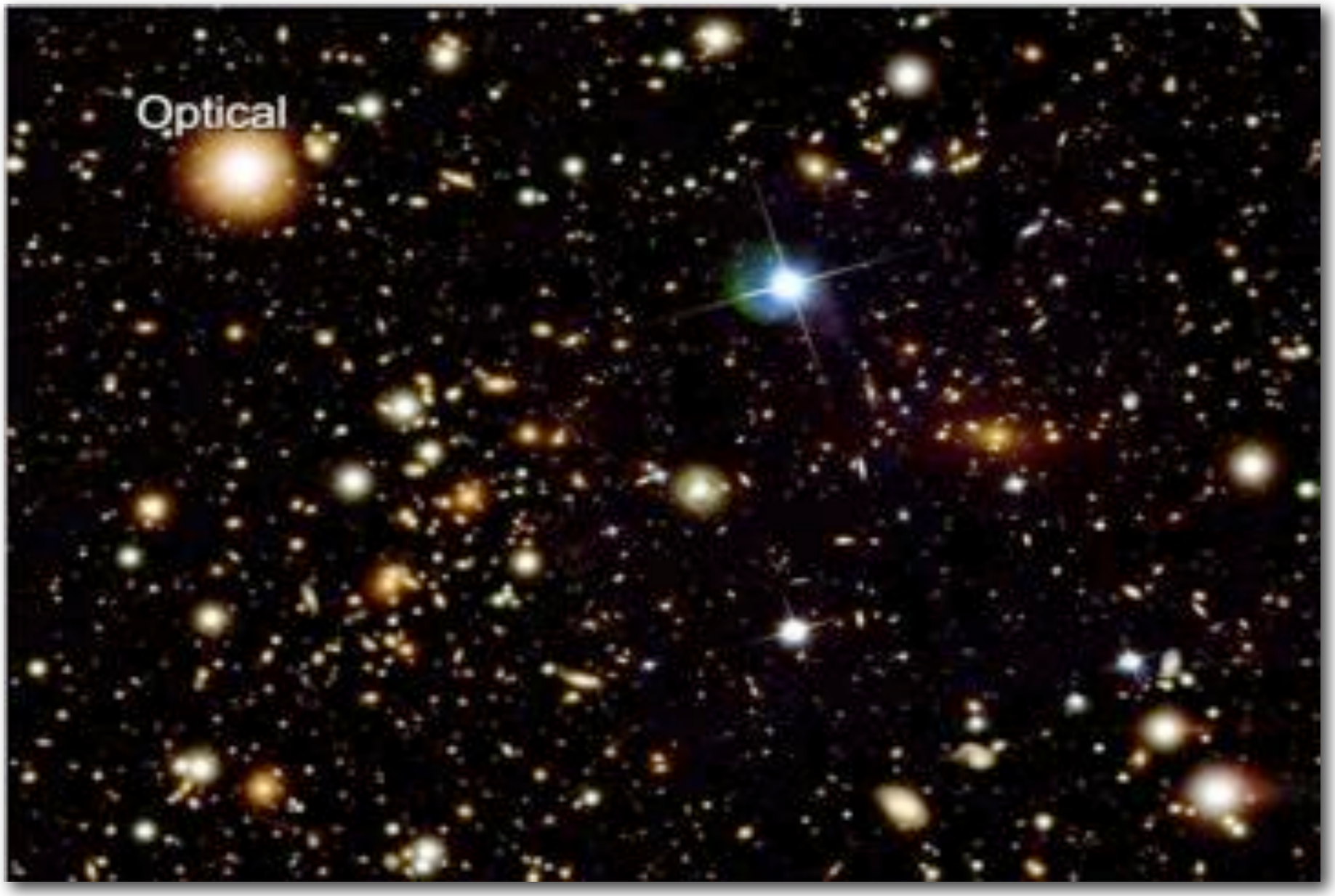

Clowe et al.(2006)

The well-known Bullet Cluster

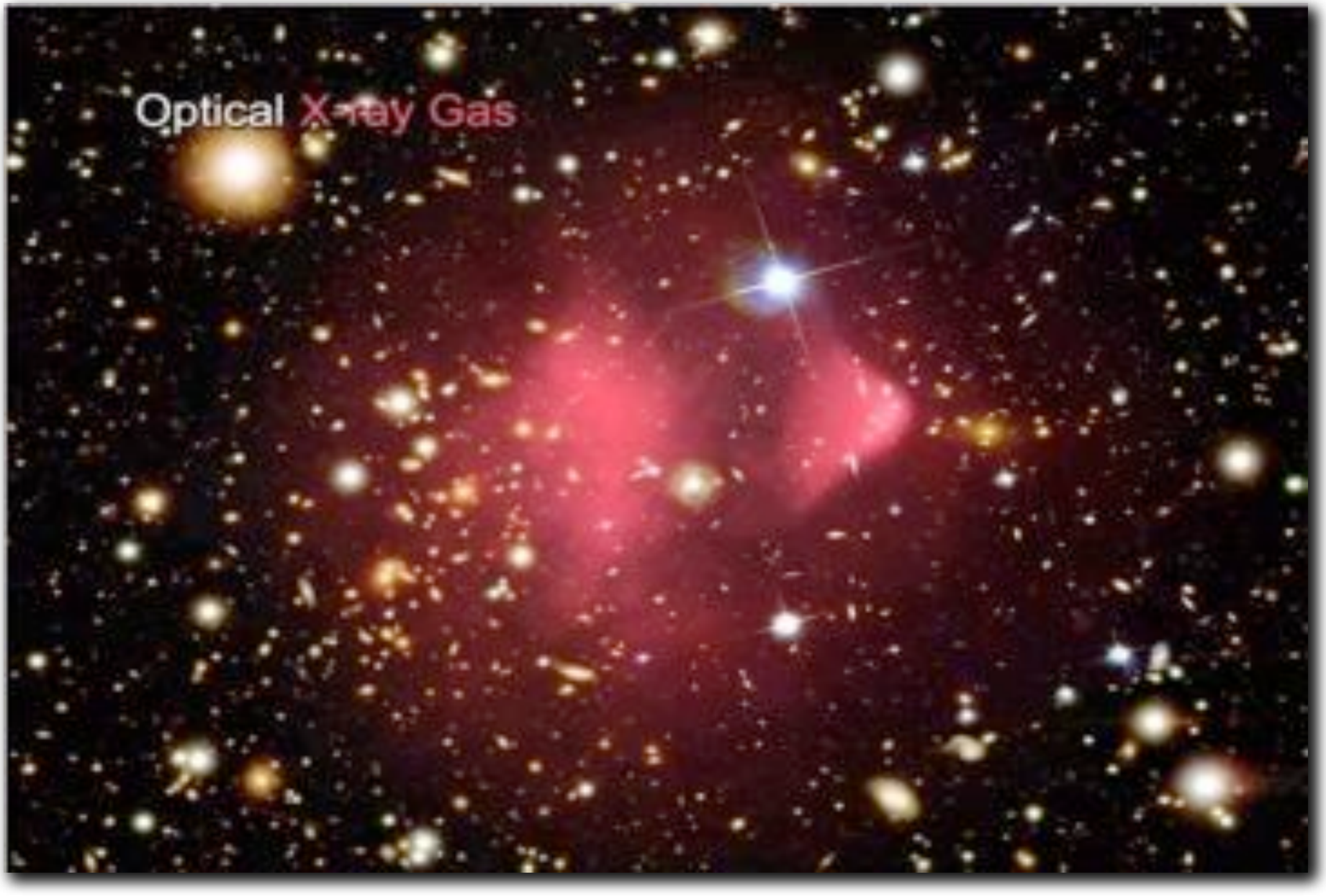

Clowe et al.(2006)

The well-known Bullet Cluster

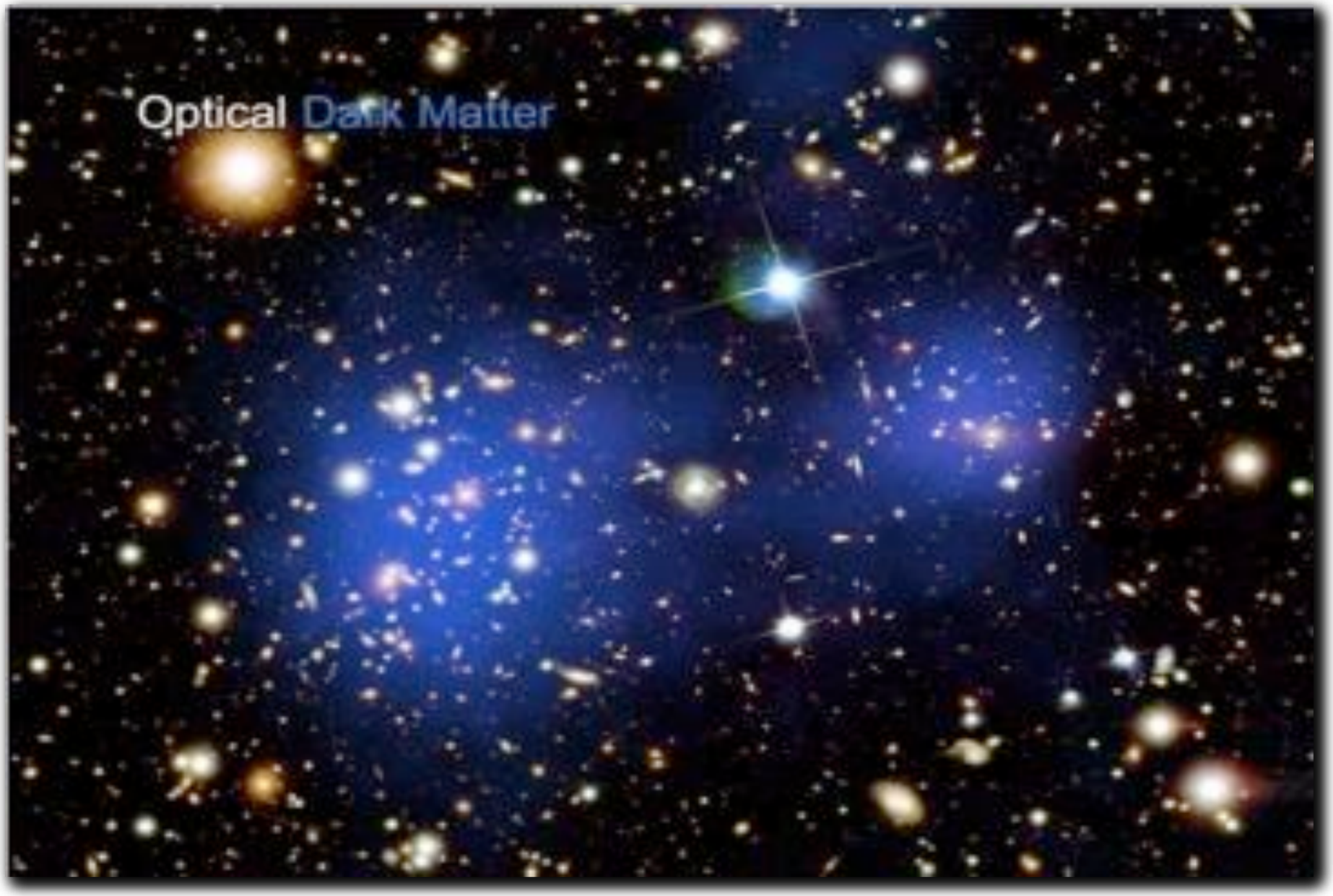

Clowe et al.(2006)

The well-known Bullet Cluster

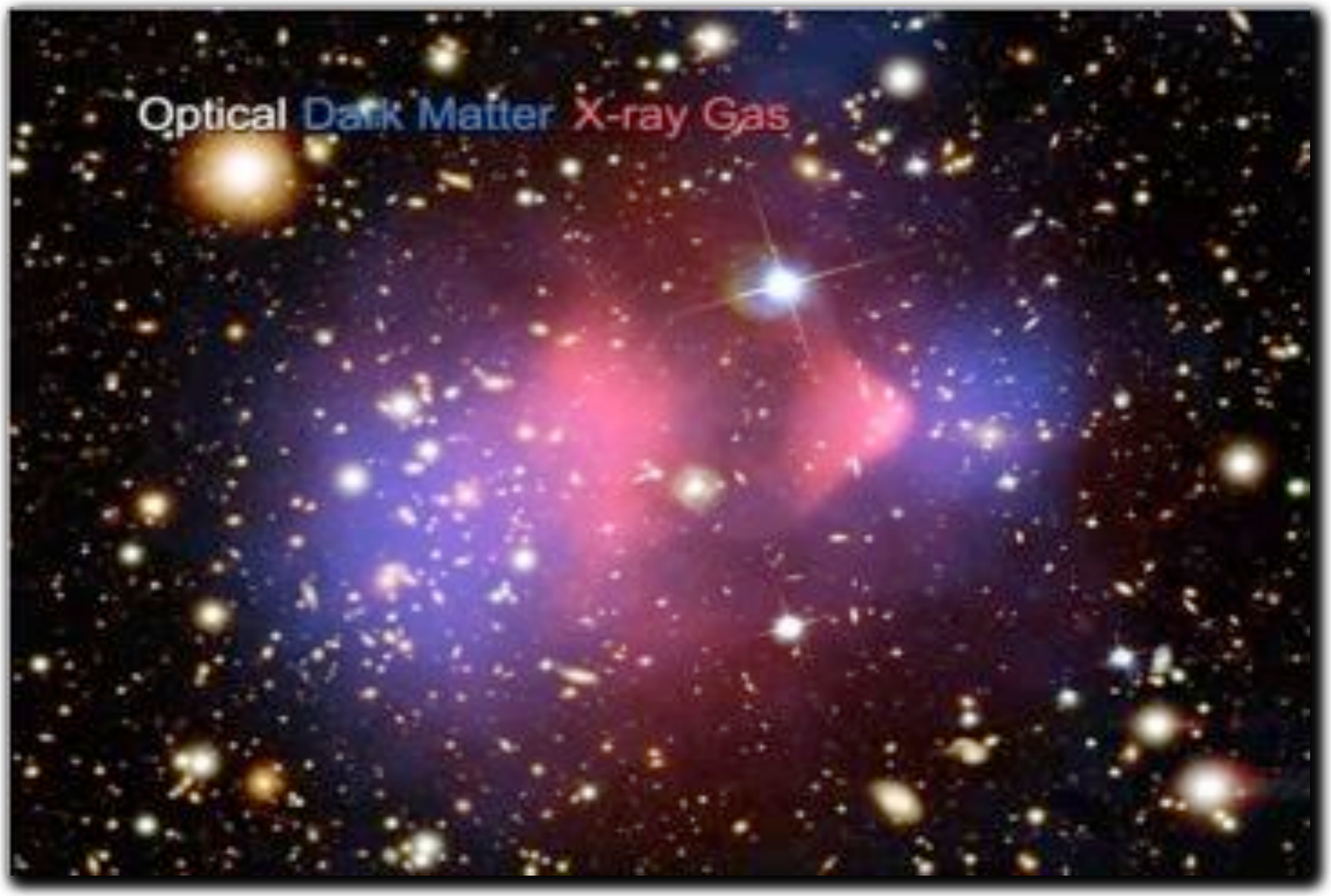

Clowe et al.(2006)

A high-z Bullet-like Cluster?

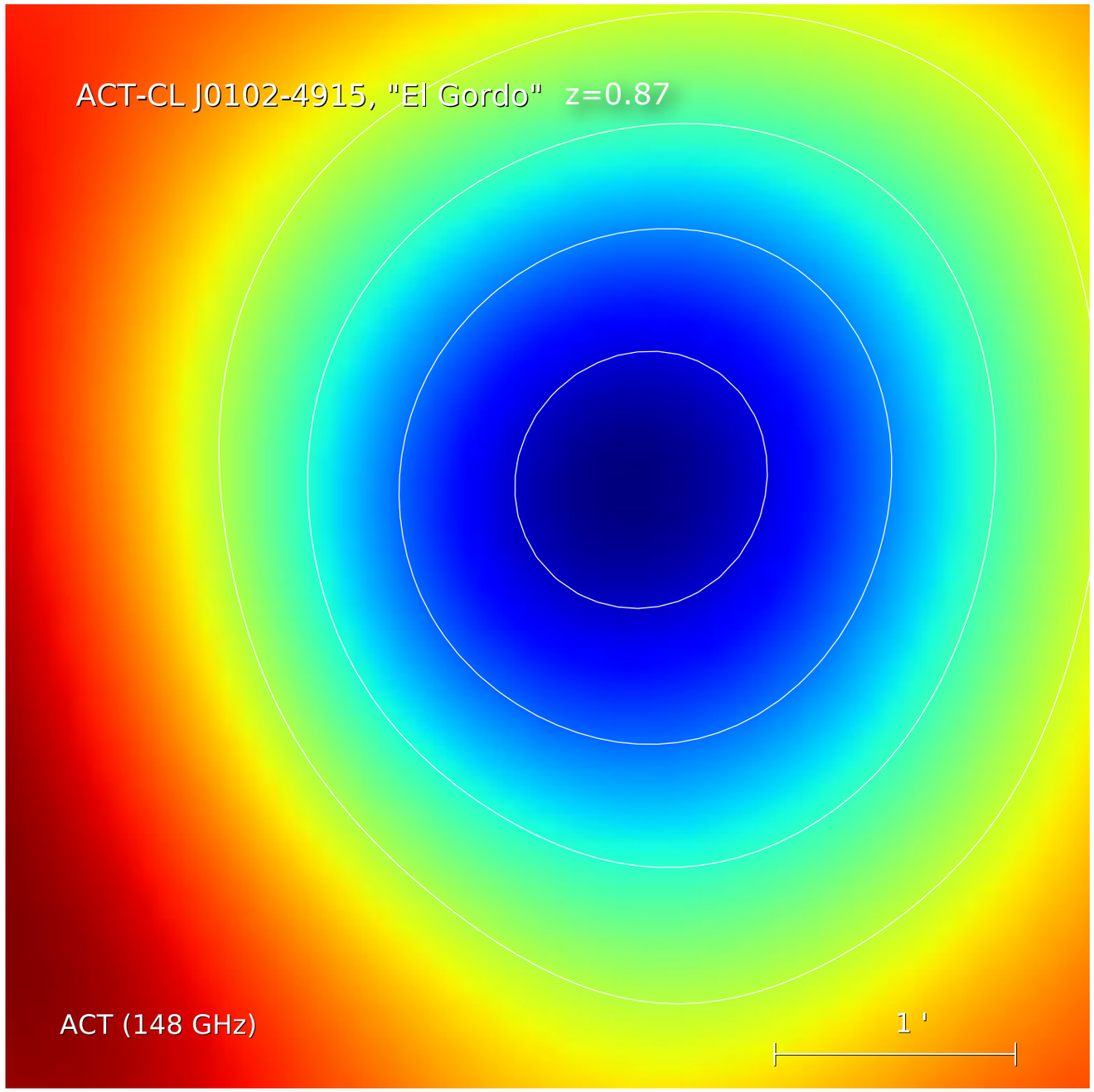

Menanteau et al. (2012, ApJ, 748,7)

A high-z Bullet-like Cluster?

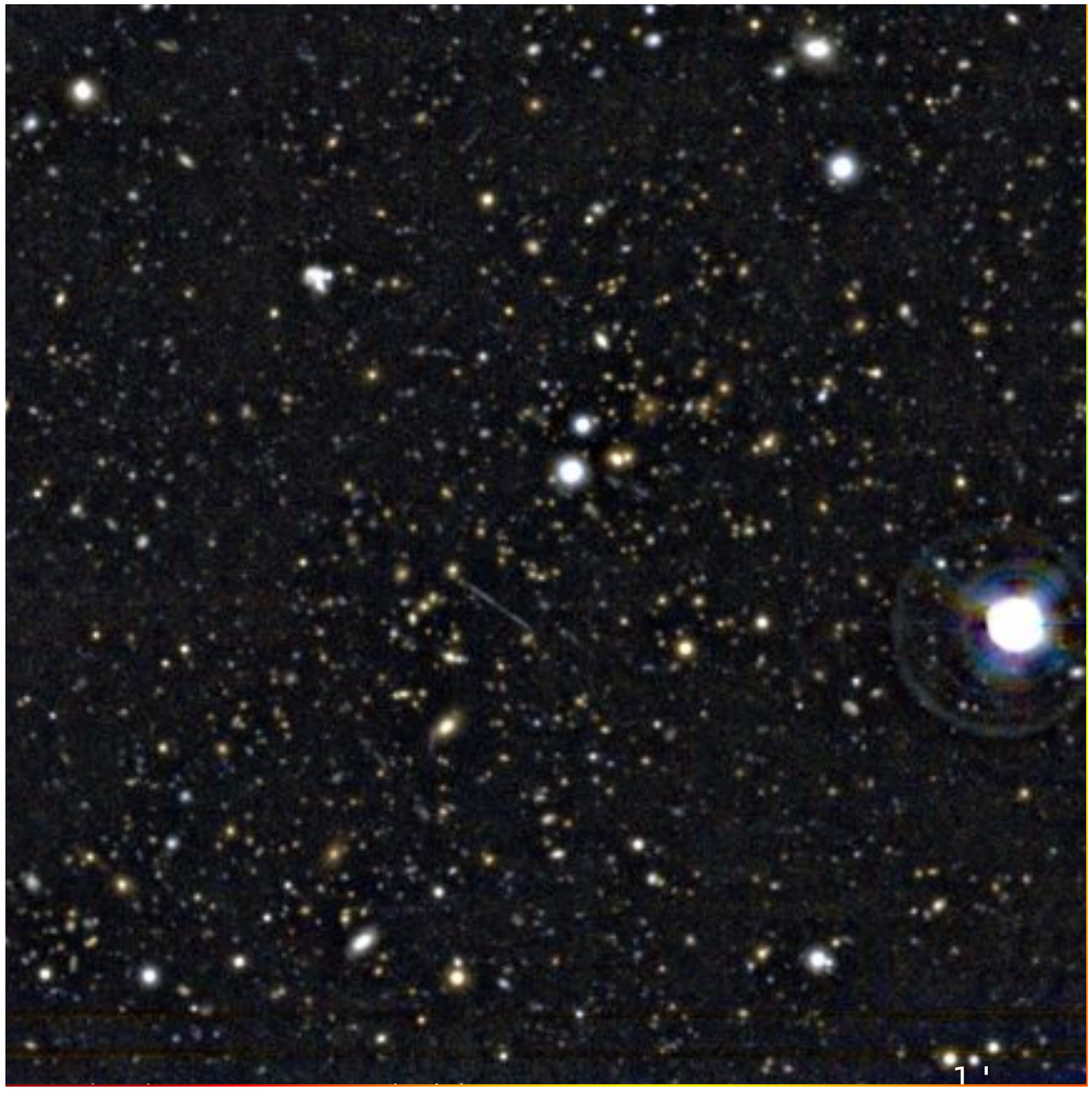

Menanteau et al. (2012, ApJ, 748,7)

A high-z Bullet-like Cluster?

The galaxies in "El Gordo" mostly lie in two distinct groups

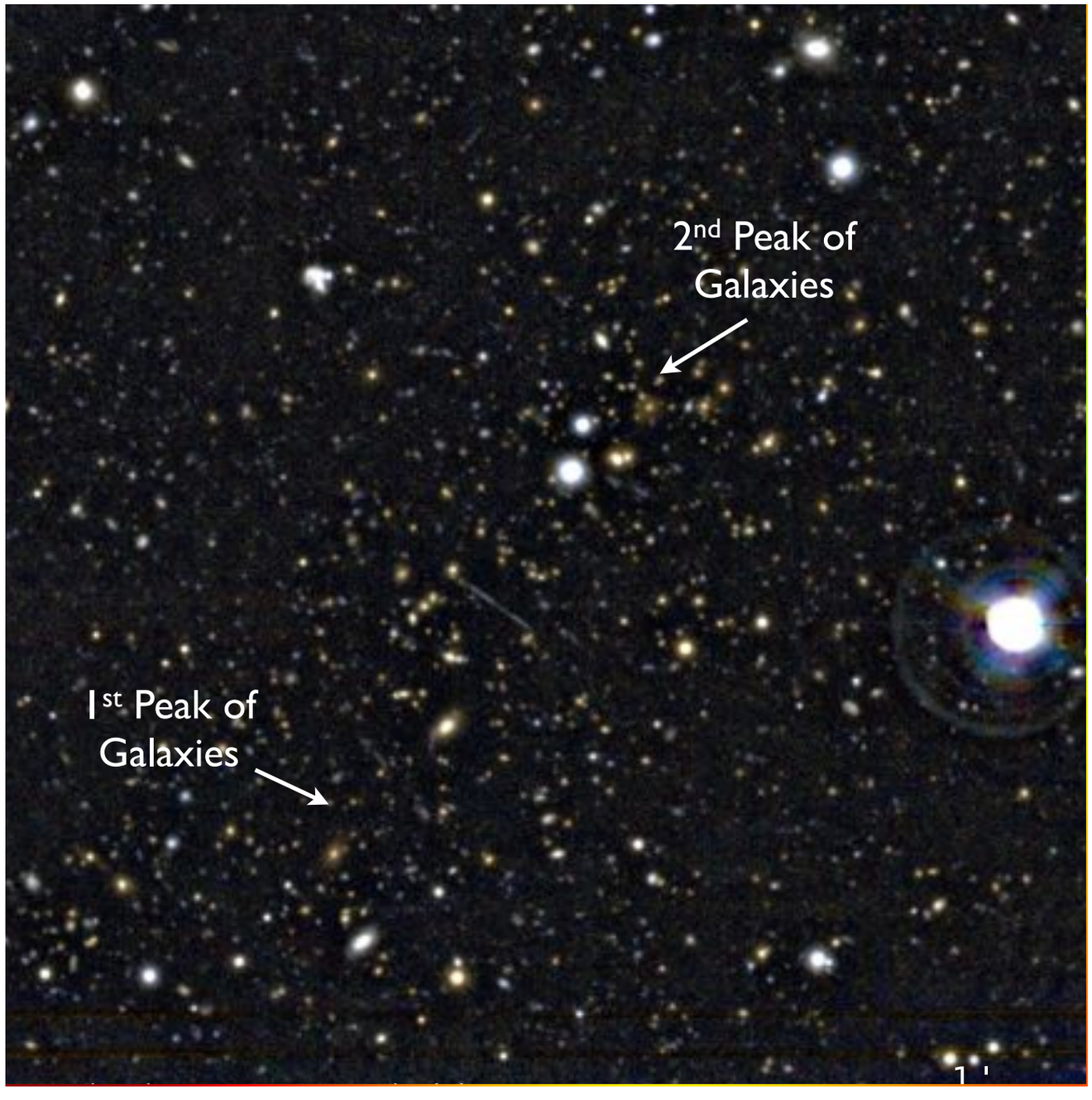

Menanteau et al. (2012, ApJ, 748,7)

A high-z Bullet-like Cluster?

The galaxies in "El Gordo" mostly lie in two distinct groups

The X-ray emission mostly lies between these two groups and shows a peculiar structure with a bright offset Gas Peak and Wake.

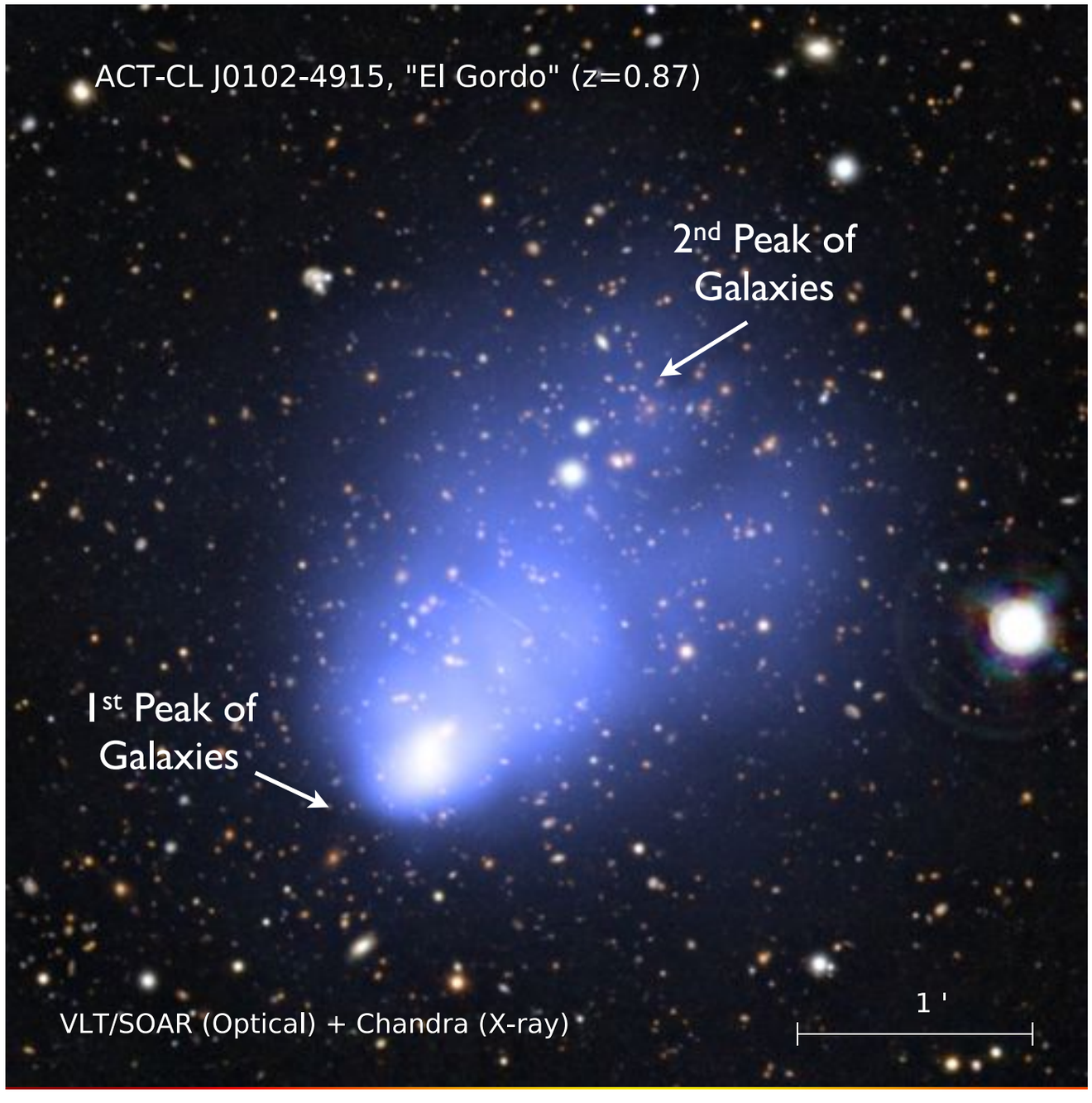

Menanteau et al. (2012, ApJ, 748,7)

A high-z Bullet-like Cluster?

The galaxies in "El Gordo" mostly lie in two distinct groups

The X-ray emission mostly lies between these two groups and shows a peculiar structure with a bright offset Gas Peak and Wake.

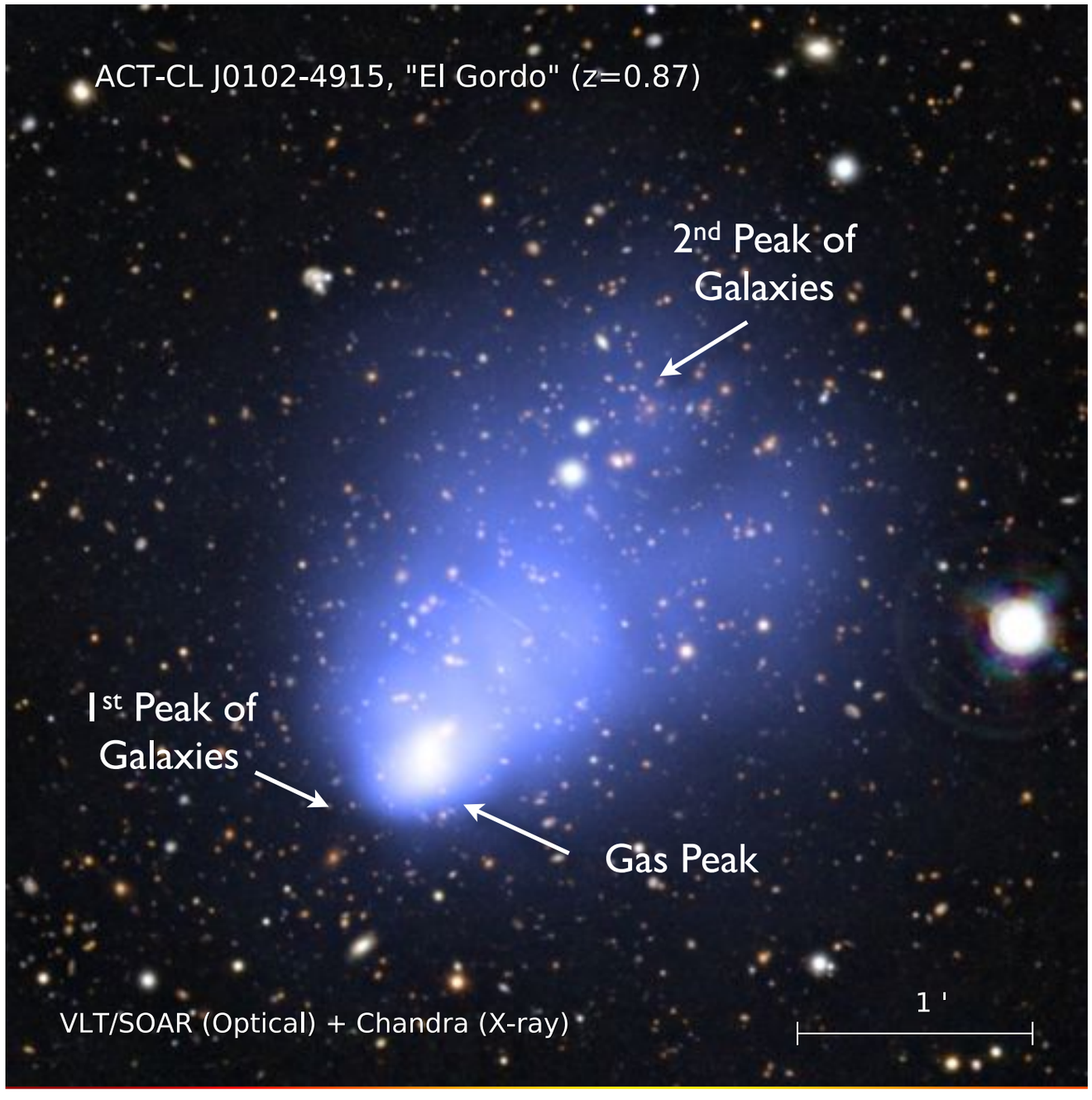

Menanteau et al. (2012, ApJ, 748,7)

A high-z Bullet-like Cluster?

The galaxies in "El Gordo" mostly lie in two distinct groups

The X-ray emission mostly lies between these two groups and shows a peculiar structure with a bright offset Gas Peak and Wake.

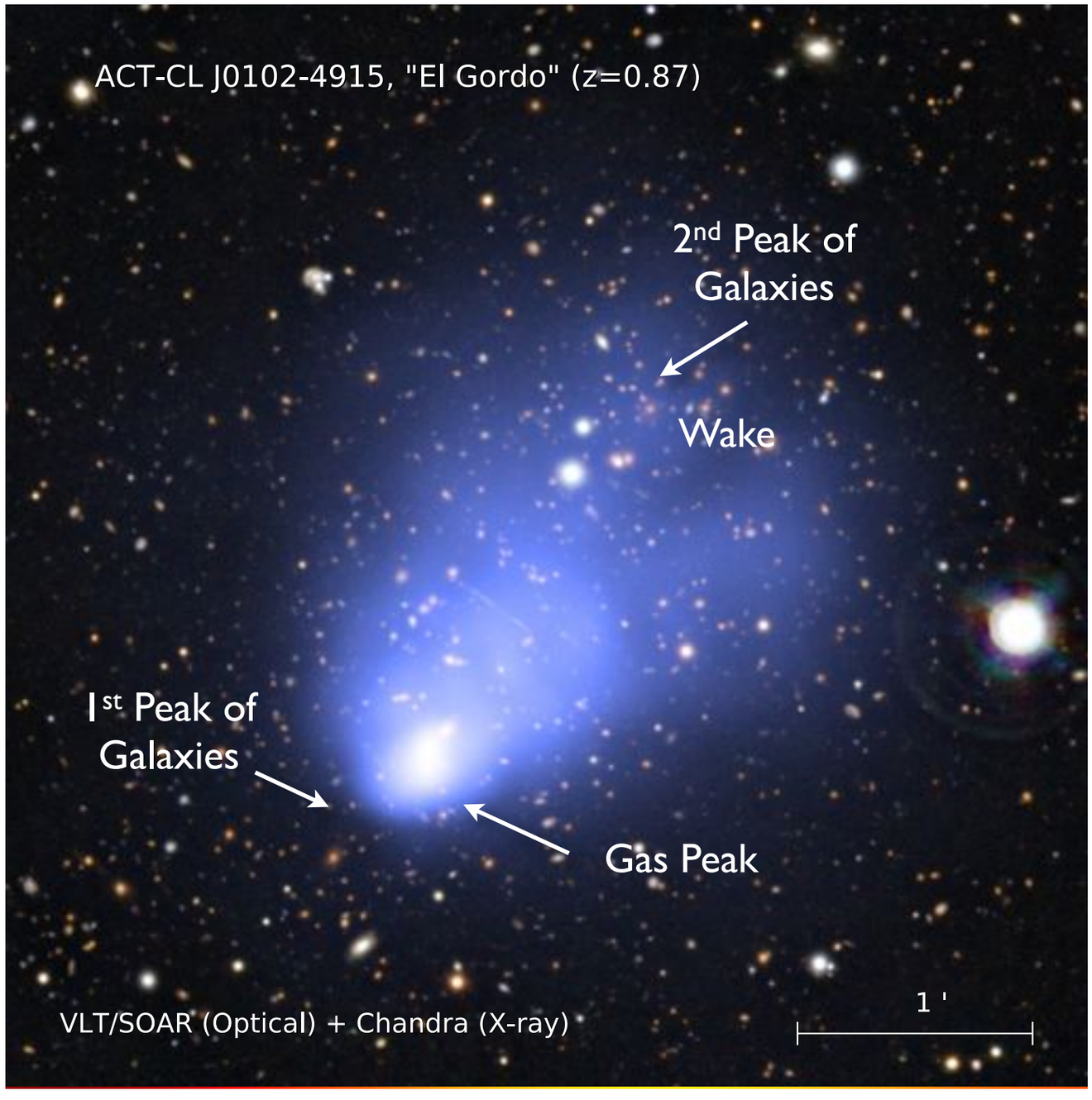

Menanteau et al. (2012, ApJ, 748,7)

A high-z Bullet-like Cluster?

The galaxies in "El Gordo" mostly lie in two distinct groups

The X-ray emission mostly lies between these two groups and shows a peculiar structure with a bright offset Gas Peak and Wake.

The offset peak is likely the core of one of the merging components; arrow indicates the approximate direction of merger.

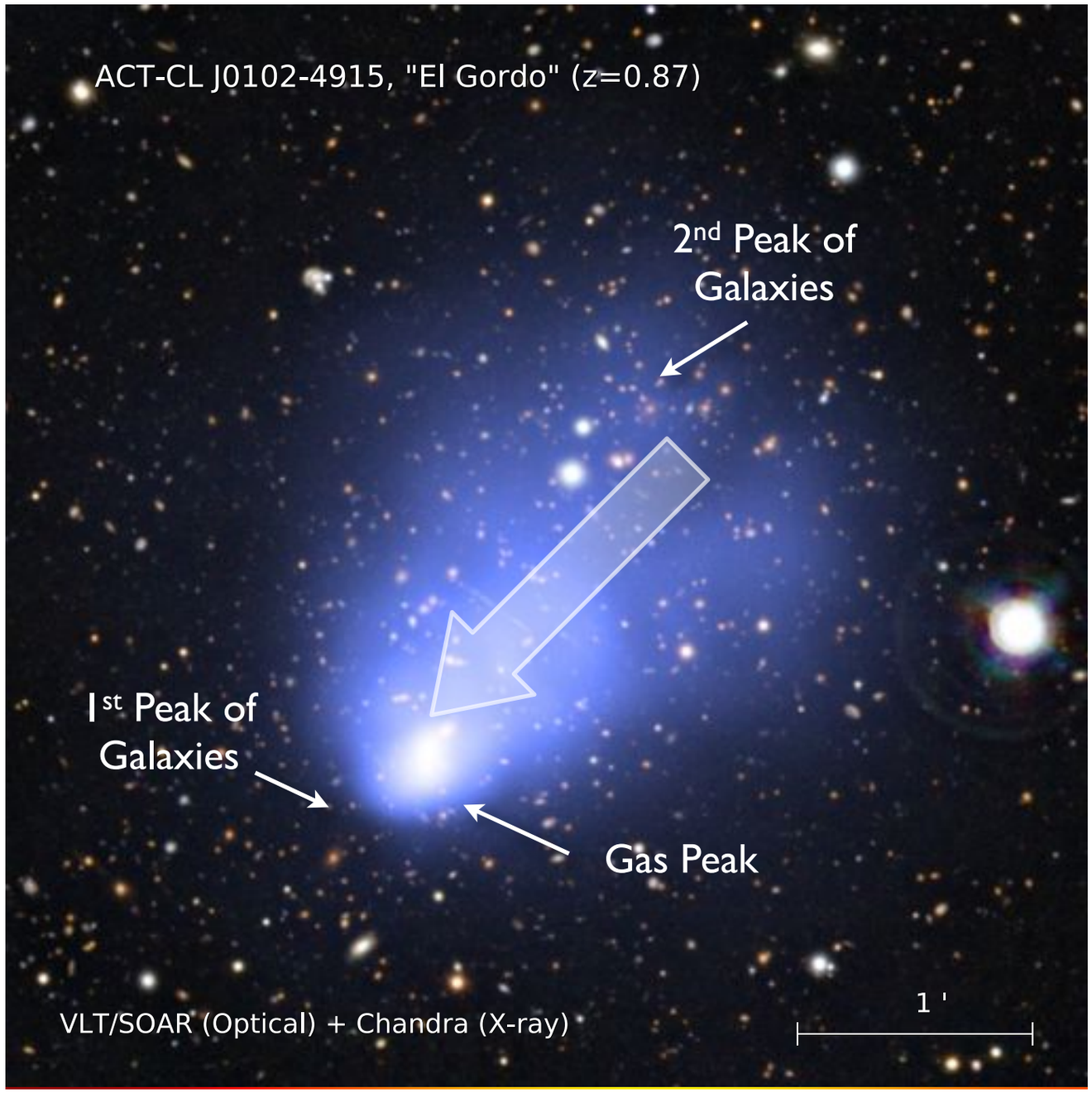

Menanteau et al. (2012, ApJ, 748,7)

A high-z Bullet-like Cluster?

The galaxies in "El Gordo" mostly lie in two distinct groups

The X-ray emission mostly lies between these two groups and shows a peculiar structure with a bright offset Gas Peak and Wake.

The offset peak is likely the core of one of the merging components; arrow indicates the approximate direction of merger.

The peak of the Galaxy distribution precedes the Gas Peak in the direction of the merger – a spatial separation like that seen in the Bullet Cluster.

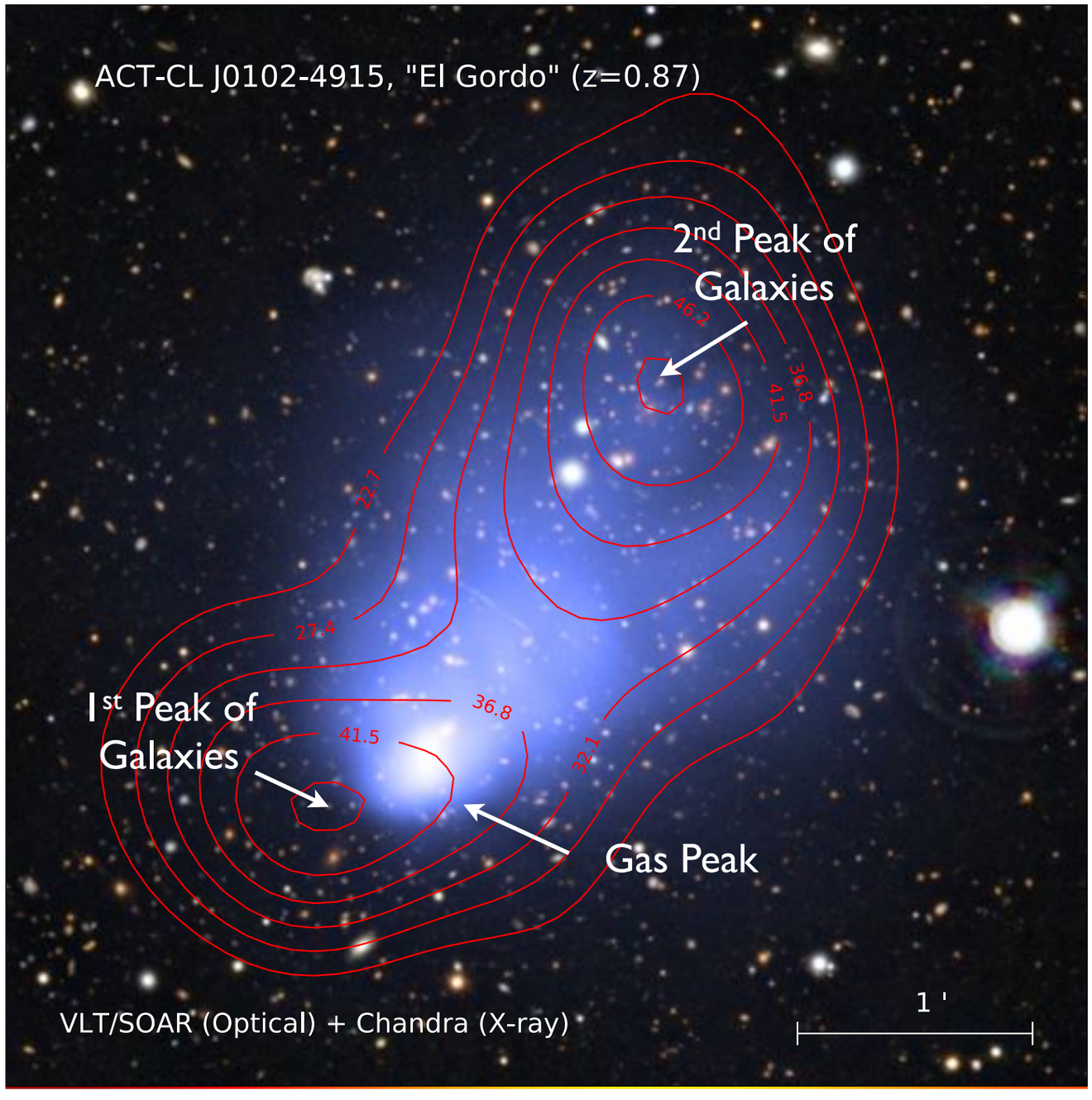

Menanteau et al. (2012, ApJ, 748,7)

A high-z Bullet-like Cluster?

The galaxies in "El Gordo" mostly lie in two distinct groups

The X-ray emission mostly lies between these two groups and shows a peculiar structure with a bright offset Gas Peak and Wake.

The offset peak is likely the core of one of the merging components; arrow indicates the approximate direction of merger.

The peak of the Galaxy distribution precedes the Gas Peak in the direction of the merger – a spatial separation like that seen in the Bullet Cluster.

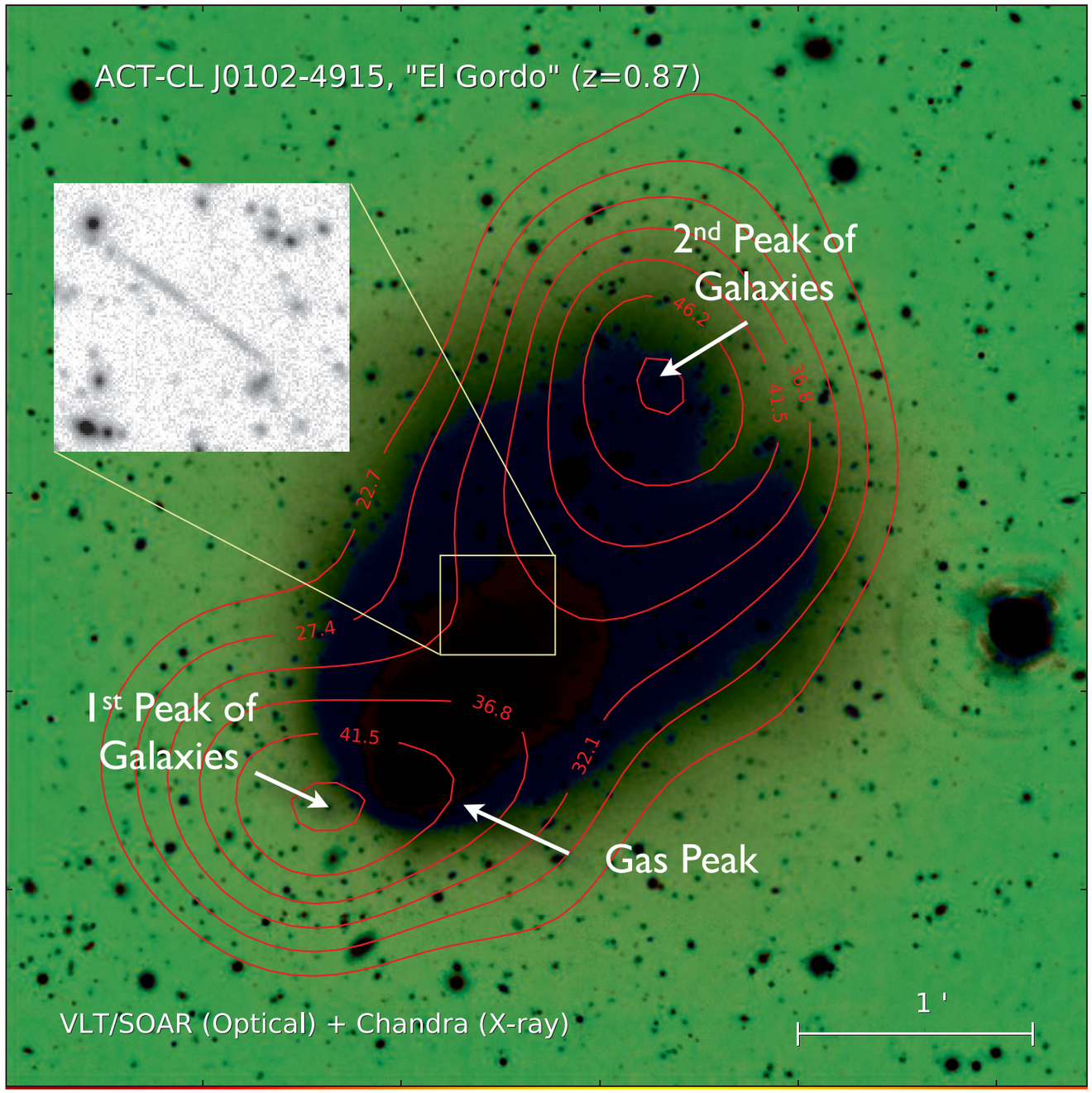

Menanteau et al. (2012, ApJ, 748,7)

A high-z Bullet-like Cluster?

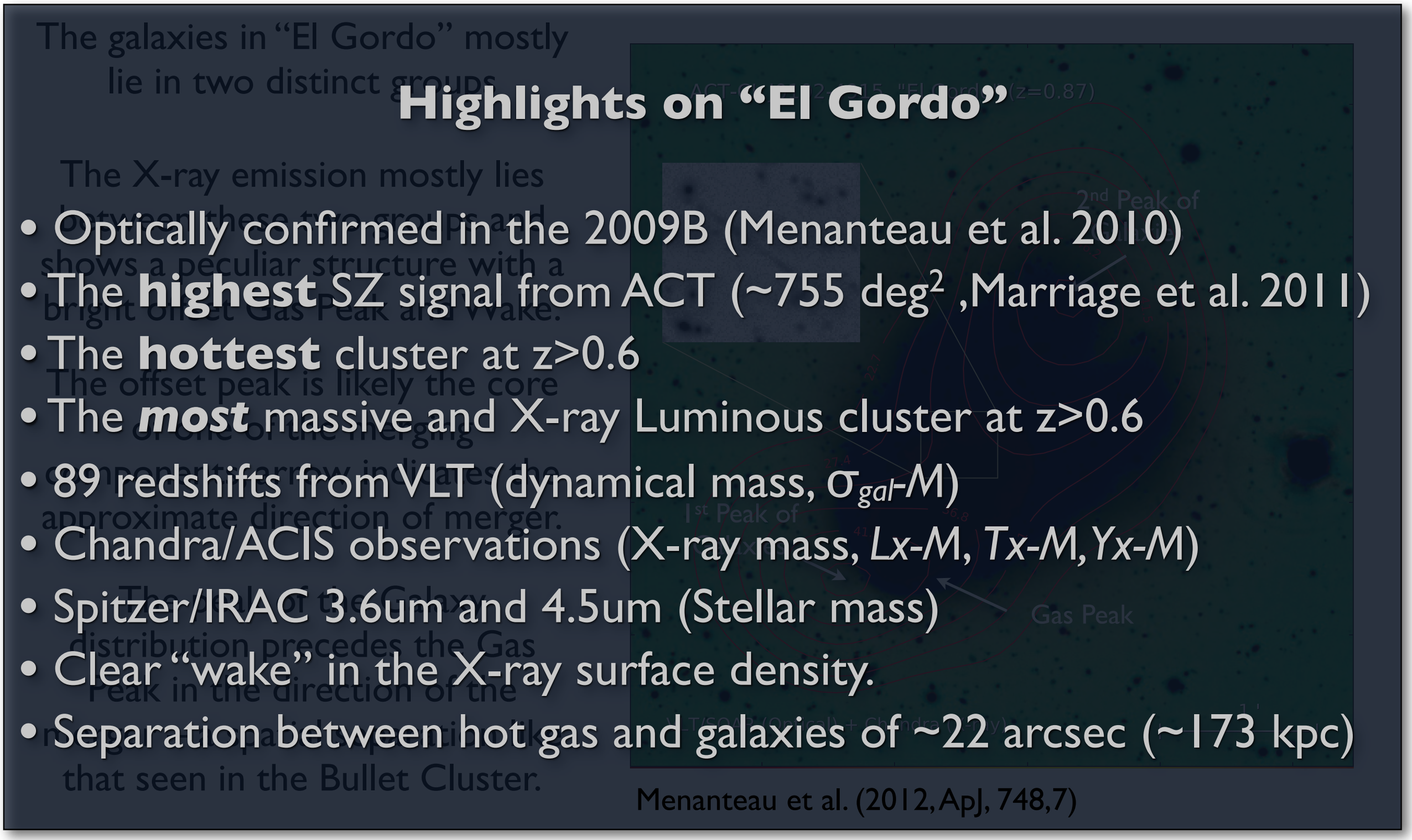

Highlights on "El Gordo"

- Optically confirmed in the 2009B (Menanteau et al. 2010)
- The **highest** SZ signal from ACT (~755 deg^2 ,Marriage et al. 2011)
- The **hottest** cluster at z>0.6
- The ***most*** massive and X-ray Luminous cluster at z>0.6
- 89 redshifts from VLT (dynamical mass, σ_{gal}-M)
- Chandra/ACIS observations (X-ray mass, *Lx-M*, *Tx-M*, *Yx-M*)
- Spitzer/IRAC 3.6um and 4.5um (Stellar mass)
- Clear "wake" in the X-ray surface density.
- Separation between hot gas and galaxies of ~22 arcsec (~173 kpc)

Menanteau et al. (2012, ApJ, 748,7)

“El Gordo” is Hot and Luminous!!

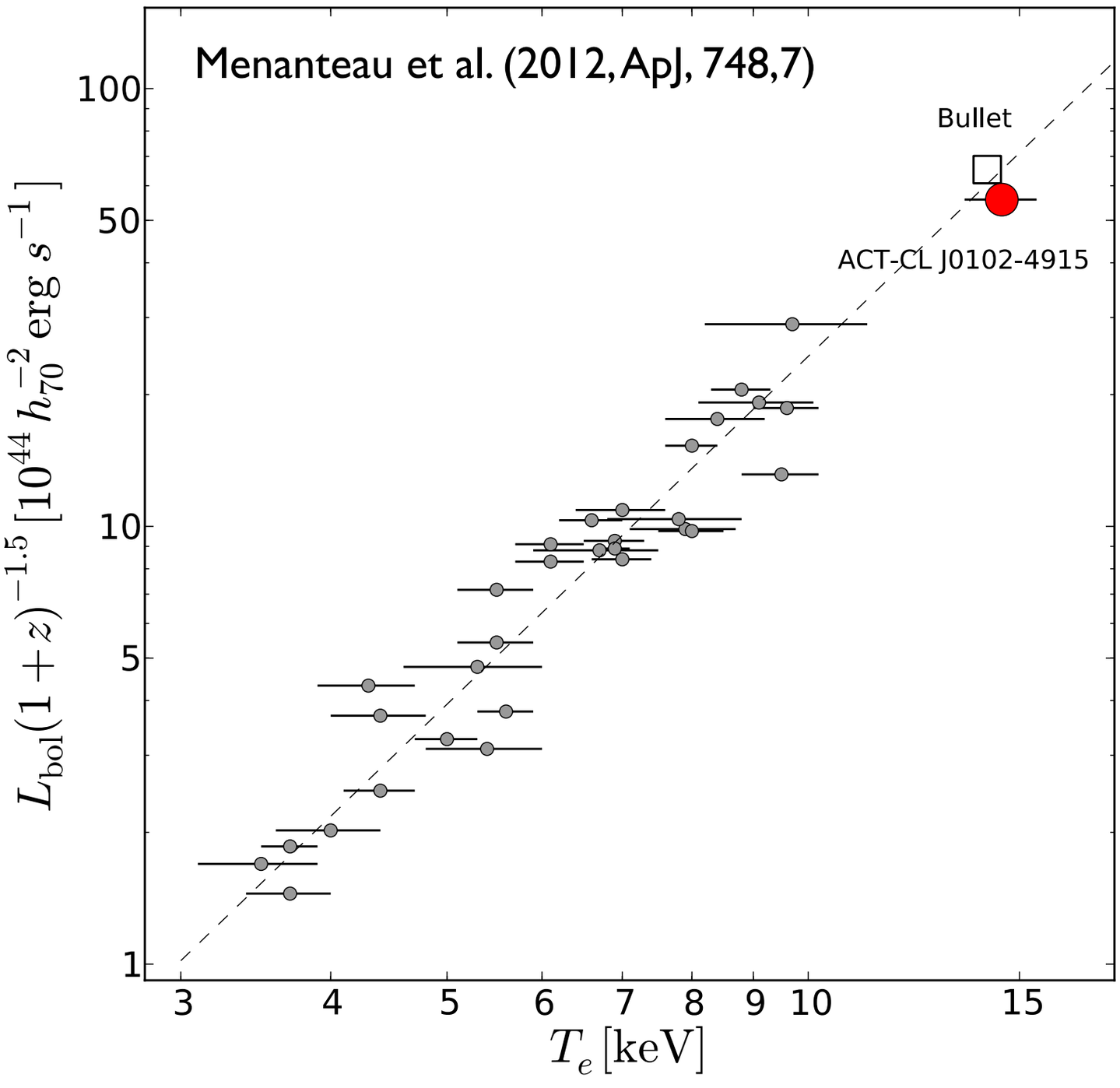

Compared with Markevitch et al. (1998)

Core-excised Integrated spectrum

$$kT = 14.5 \pm 0.1 \text{ keV}$$
$$L_X = 2.19 \times 10^{45} \text{ erg s}^{-1}$$
$$L_{\mathrm{bol}} = 1.36 \times 10^{46} \text{ erg s}^{-1}$$

Combined measurements for the Most Massive Cluster at z>0.6

Combined measurements for the Most Massive Cluster at z>0.6

- VLT FORS2 (10hrs), redshifts for 89 members:

$$z = 0.8701 \pm 0.0001$$

$$\sigma_{\rm gal} = 1321 \pm 106 \ {\rm km \ s^{-1}}$$

$$M_{200,{\rm dyn}} = 1.86^{+0.54}_{-0.49} \times 10^{15} \, h_{70}^{-1} \, M_{\odot}$$

Evrard et al. (2008)

Combined measurements for the Most Massive Cluster at z>0.6

- VLT FORS2 (10hrs), redshifts for 89 members:

$$z = 0.8701 \pm 0.0001$$
$$\sigma_{\rm gal} = 1321 \pm 106 \ {\rm km \ s^{-1}}$$
$$M_{200,{\rm dyn}} = 1.86^{+0.54}_{-0.49} \times 10^{15} \, h_{70}^{-1} \, M_\odot$$

Evrard et al. (2008)

- *Chandra*/ACIS (60 ks exposure):

$$T_X = 14.5 \pm 1.0 \ {\rm keV}; f_{\rm gas} = 0.133$$

Kravtsov, Vikhlinin & Nagai (2006)
Vikhlinin et al. (2009)

$$M_{200,Y_X} = 2.88^{+0.78}_{-0.55} \times 10^{15} \, h_{70}^{-1} \, M_\odot$$

Combined measurements for the Most Massive Cluster at z>0.6

- VLT FORS2 (10hrs), redshifts for 89 members:

$$z = 0.8701 \pm 0.0001$$
$$\sigma_{\rm gal} = 1321 \pm 106 \ {\rm km \ s^{-1}}$$
$$M_{200,{\rm dyn}} = 1.86^{+0.54}_{-0.49} \times 10^{15} \, h_{70}^{-1} \, M_{\odot}$$

Evrard et al. (2008)

- *Chandra*/ACIS (60 ks exposure):

$$T_X = 14.5 \pm 1.0 \ {\rm keV}; f_{\rm gas} = 0.133$$

Kravtsov, Vikhlinin & Nagai (2006)
Vikhlinin et al. (2009)

$$M_{200,Y_X} = 2.88^{+0.78}_{-0.55} \times 10^{15} \, h_{70}^{-1} \, M_{\odot}$$

- ACT/SZ decrement, yT_{CMB} - *Mass*

$$yT_{\rm CMB} = 490 \pm 60 \mu K$$
$$M_{200,{\rm SZ}} = 1.64^{+0.62}_{-0.42} \times 10^{15} \, h_{70}^{-1} M_{\odot}$$

Sehgal et al. (2011)

Combined measurements for the Most Massive Cluster at z>0.6

- VLT FORS2 (10hrs), redshifts for 89 members:

$$z = 0.8701 \pm 0.0001$$
$$\sigma_{\rm gal} = 1321 \pm 106 \ {\rm km \ s^{-1}}$$
$$M_{200,\rm dyn} = 1.86^{+0.54}_{-0.49} \times 10^{15} \, h_{70}^{-1} \, M_\odot$$

Evrard et al. (2008)

- *Chandra*/ACIS (60 ks exposure):

$$T_X = 14.5 \pm 1.0 \ {\rm keV}; f_{\rm gas} = 0.133$$

Kravtsov, Vikhlinin & Nagai (2006)
Vikhlinin et al. (2009)

$$M_{200,Y_X} = 2.88^{+0.78}_{-0.55} \times 10^{15} \, h_{70}^{-1} \, M_\odot$$

- ACT/SZ decrement, yT_{CMB} - *Mass*

$$yT_{\rm CMB} = 490 \pm 60 \mu K$$
$$M_{200,\rm SZ} = 1.64^{+0.62}_{-0.42} \times 10^{15} \, h_{70}^{-1} M_\odot$$

Sehgal et al. (2011)

- Combined (χ^2 combined) optical+X-ray+SZ:

$$M_{200} = (2.16 \pm 0.32) \times 10^{15} \, h_{70}^{-1} M_\odot$$

Combined measurements for the Most Massive Cluster at z>0.6

- VLT FORS2 (10hrs), redshifts for 89 members:

$$z = 0.8701 \pm 0.0001$$
$$\sigma_{\rm gal} = 1321 \pm 106 \ {\rm km \ s^{-1}}$$
$$M_{200,{\rm dyn}} = 1.86^{+0.54}_{-0.49} \times 10^{15} \, h_{70}^{-1} \, M_\odot$$

Evrard et al. (2008)

- *Chandra*/ACIS (60 ks exposure):

$$T_X = 14.5 \pm 1.0 \ {\rm keV}; f_{\rm gas} = 0.133$$ Kravtsov, Vikhlinin & Nagai (2006)
Vikhlinin et al. (2009)

$$M_{200,Y_X} = 2.88^{+0.78}_{-0.55} \times 10^{15} \, h_{70}^{-1} \, M_\odot$$

- ACT/SZ decrement, yT_{CMB} - *Mass*

$$yT_{\rm CMB} = 490 \pm 60 \mu K$$
$$M_{200,{\rm SZ}} = 1.64^{+0.62}_{-0.42} \times 10^{15} \, h_{70}^{-1} M_\odot$$

CL J1226+3332 (z=0.89)
$M_{200} = (1.38 \pm 0.20) \times 10^{15} \, h_{70}^{-1} \, M_\odot$

SPT-CL J2106-5844 (z=1.14)
$M_{200} = (1.27 \pm 0.21) \times 10^{15} \, h_{70}^{-1} \, M_\odot$

- Combined (χ^2 combined) optical+X-ray+SZ:

$$M_{200} = (2.16 \pm 0.32) \times 10^{15} \, h_{70}^{-1} M_\odot$$

Rarity of "El Gordo" (Based on its exceptional mass)

- Combined Mass from optical +X-ray+SZ:

$$M_{200} = (2.16 \pm 0.32) \times 10^{15}\, h_{70}^{-1} M_\odot$$

- Area of survey:

  ACT: 755 deg^2

  ACT+SPT: 2800 deg^2

- Mortonson et al. (2011) exclusion curves for ΛCDM and quintenssence parameter distribution.

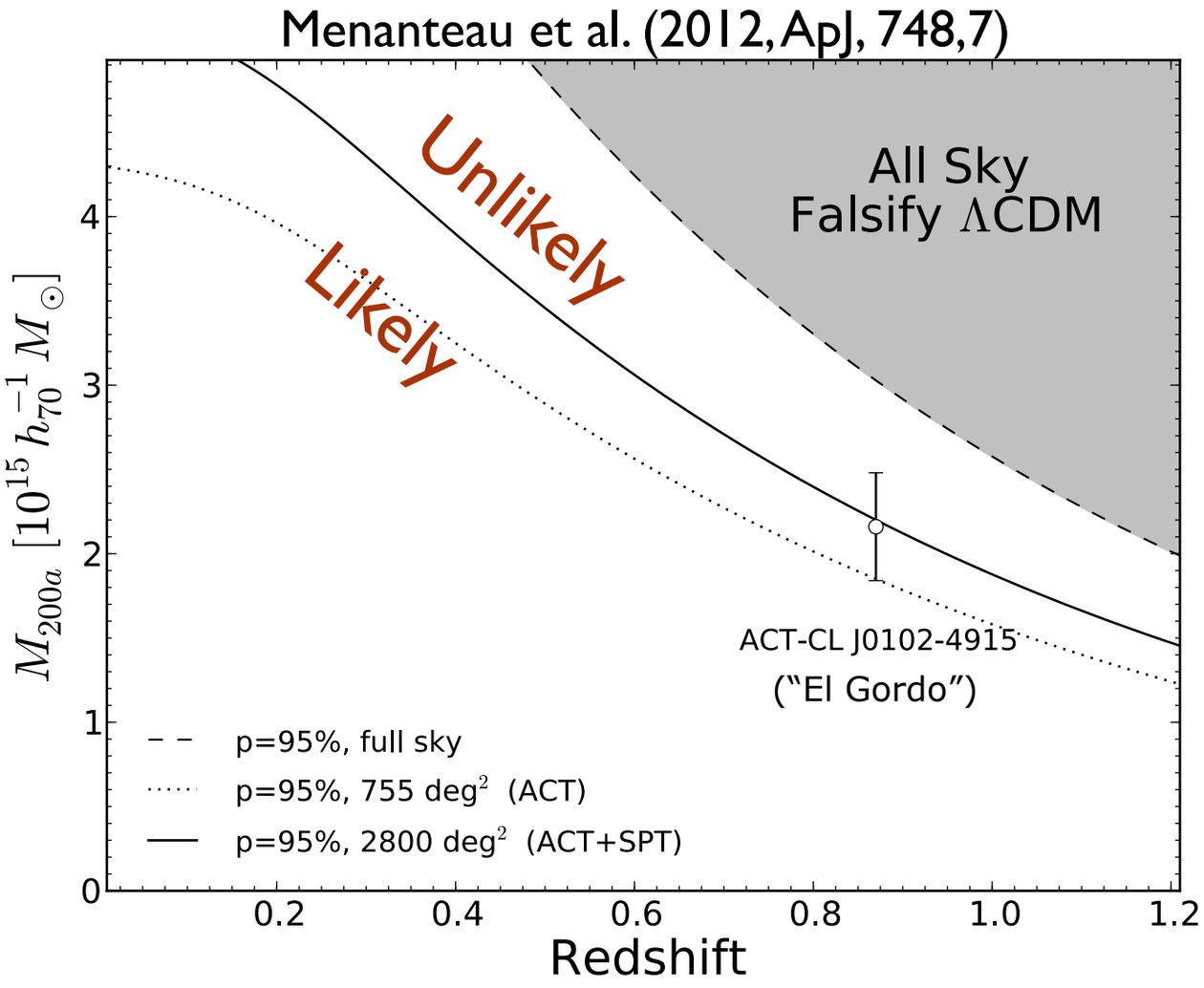

- Cluster is very unlikely in the ACT survey area alone (3σ), but still allowed in the ACT+SPT sky region if its mass is 1-σ or more below the nominal mass.

"El Gordo," *Chandra* Imaging

Menanteau et al. (2012, ApJ, 748,7)

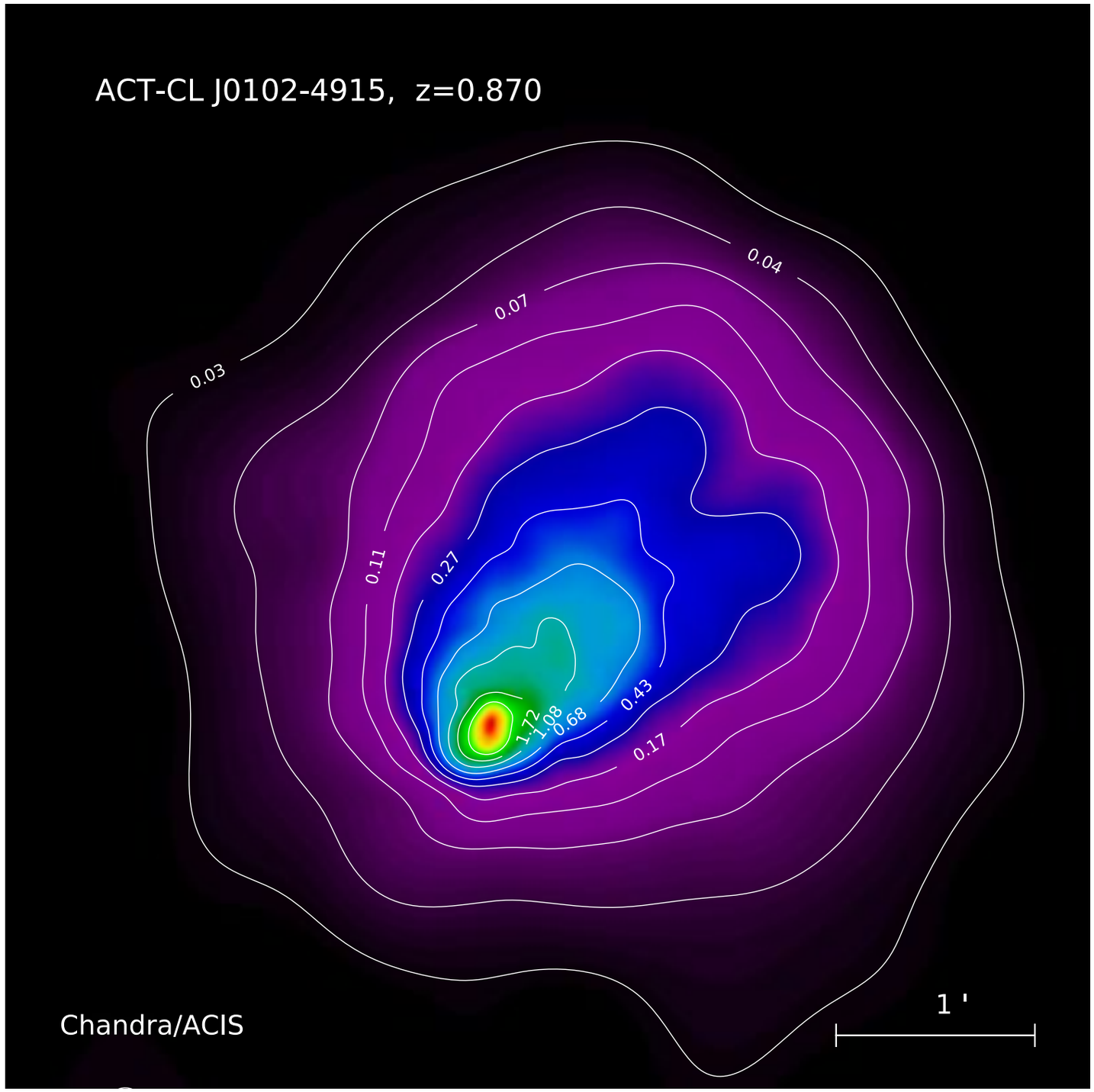

"El Gordo," *Chandra* Imaging

Menanteau et al. (2012, ApJ, 748,7)

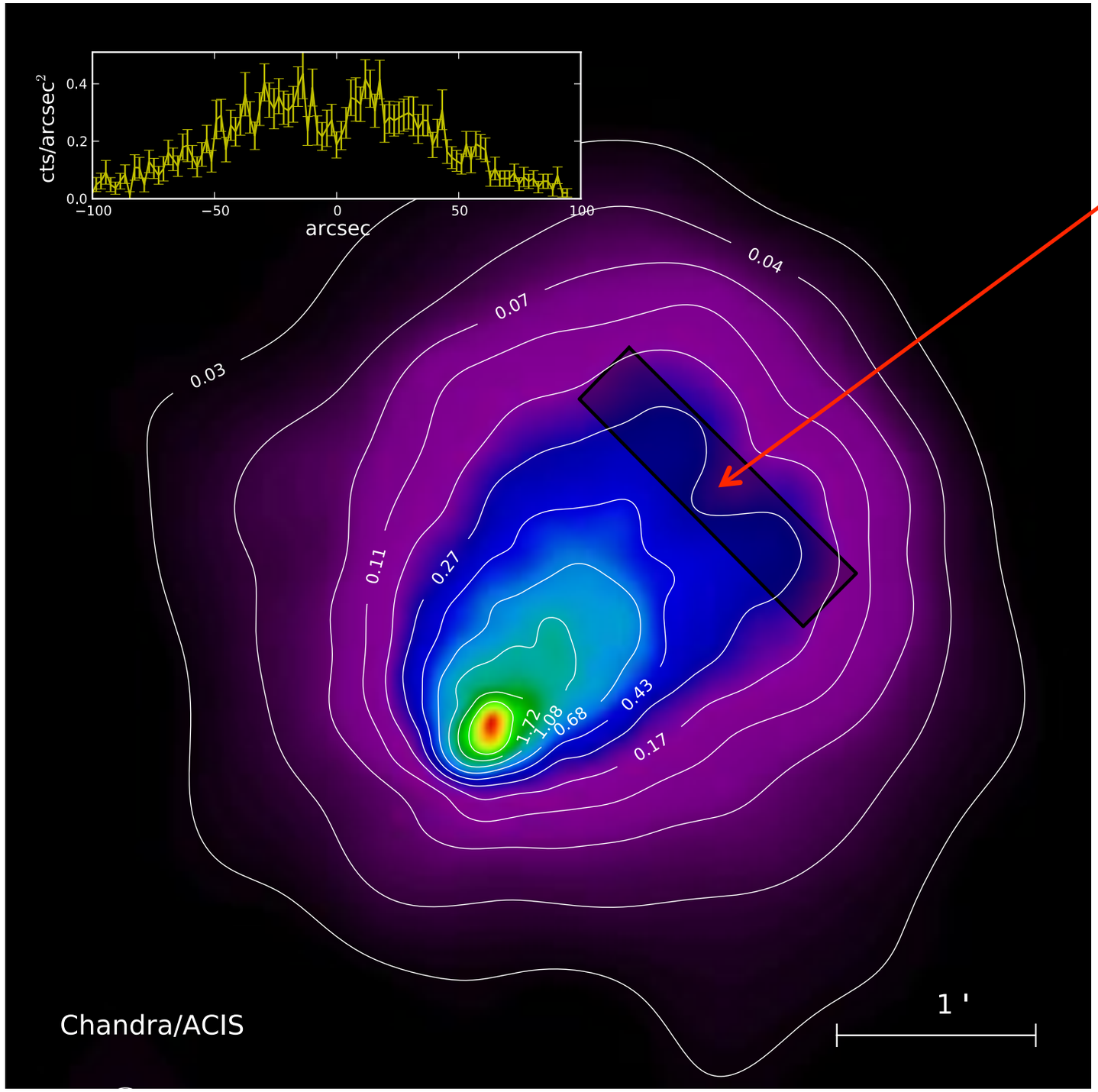

Wake! Cometary shape (even 2 tails!) 20-40% surface brightness suppression ≈35"x60"

“El Gordo,” *Chandra* Imaging

Menanteau et al. (2012, ApJ, 748,7)

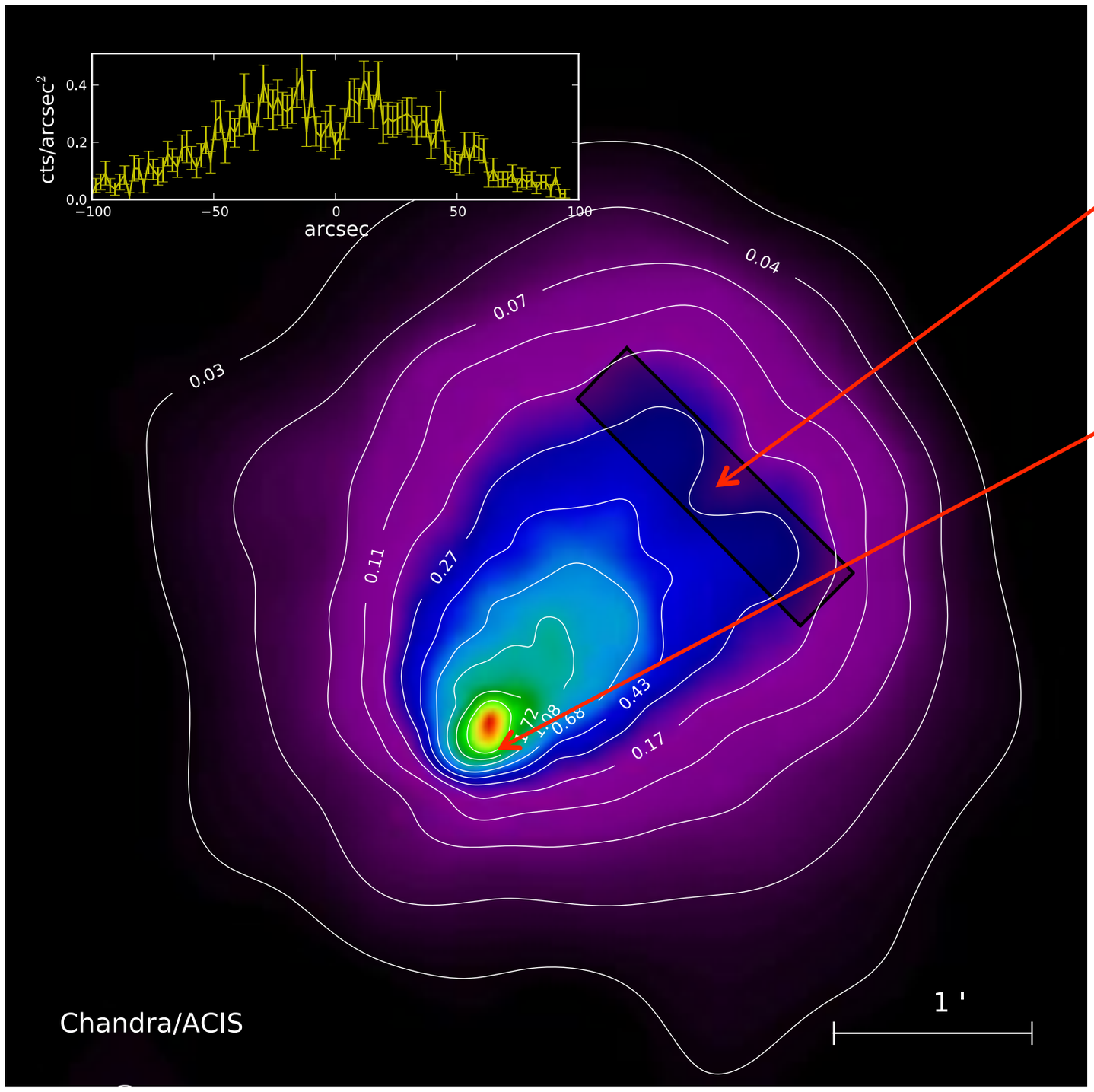

Wake! Cometary shape (even 2 tails!) 20-40% surface brightness suppression ≈35”x60”

Low entropy, bright, offset peak

"El Gordo," *Chandra* Imaging

Menanteau et al. (2012, ApJ, 748,7)

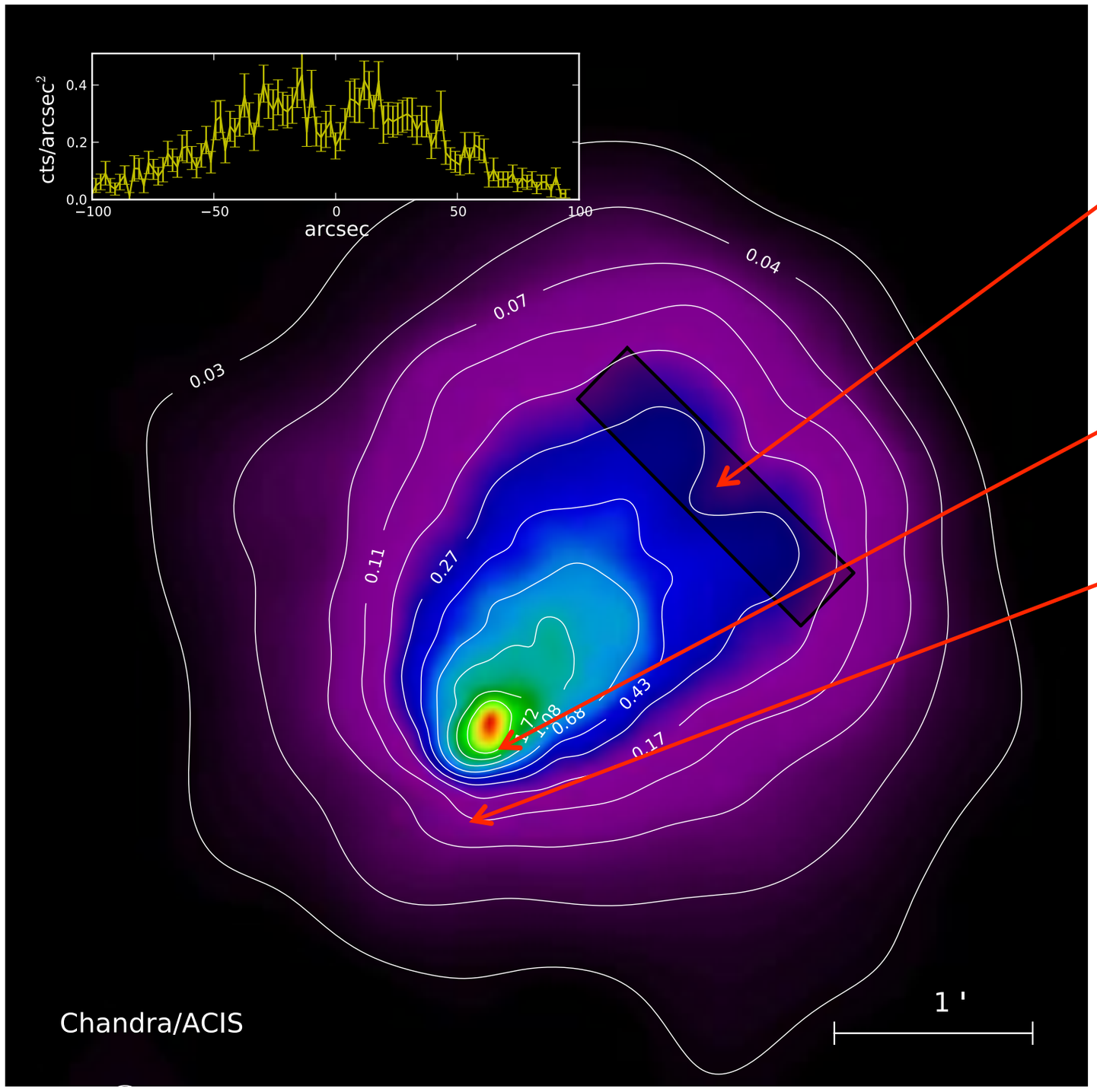

Wake! Cometary shape (even 2 tails!) 20-40% surface brightness suppression ≈35"x60"

Low entropy, bright, offset peak

Steep brightness gradient

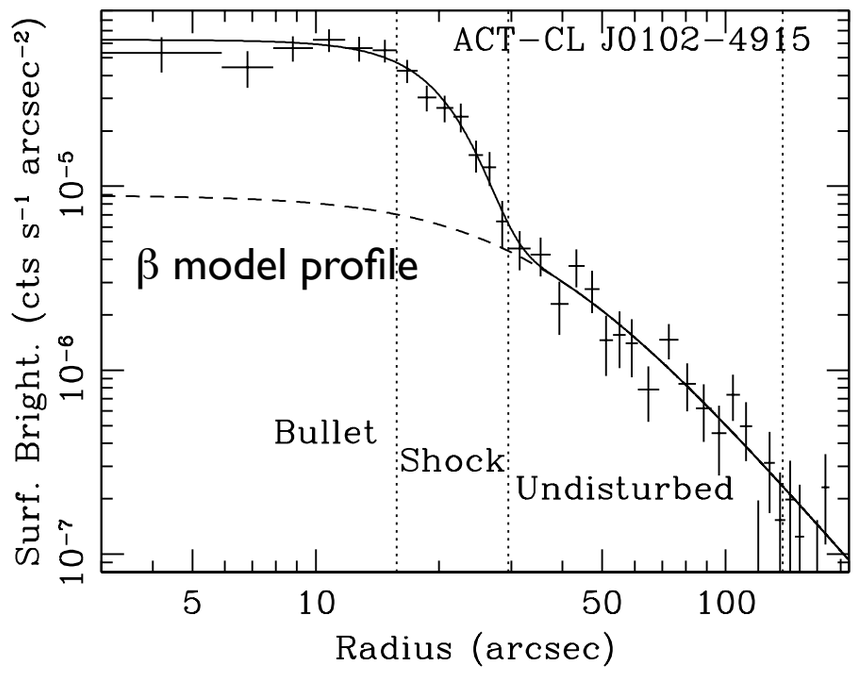

Chandra Spectro-Imaging Analysis

Menanteau et al. (2012, ApJ, 748,7)

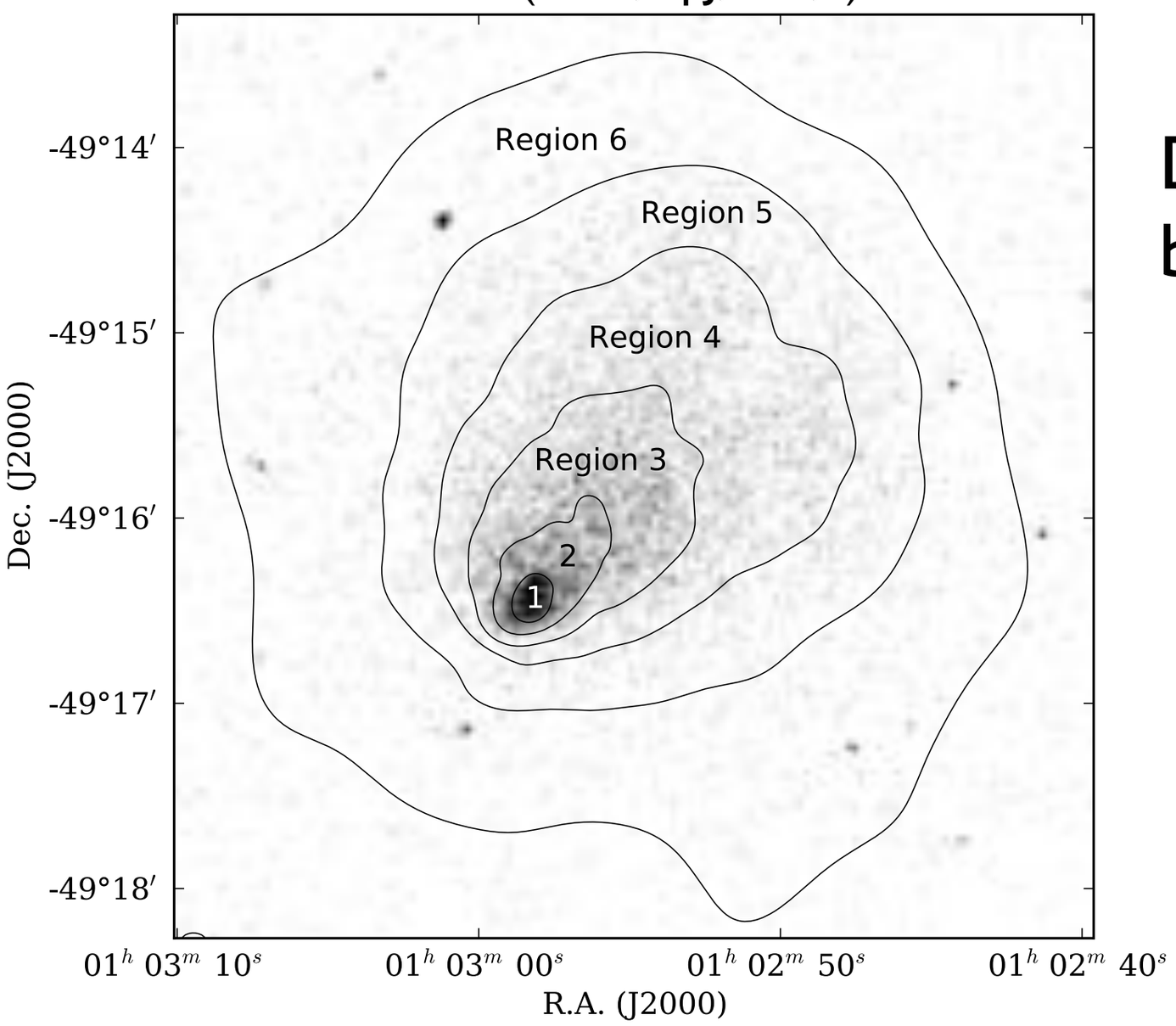

Divide cluster in six regions based on surface brightness

Region 1 : 1000 cts
Region 4 : 4300 cts
Others : 2000 – 3600 cts

Chandra Spectro-Imaging Analysis

Menanteau et al. (2012, ApJ, 748,7)

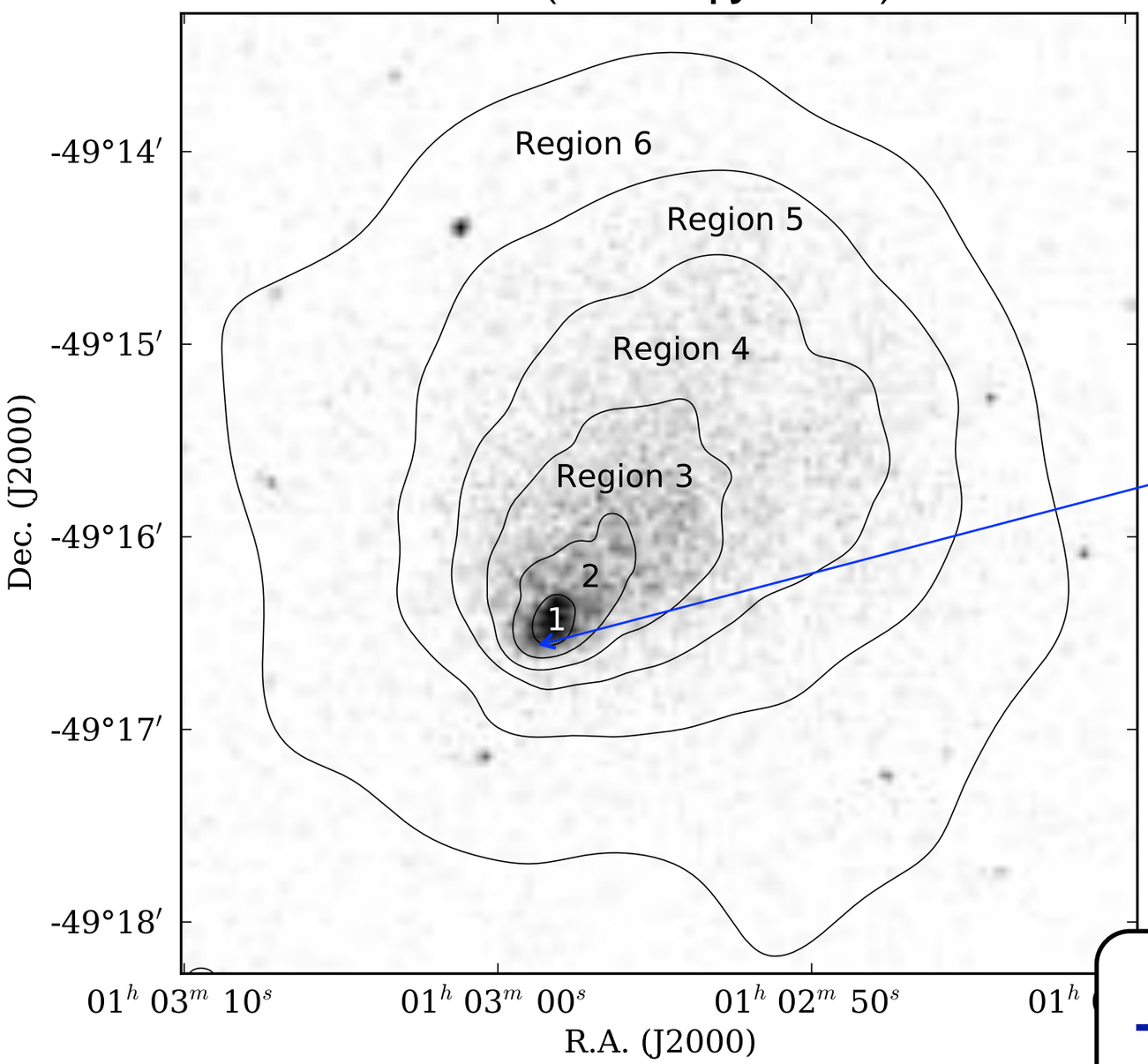

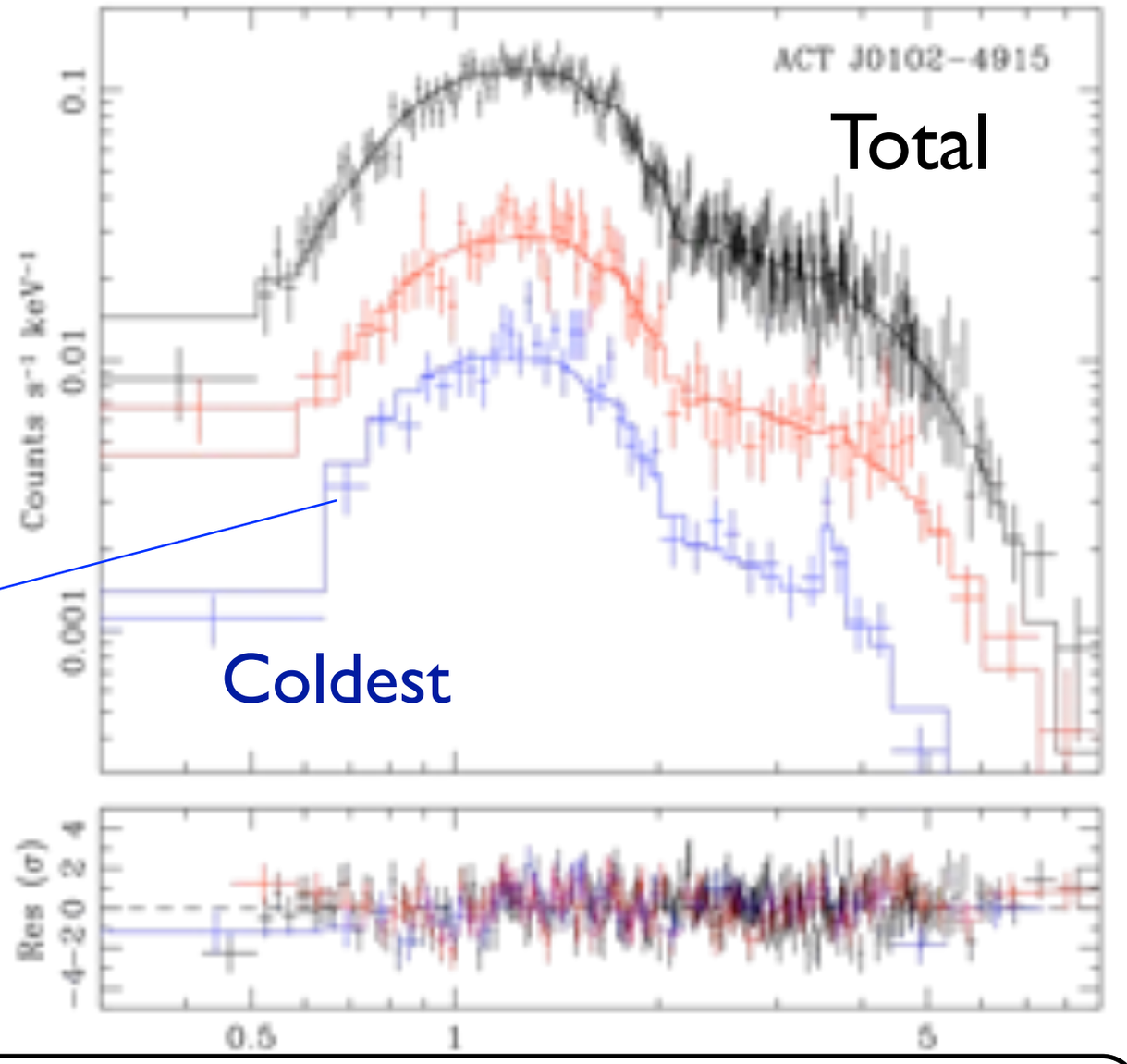

- X-ray peak is cold (kT=6.6±0.7 keV)
- Highest Fe abundance (Z=0.57±0.20)
- low entropy bullet, i.e., the cool core of a merging cluster

Felipe Menanteau

Chandra Spectro-Imaging Analysis

Menanteau et al. (2012, ApJ, 748,7)

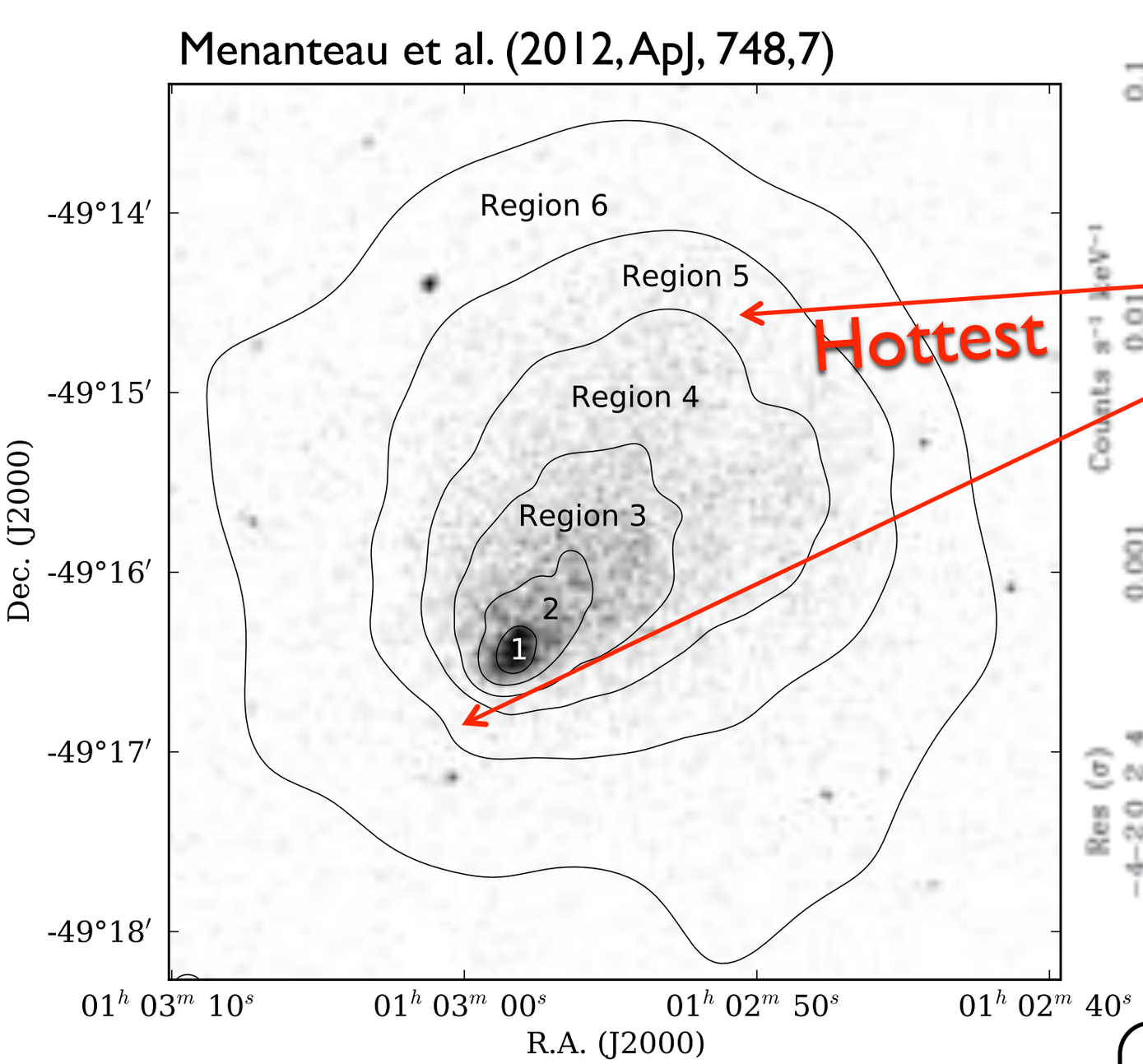

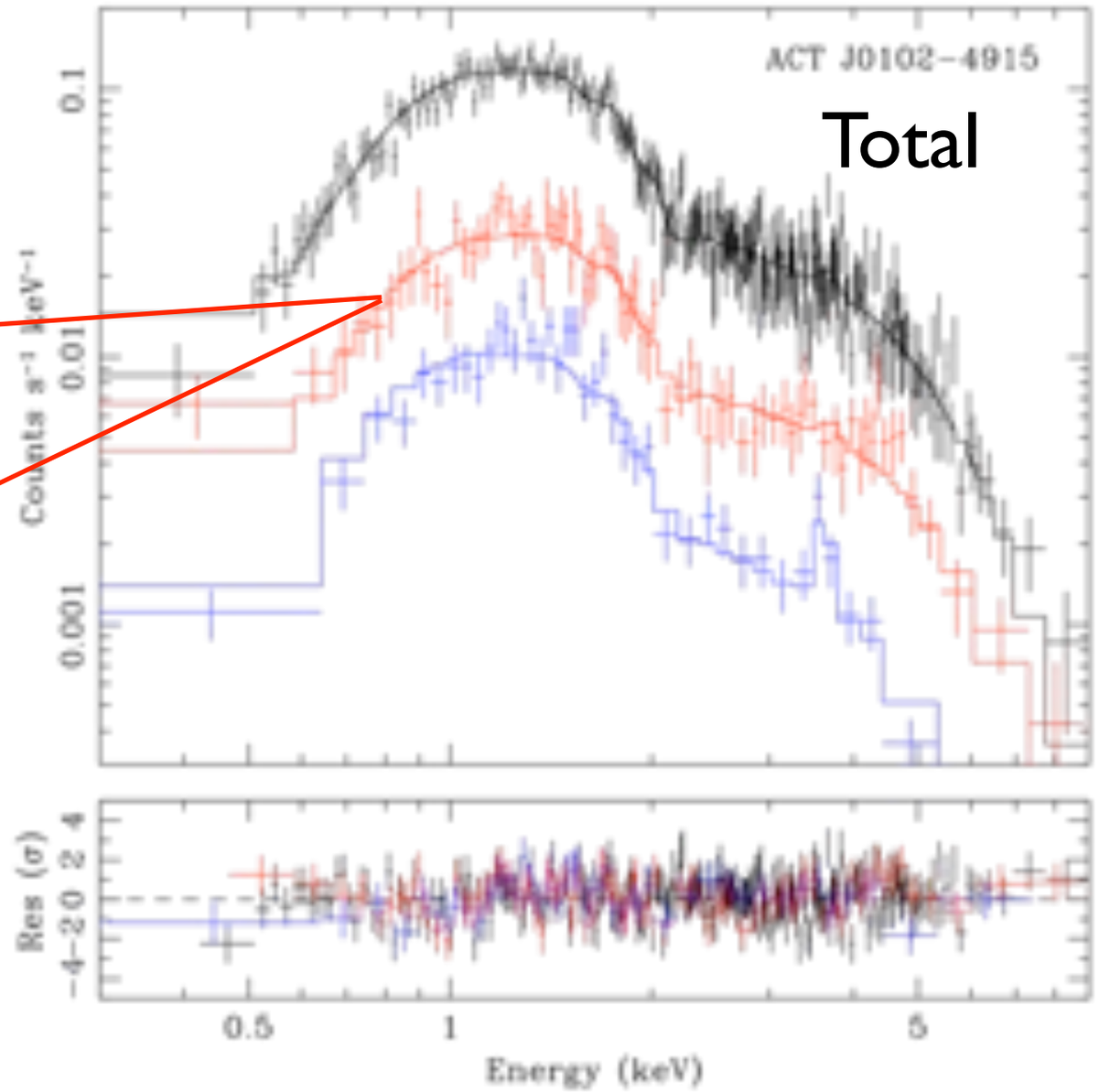

Hottest region is kT=22(+6,-5) keV (source frame) – shock heating?

Chandra Spectro-Imaging Analysis

Menanteau et al. (2012, ApJ, 748,7)

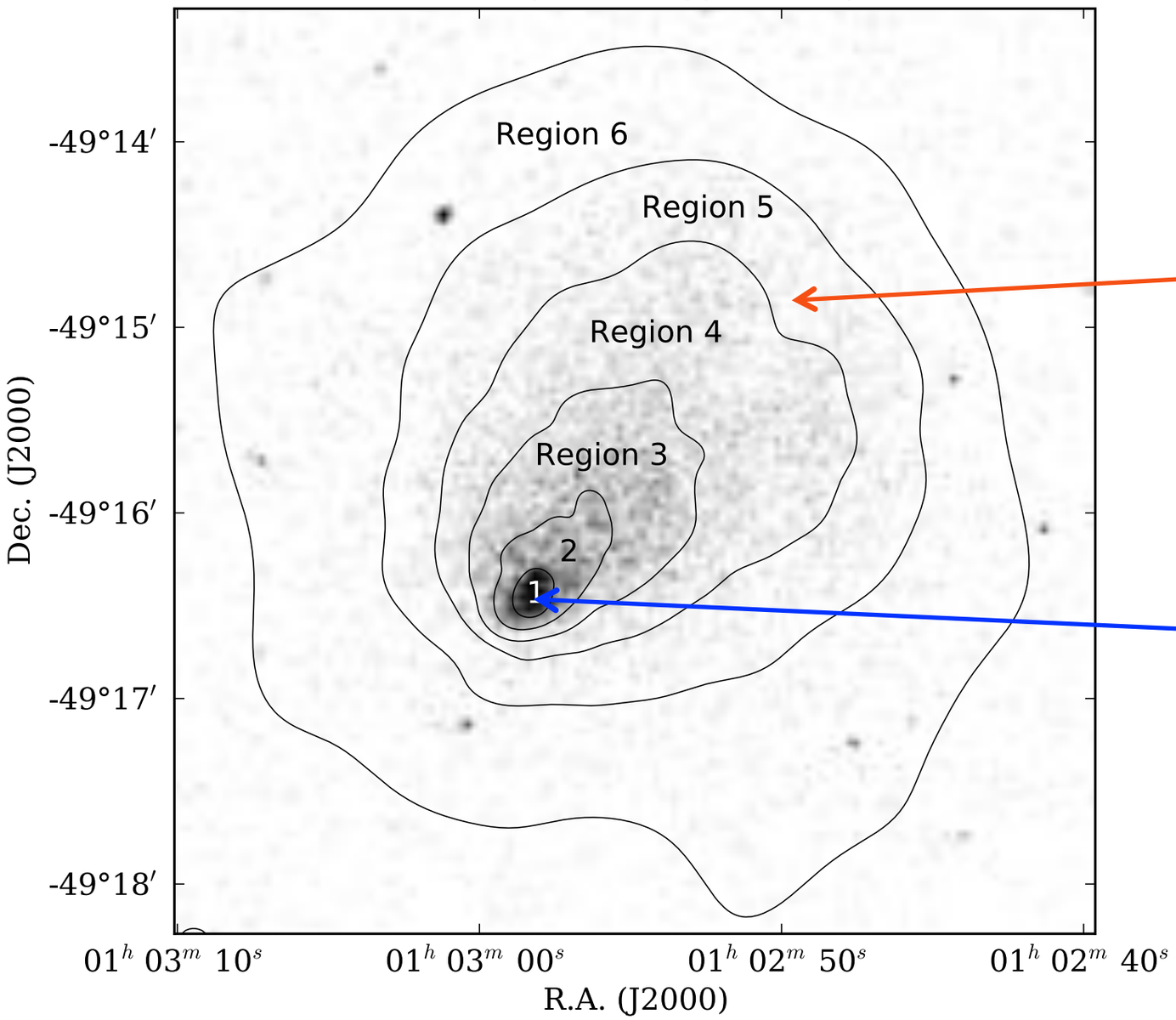

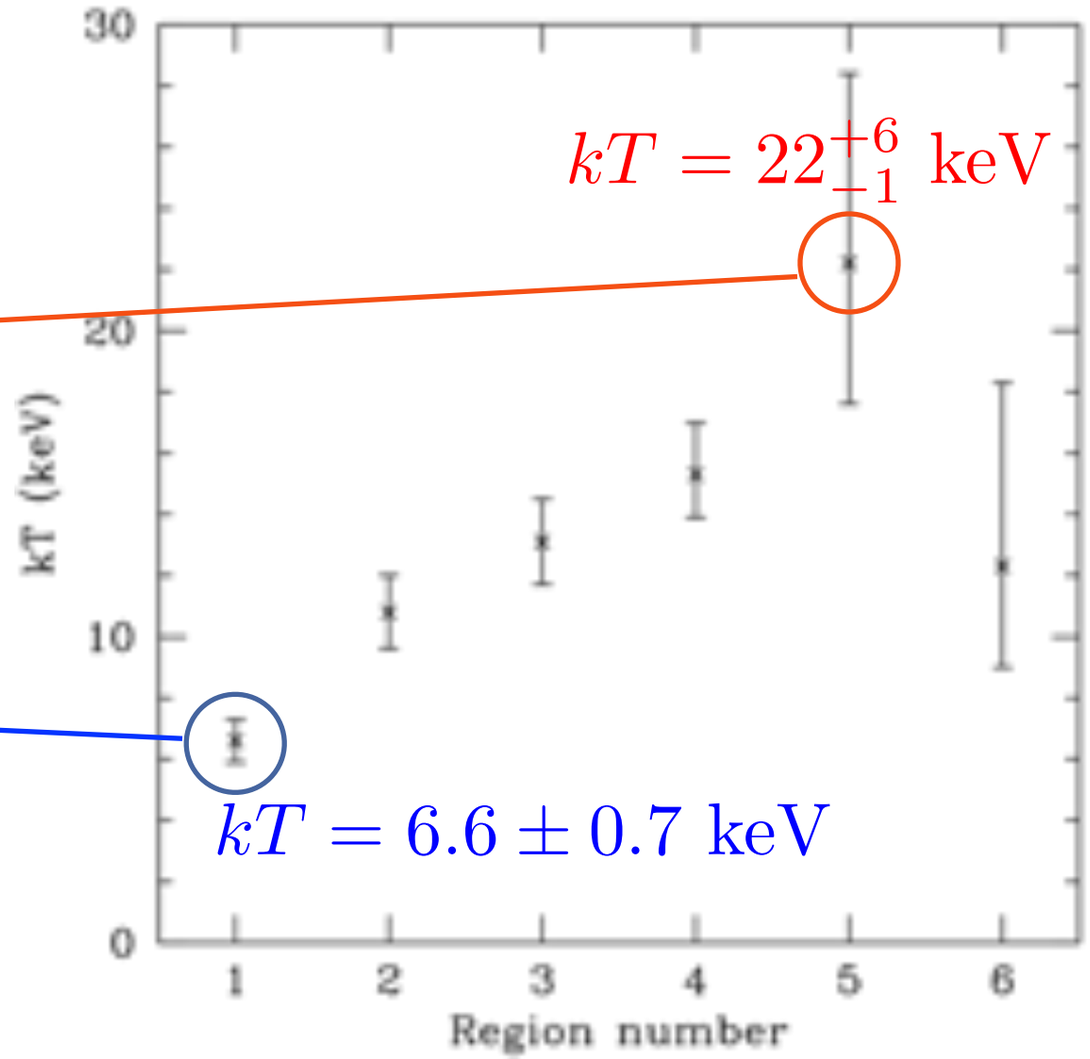

Merger Structure of "El Gordo"

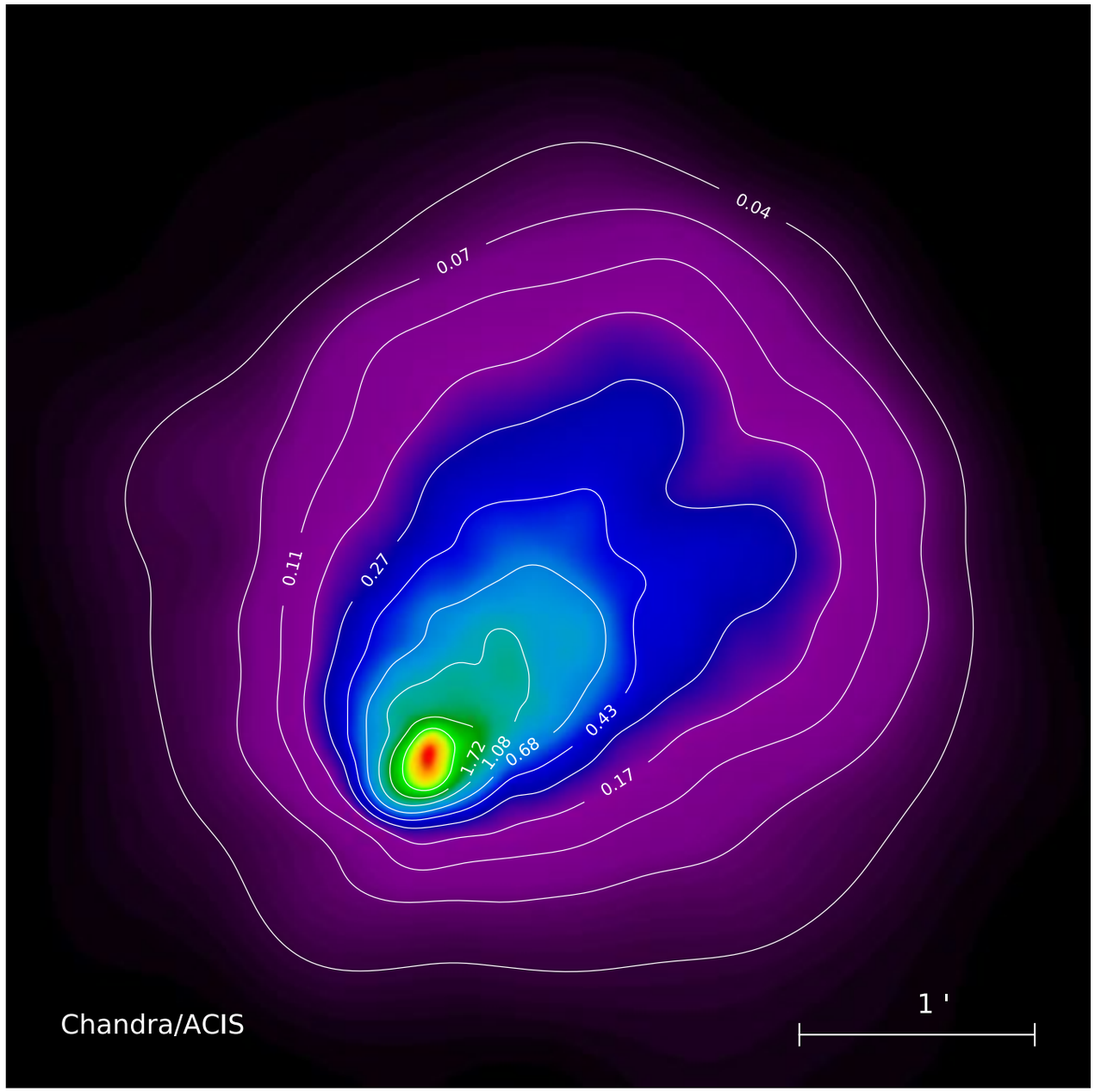

Menanteau et al. (2012, ApJ, 748,7)

Merger Structure of “El Gordo”

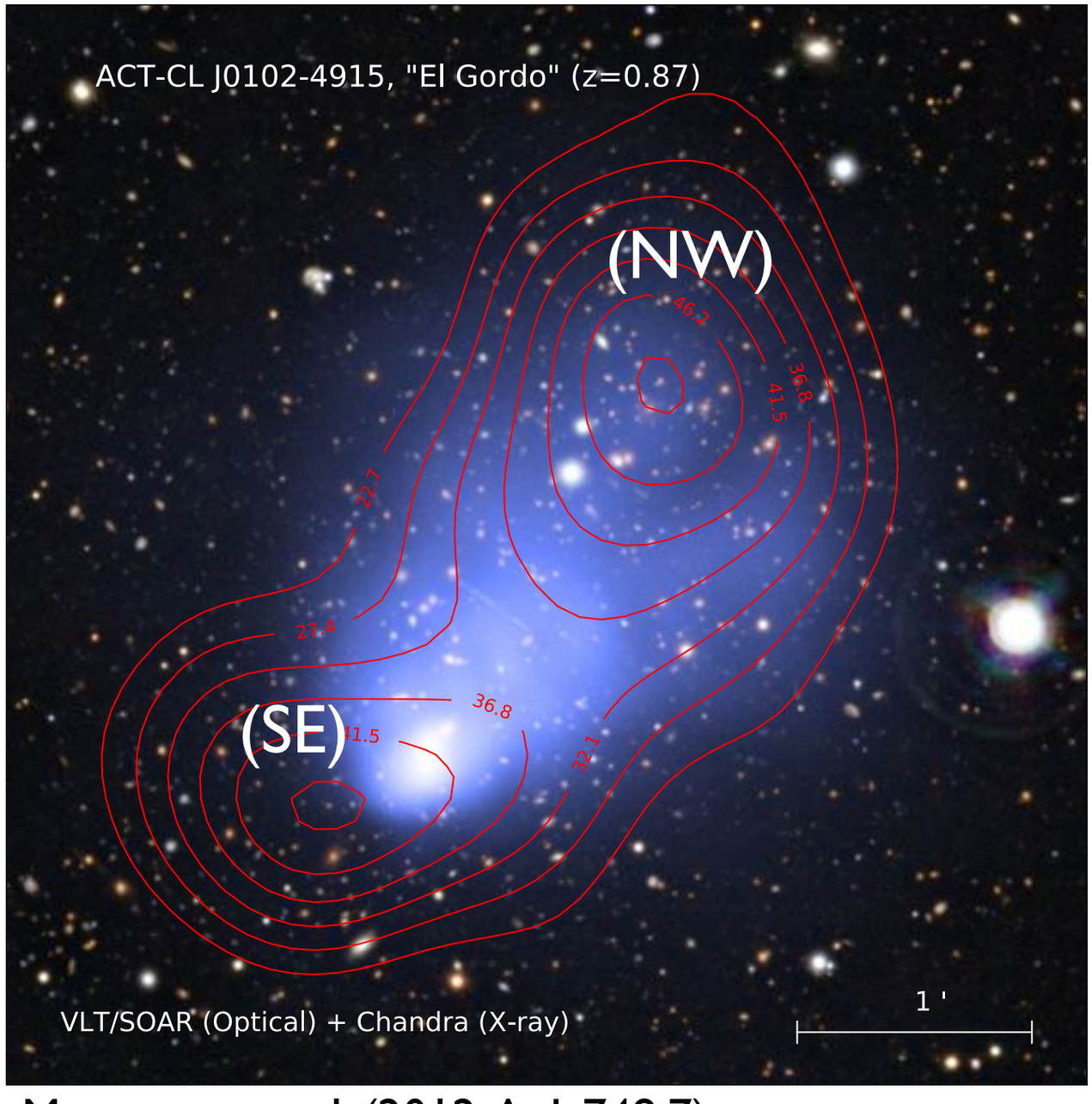

Menanteau et al. (2012, ApJ, 748,7)

Merger Structure of "El Gordo"

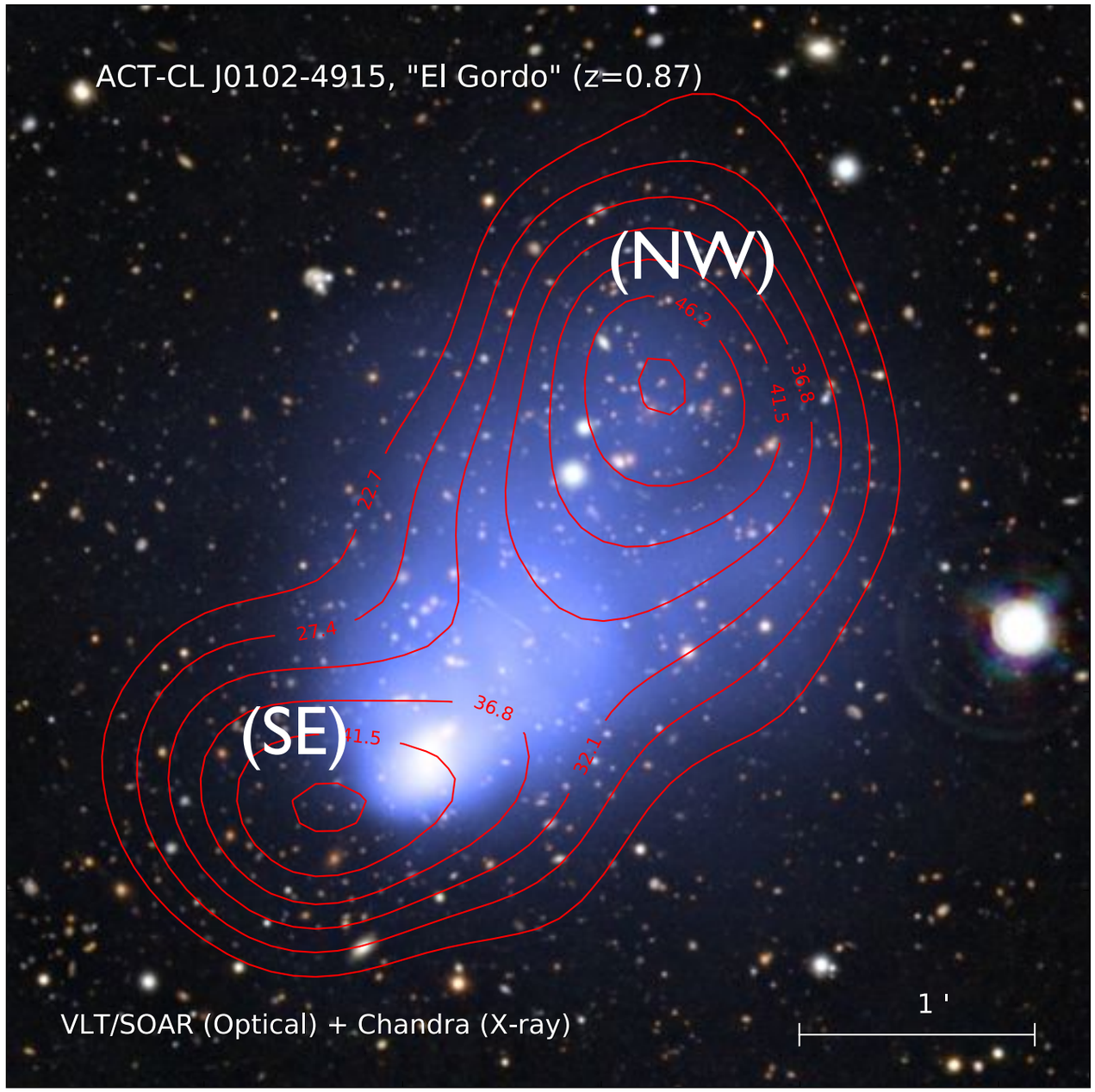

Menanteau et al. (2012, ApJ, 748,7)

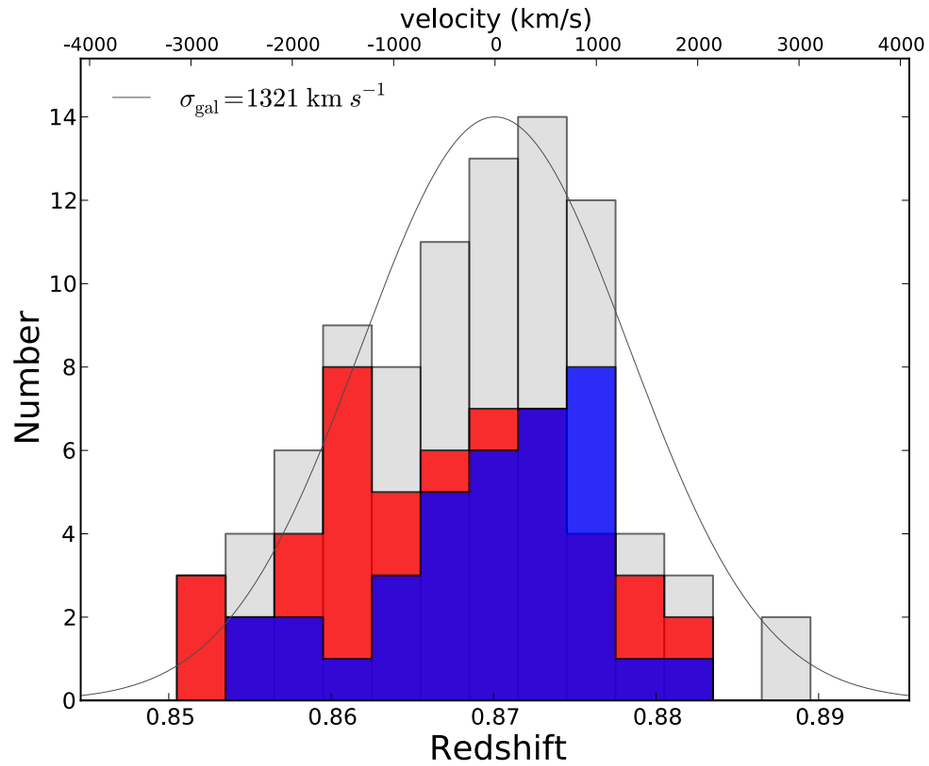

$$M_{200} = 1.76^{+0.62}_{-0.58} \times 10^{15}\, h_{70}^{-1} M_{\odot}(\mathrm{NW})$$

$$M_{200} = 1.06^{+0.64}_{-0.59} \times 10^{15}\, h_{70}^{-1} M_{\odot}(\mathrm{SE})$$

Mass ratio ~ 2 to 1

No such high-z mergers find in current large N-body Simulations (Cube3pm)

Merger Structure of "El Gordo"

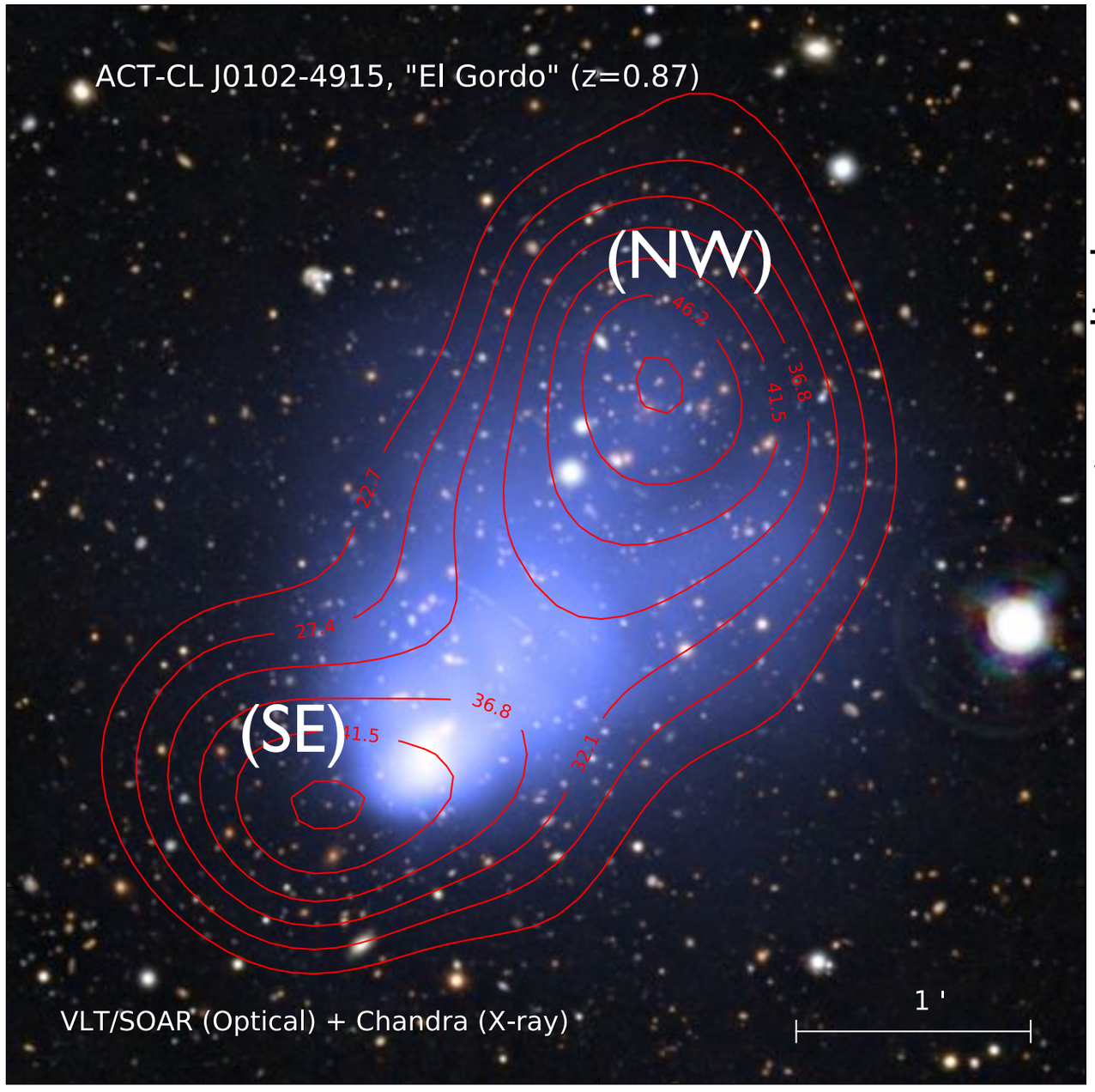

Menanteau et al. (2012, ApJ, 748,7)

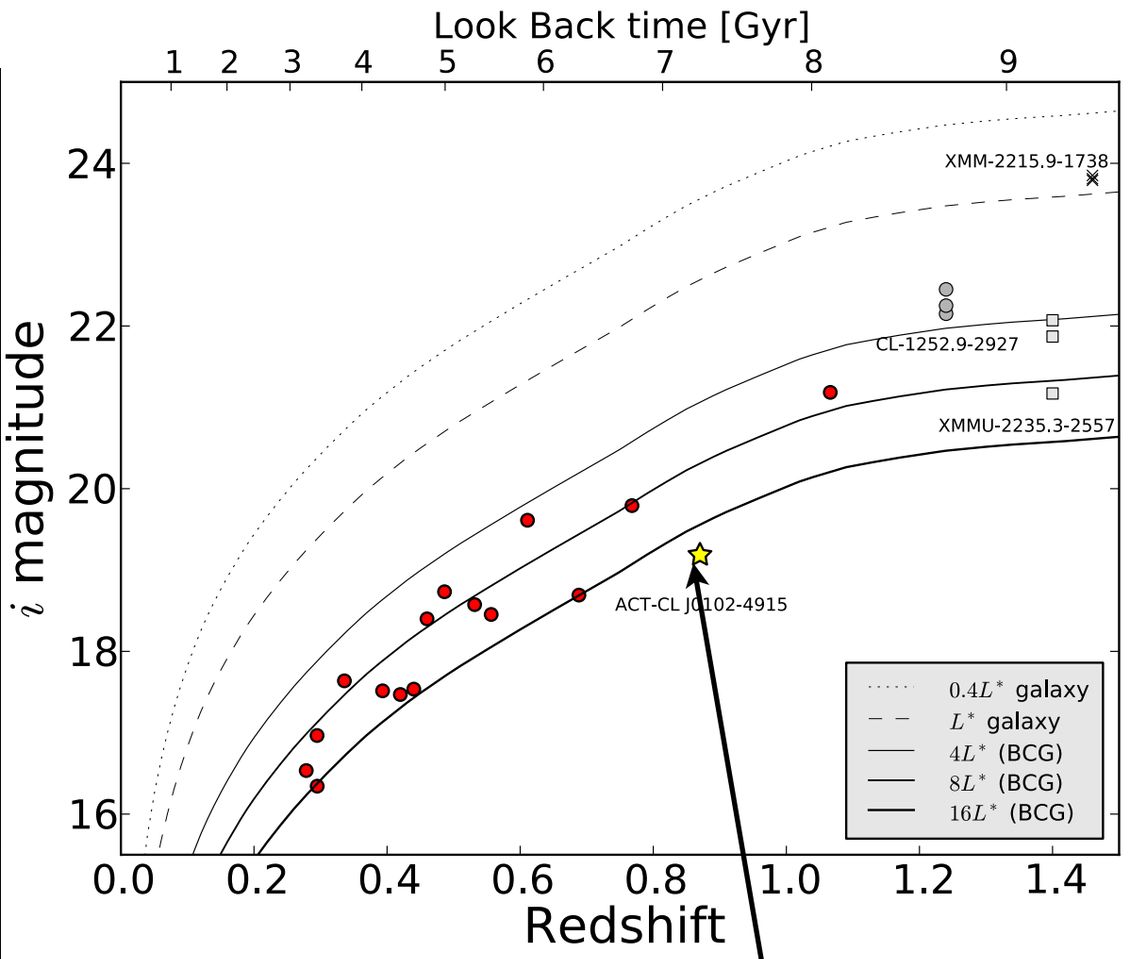

Very luminous BCG

Color-magnitude for “El Gordo”

Optical colors

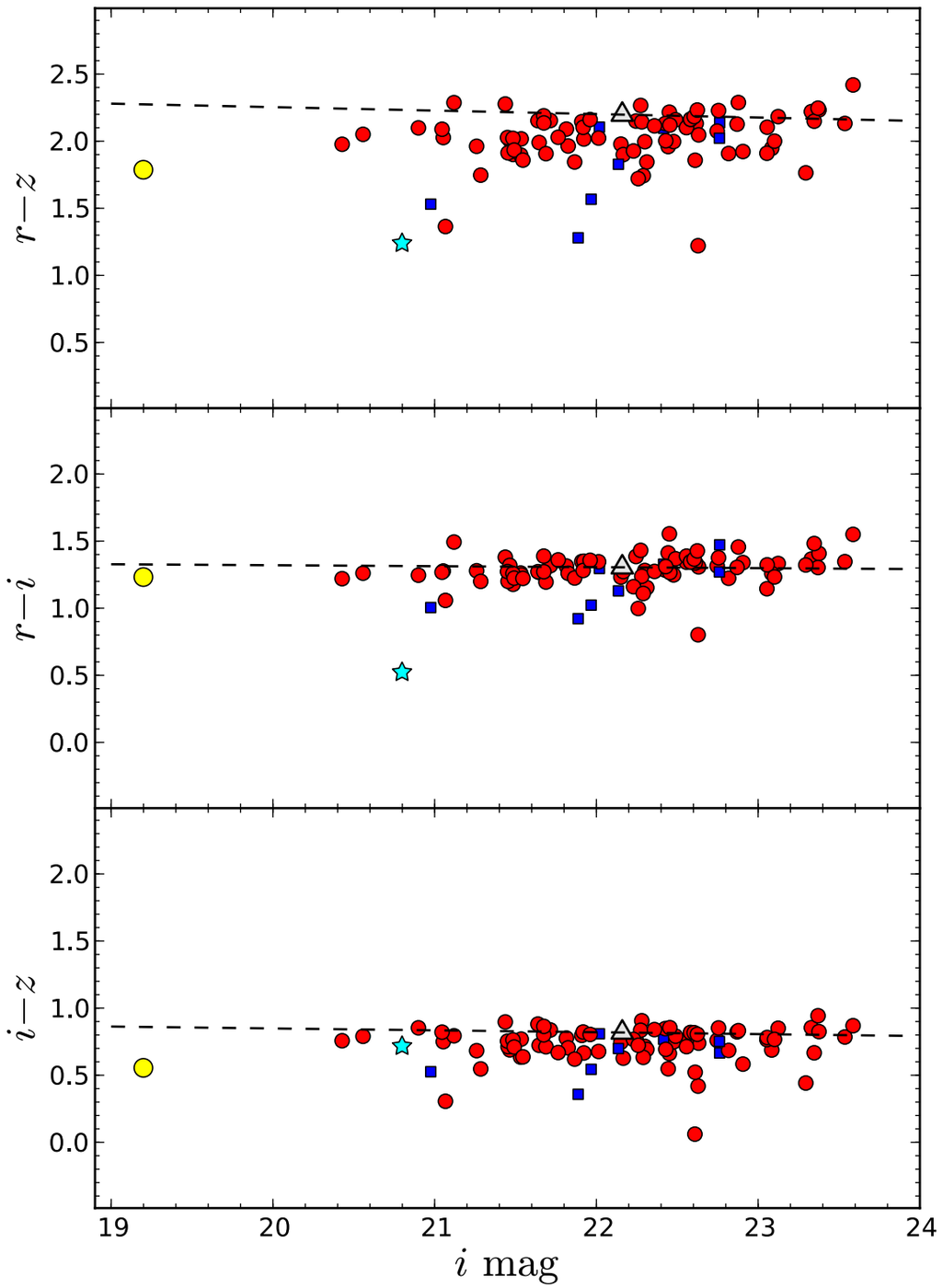

Menanteau et al. (2012, ApJ, 748,7)

Color-magnitude for "El Gordo"

Optical colors

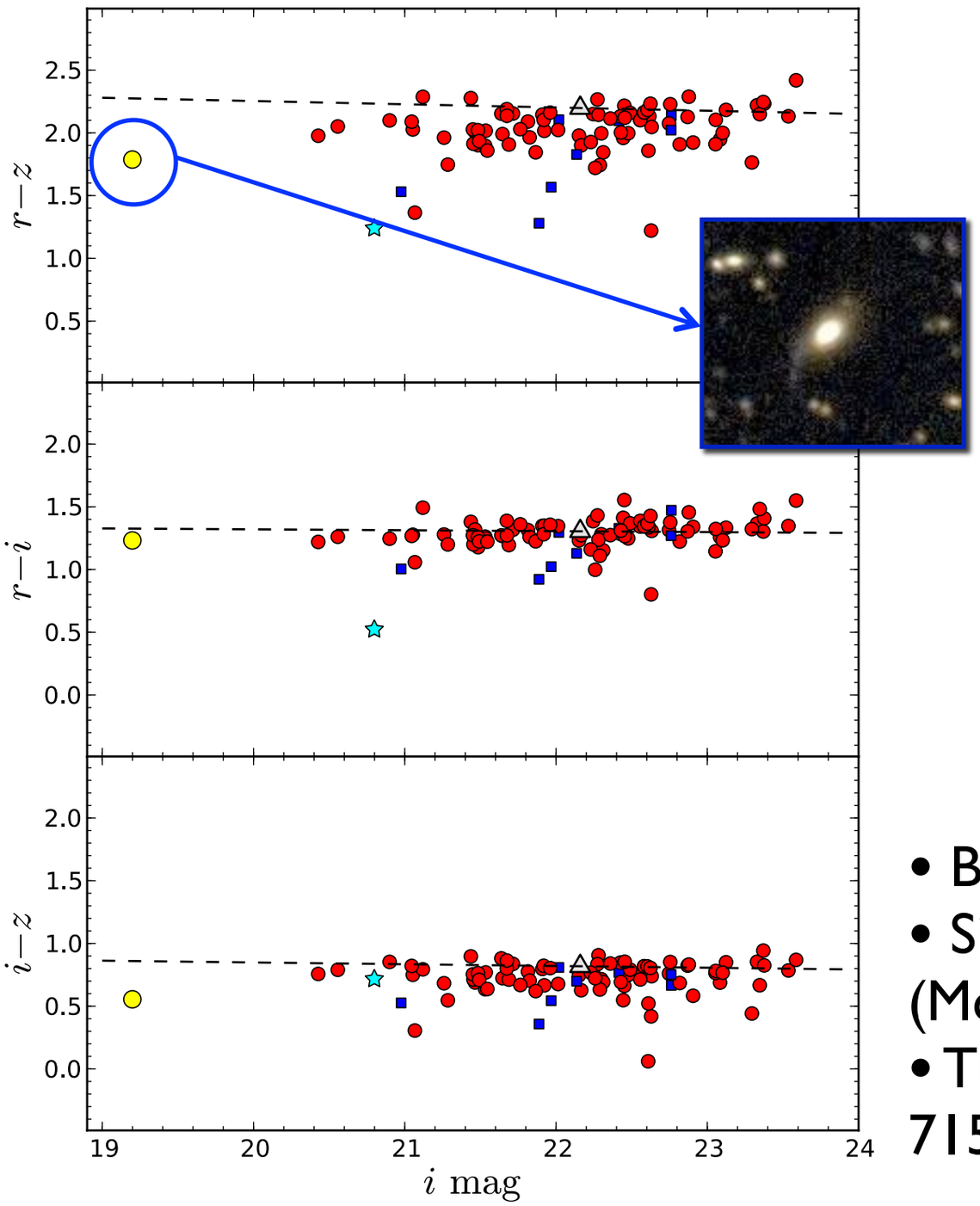

Menanteau et al. (2012, ApJ, 748,7)

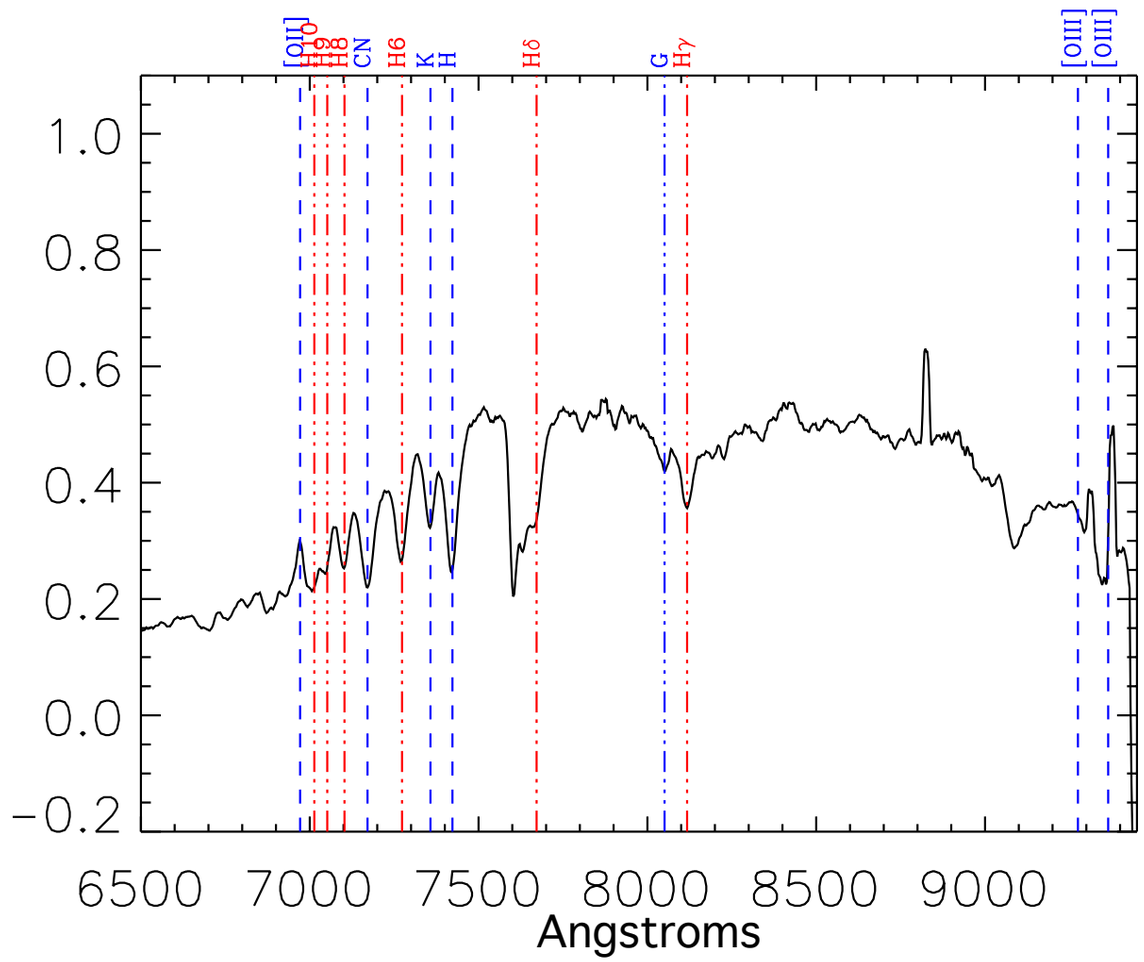

- BCG is an E+A+[OII] galaxy (not red and dead)
- Similar to NGC 1275 in Perseus Clusters (McNamara 1996) and RXJ 1347 (z=0.45)
- The BCG sample in Donahue et al.(2010), ApJ 715, 881

The Highest Redshift Radio Relic

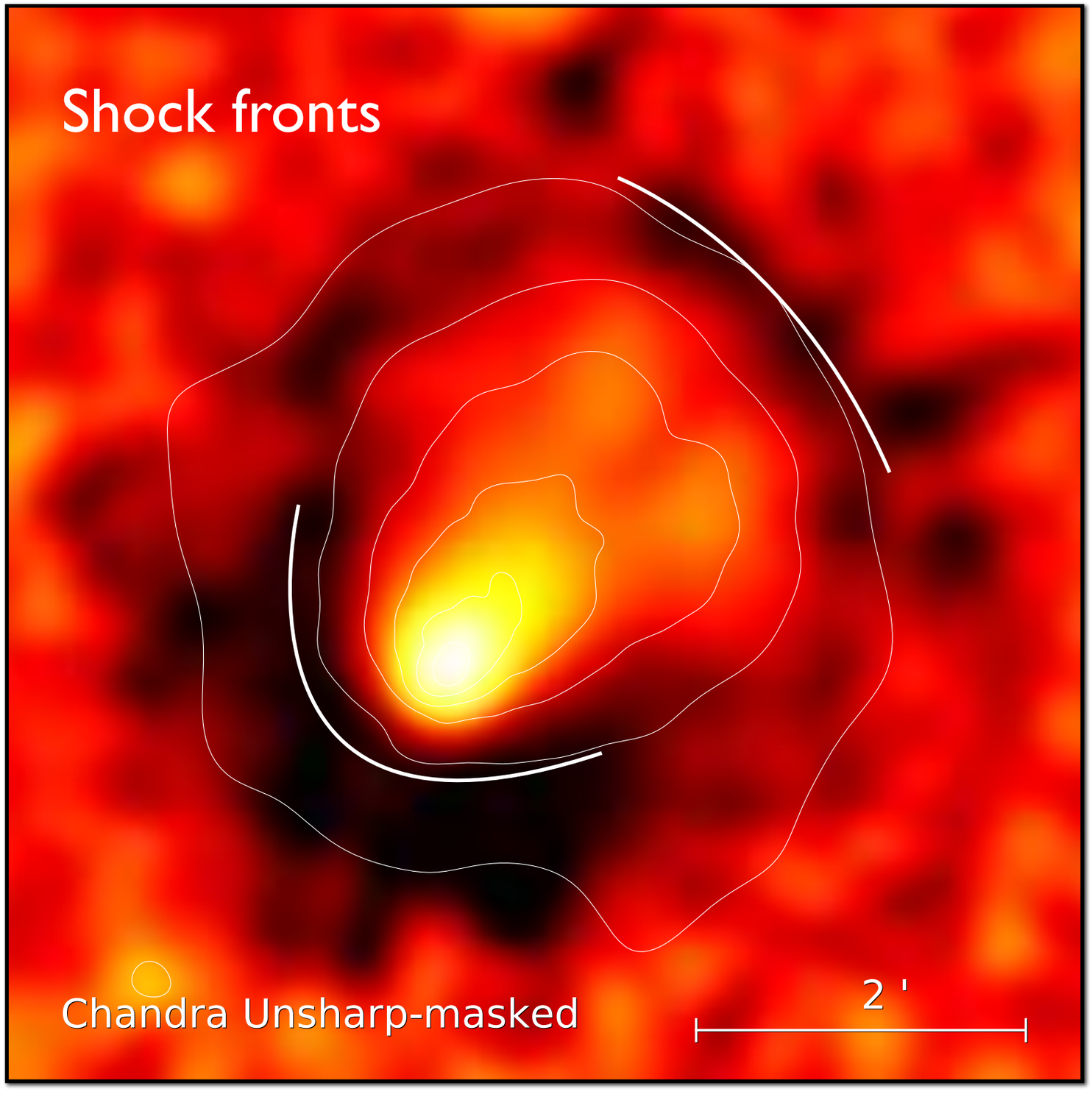

Evidence of Giant Radio Relic from archival SUMSS 843 MHz

Potentially the most powerful radio halo known

New ATCA 2.1 GHz observations (Dec 2011) shows clear extended structure.

Double Radio Relic, associated location of shock fronts.

The Highest Redshift Radio Relic

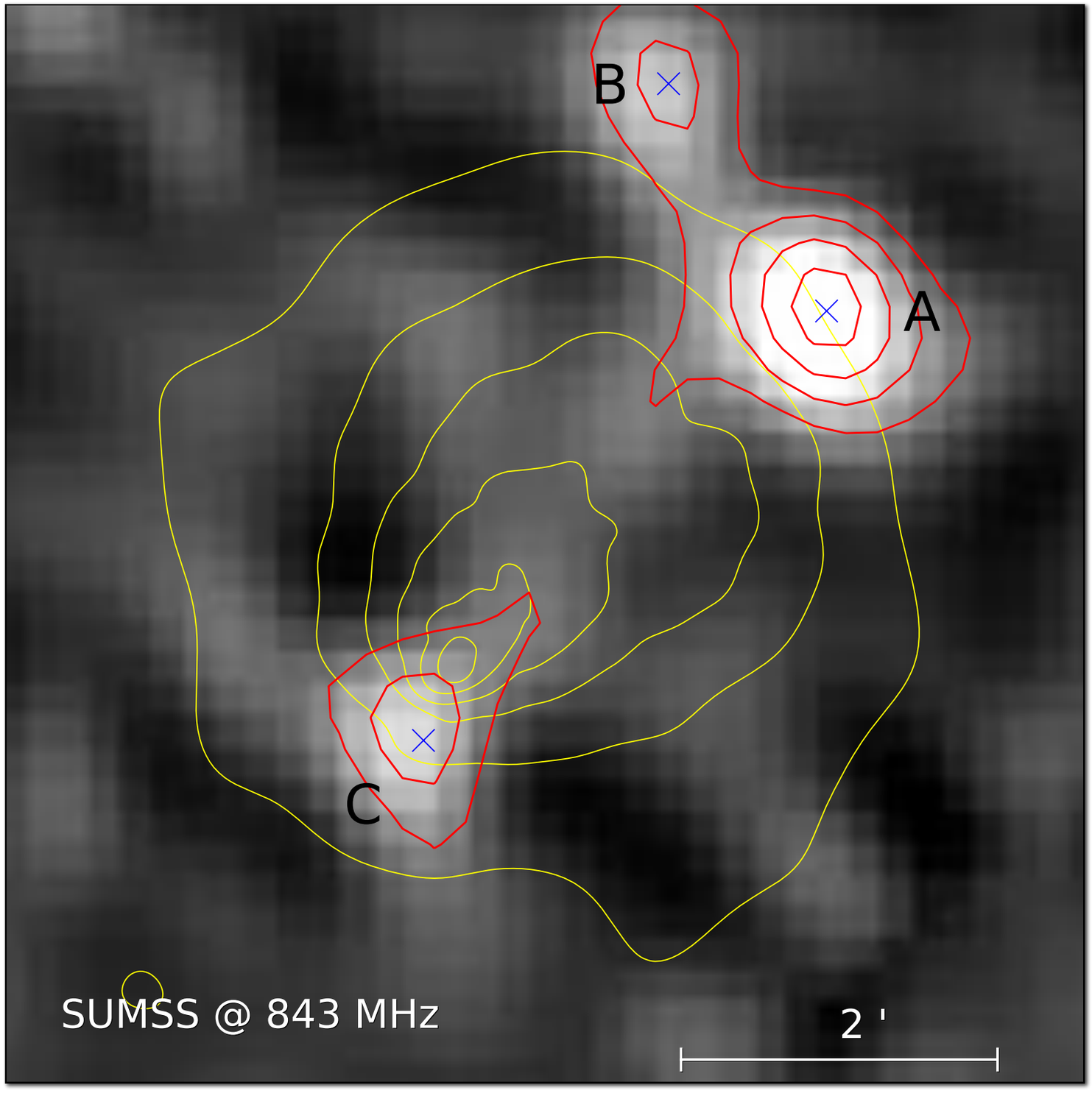

Evidence of Giant Radio Relic from archival SUMSS 843 MHz

Potentially the most powerful radio halo known

New ATCA 2.1 GHz observations (Dec 2011) shows clear extended structure.

Double Radio Relic, associated location of shock fronts.

The Highest Redshift Radio Relic

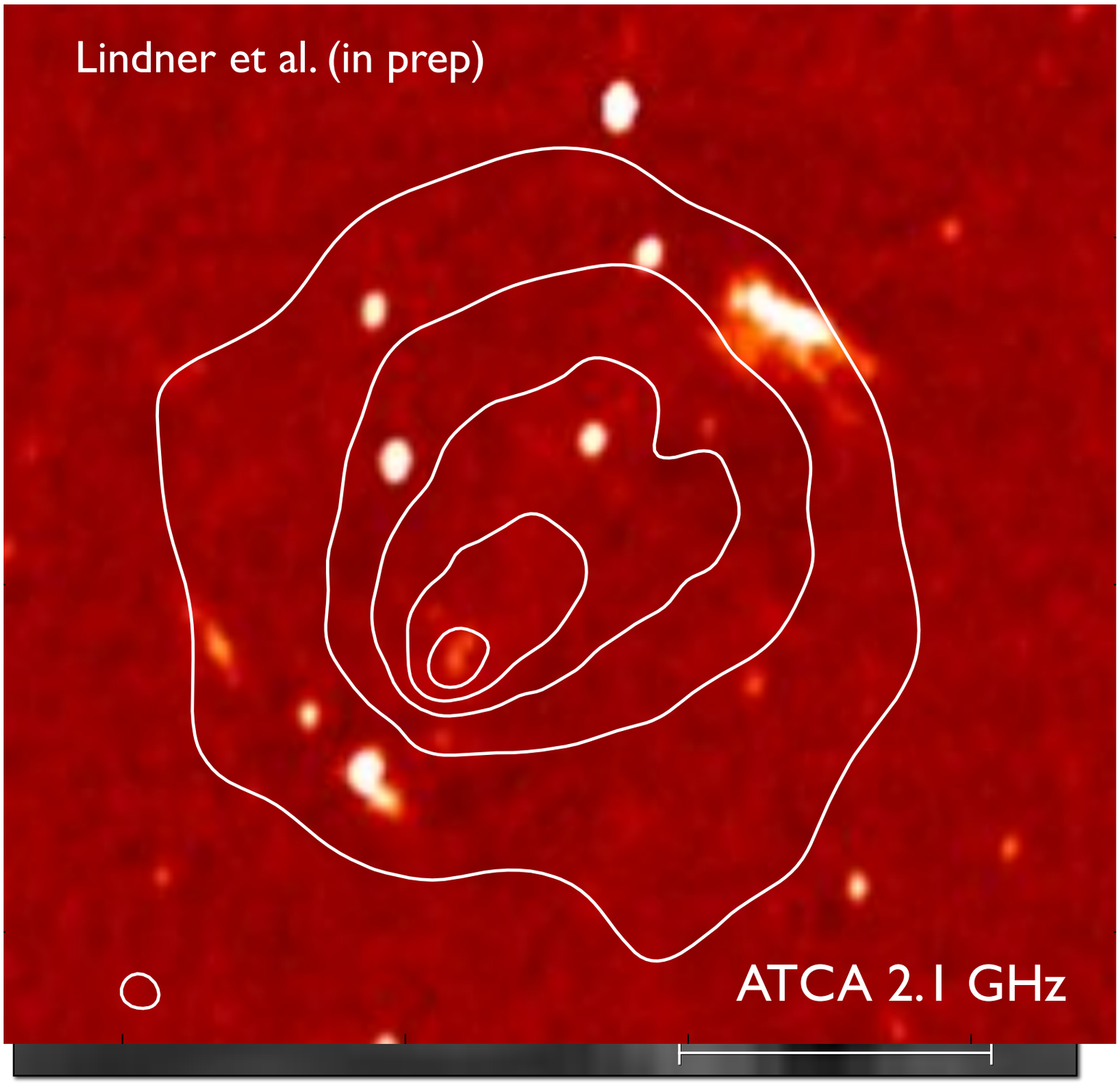

Evidence of Giant Radio Relic from archival SUMSS 843 MHz

Potentially the most powerful radio halo known

New ATCA 2.1 GHz observations (Dec 2011) shows clear extended structure.

Double Radio Relic, associated location of shock fronts.

Next Steps for "El Gordo"

Approved Programs:

- F625W(r), F775W(i) and F850LP(z) HST/ACS observations will be used to create WL maps. (yesterday)

- Deeper 300 ks Chandra/ACIS X-ray observation (Feb 2012) to study hot gas of merger shock and temperature map of El Gordo (in progress)

- ATCA and GMRT radio observation to search for Radio Halo emission. (2012B)

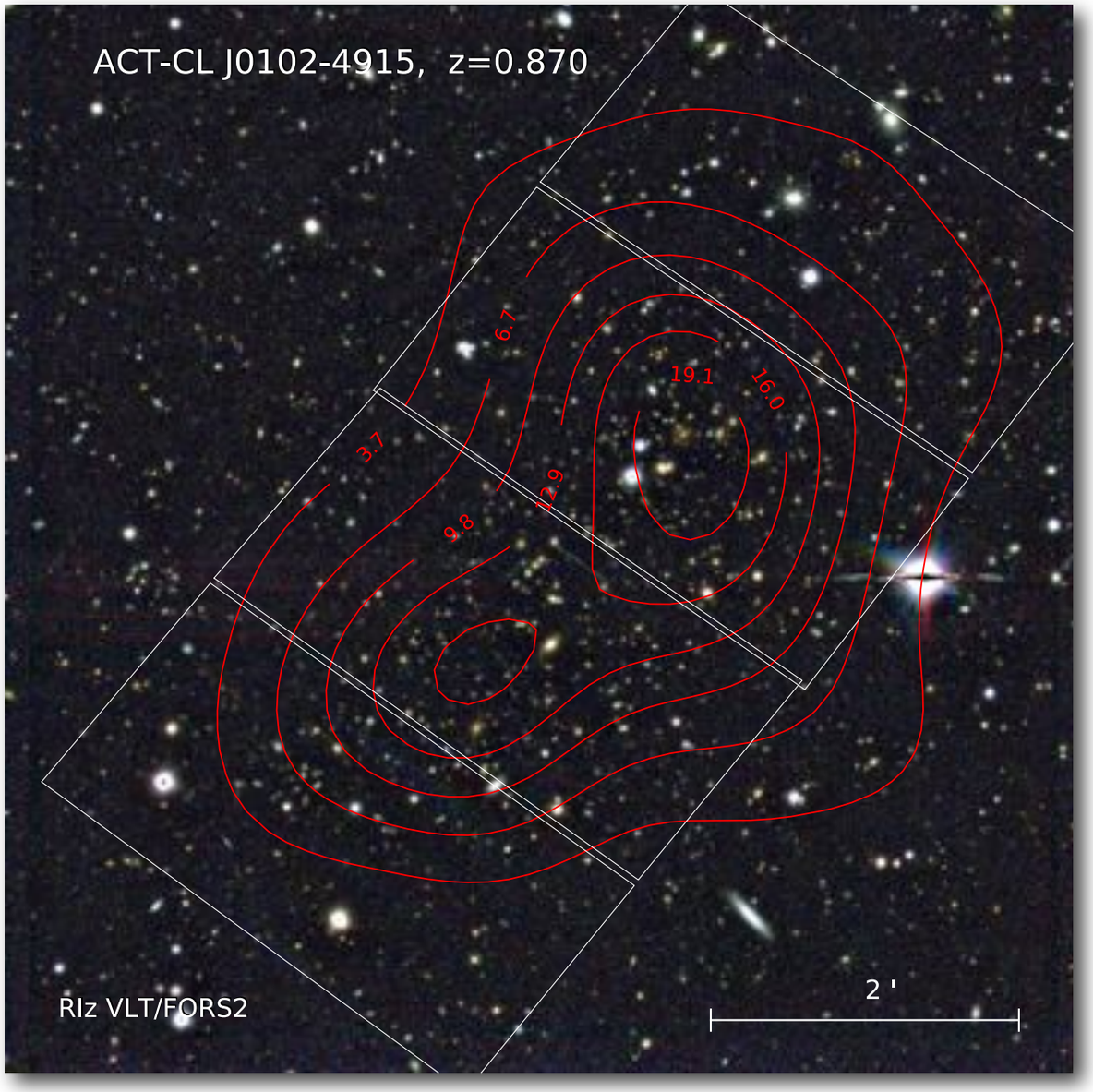

Towards a better *y*-Mass calibration

- *Ongoing*: Dynamic Masses and Scaling Relations of ACT SZE-selected Galaxy Clusters. (see Sifon, Menanteau et al. 2012, arXiv:1201.0991S)
- *Lesson:* Strength not coming from numbers (yet!)

Cosmology Constraints Fixing the SZ Signal Mass Relation

WMAP7 alone

WMAP7 plus ACT Clusters

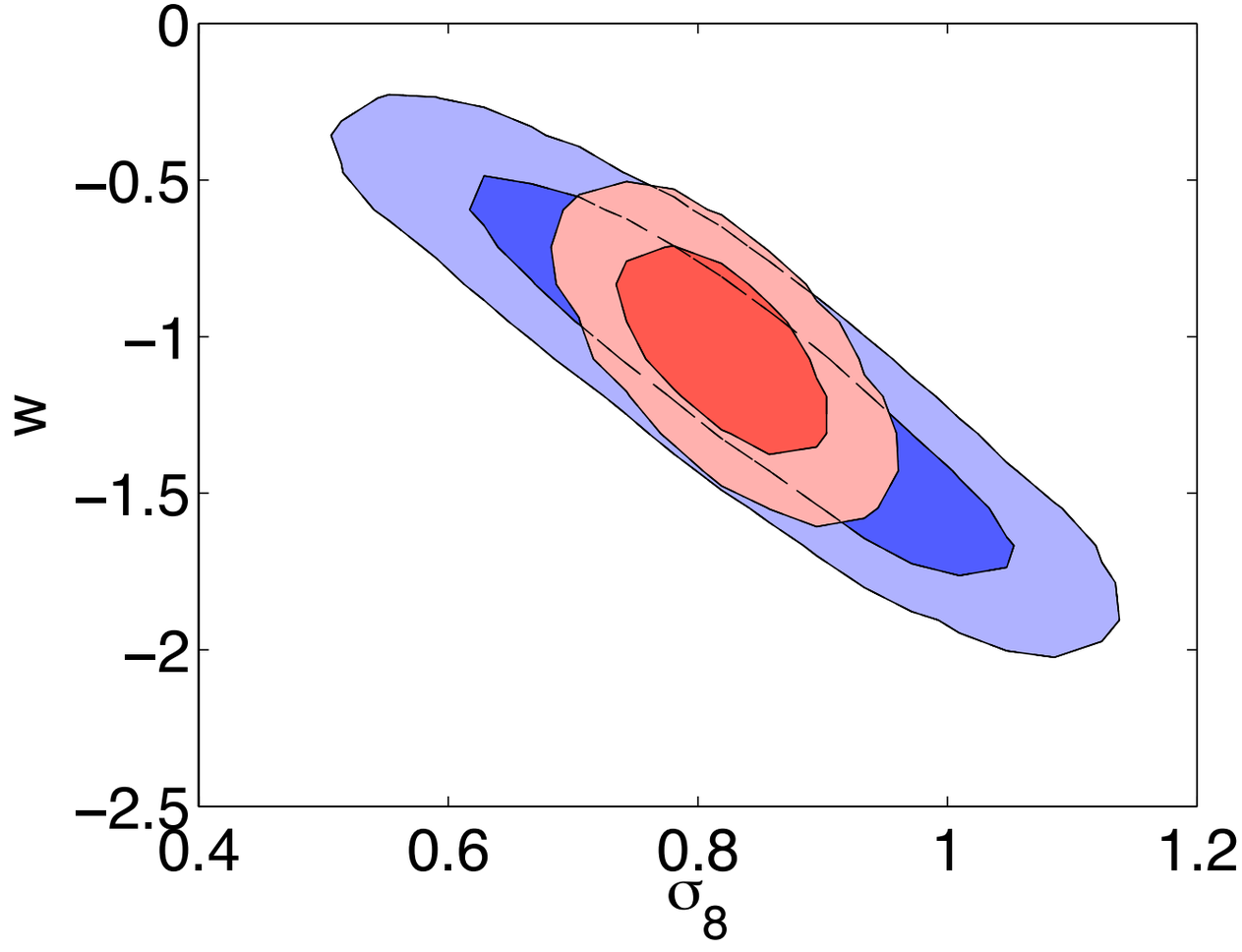

Y-M relation fixed to fiducial model

Spatially flat wCDM model

- ACT results for ~10 Clusters
- SPT similar results with ~20 clusters (see Benson et al. 2012)

$$\sigma_8 = 0.821 \pm 0.044$$
$$w = -1.05 \pm 0.20$$

Sehgal et al. (2011), ApJ 732,44

Cosmology Constraints Marginalizing over the SZ Signal Mass Relation

WMAP7 alone

WMAP7 plus ACT Clusters

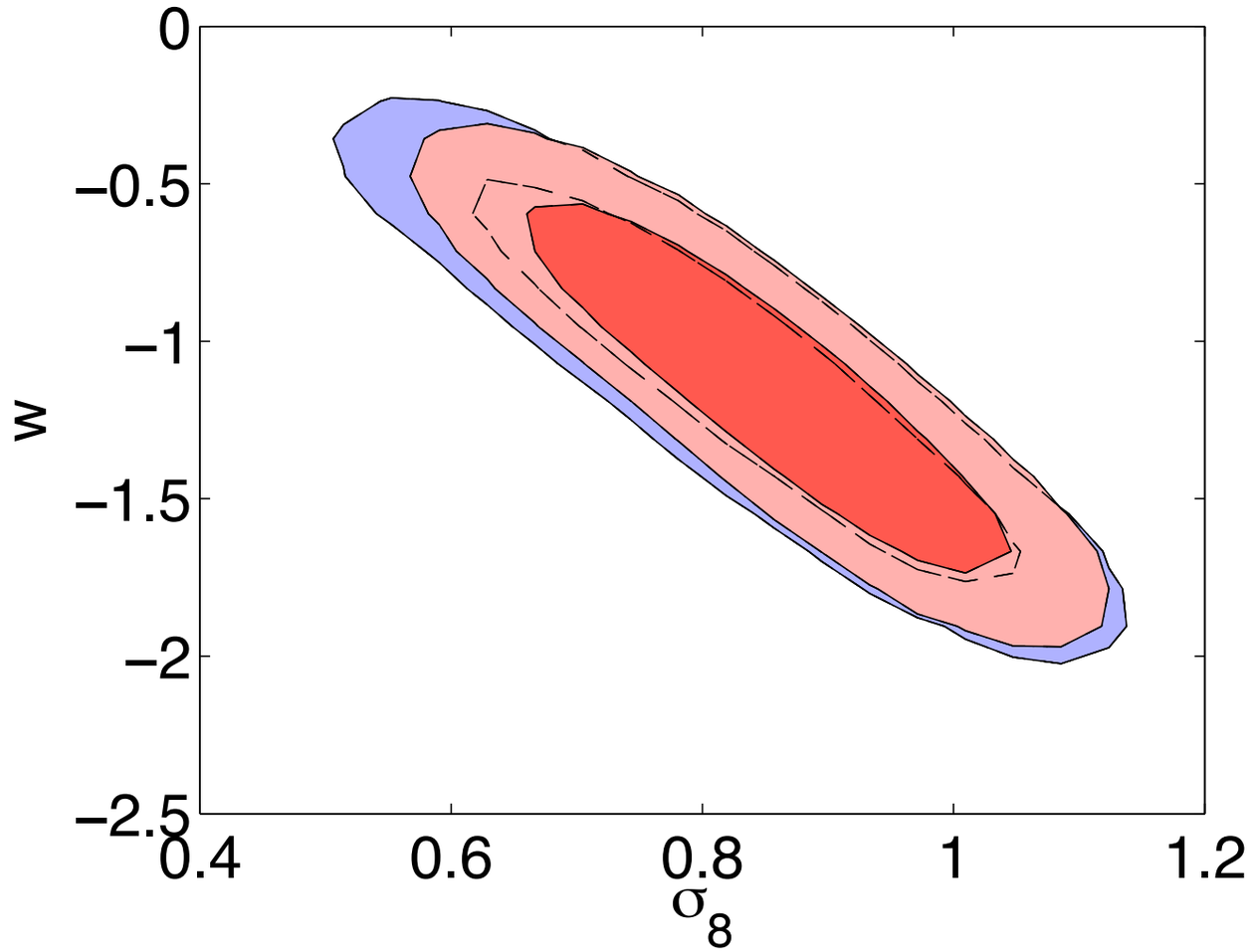

Priors for Y-M relation given by range of nonthermal and adiabatic models

$$\sigma_8 = 0.851 \pm 0.115$$

$$w = -1.14 \pm 0.35$$

Sehgal et al. (2011), ApJ 732,44

Cosmology Constraints Marginalizing over the SZ Signal Mass Relation

WMAP7 alone

WMAP7 plus ACT Clusters

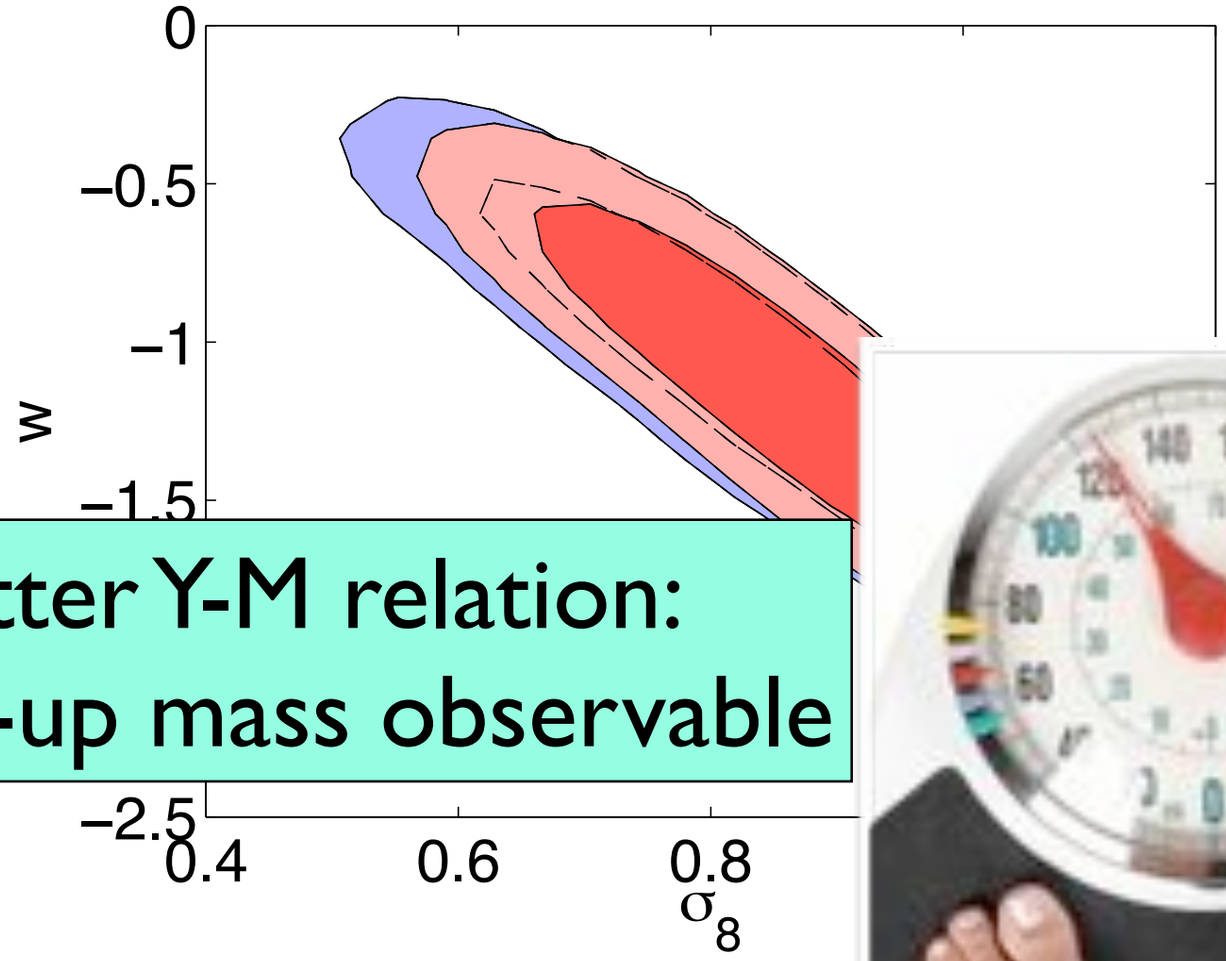

Priors for Y-M relation given
ge of
ermal
iabatic
dels

Need better Y-M relation:
How: Follow-up mass observable

$$\sigma_8 = 0.851 \pm$$

$$w = -1.14 \pm 0.35$$

Sehgal et al. (2011), ApJ 732,44

Improving Cluster Scaling Relations

(using optical data)

Table 3
Dynamical Properties of ACT 2008 Clusters

ACT Descriptor	N_{gal}[a]	z_{BI}	S_{BI} ($km\,s^{-1}$)	r_{200c} (h_{70}^{-1} kpc)	M_{200c} ($10^{14}\,h_{70}^{-1}\,M_\odot$)
ACT-CL J0102–4915[b]	89	0.87008 ± 0.00010	1321 ± 106	1789 ± 140	16.3 ± 3.8
ACT-CL J0215–5212	55	0.48009 ± 0.00012	1025 ± 102	1736 ± 173	9.6 ± 2.8
ACT-CL J0232–5257	64	0.55595 ± 0.00009	884 ± 110	1438 ± 177	5.9 ± 2.2
ACT-CL J0235–5121	82	0.27768 ± 0.00006	1063 ± 101	2007 ± 190	11.9 ± 3.4
ACT-CL J0237–4939	65	0.33438 ± 0.00009	1280 ± 89	2339 ± 162	20.0 ± 4.2
ACT-CL J0304–4921	71	0.39219 ± 0.00008	1109 ± 89	1971 ± 155	12.7 ± 3.0
ACT-CL J0330–5227[c]	71	0.44173 ± 0.00009	1238 ± 98	2138 ± 166	17.1 ± 4.0
ACT-CL J0346–5438	88	0.52973 ± 0.00007	1075 ± 74	1770 ± 122	10.7 ± 2.2
ACT-CL J0438–5419[d]	65	0.42141 ± 0.00011	1324 ± 105	2310 ± 182	21.1 ± 5.0
ACT-CL J0509–5341[e]	76	0.46072 ± 0.00006	846 ± 111	1451 ± 189	5.5 ± 2.1
ACT-CL J0521–5104[f]	24	0.67549 ± 0.00032	1150 ± 163	1744 ± 245	12.1 ± 5.1
ACT-CL J0528–5259[g]	55	0.76780 ± 0.00010	928 ± 111	1337 ± 159	6.1 ± 2.2
ACT-CL J0546–5345[h]	48	1.06628 ± 0.00020	1082 ± 187	1319 ± 226	8.1 ± 4.2
ACT-CL J0559–5249[i]	31	0.60910 ± 0.00026	1219 ± 118	1916 ± 184	14.9 ± 4.3
ACT-CL J0616–5227	18	0.68380 ± 0.00044	1124 ± 165	1699 ± 244	11.2 ± 4.9
ACT-CL J0707–5522	58	0.29625 ± 0.00006	832 ± 82	1561 ± 156	5.7 ± 1.7

(Sifón, Menanteau et al. 2012, arXiv:1201.0991)

Gemini-S/GMOS

VLT/FORS2

Ongoing Gemini-S/GMOS, 2010B, 2011B, 2012A, 2012B

Improving Cluster Scaling Relations

(using optical data)

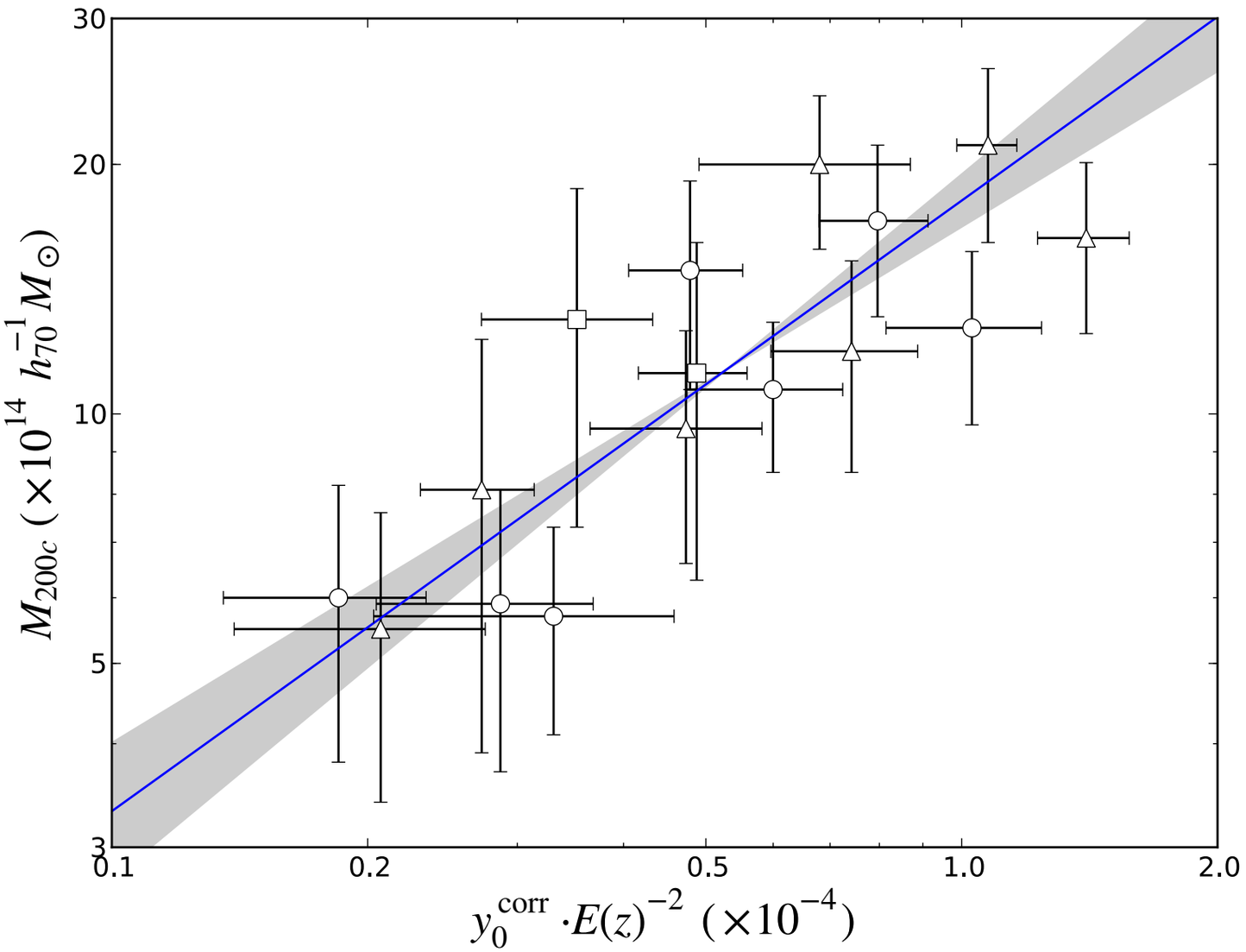

Sifón, Menanteau et al. (2012, arXiv:1201.0991)

Gemini-S/GMOS
Dec, 2010

VLT/FORS2
Jan 2011

Improving Cluster Scaling Relations

(using optical data)

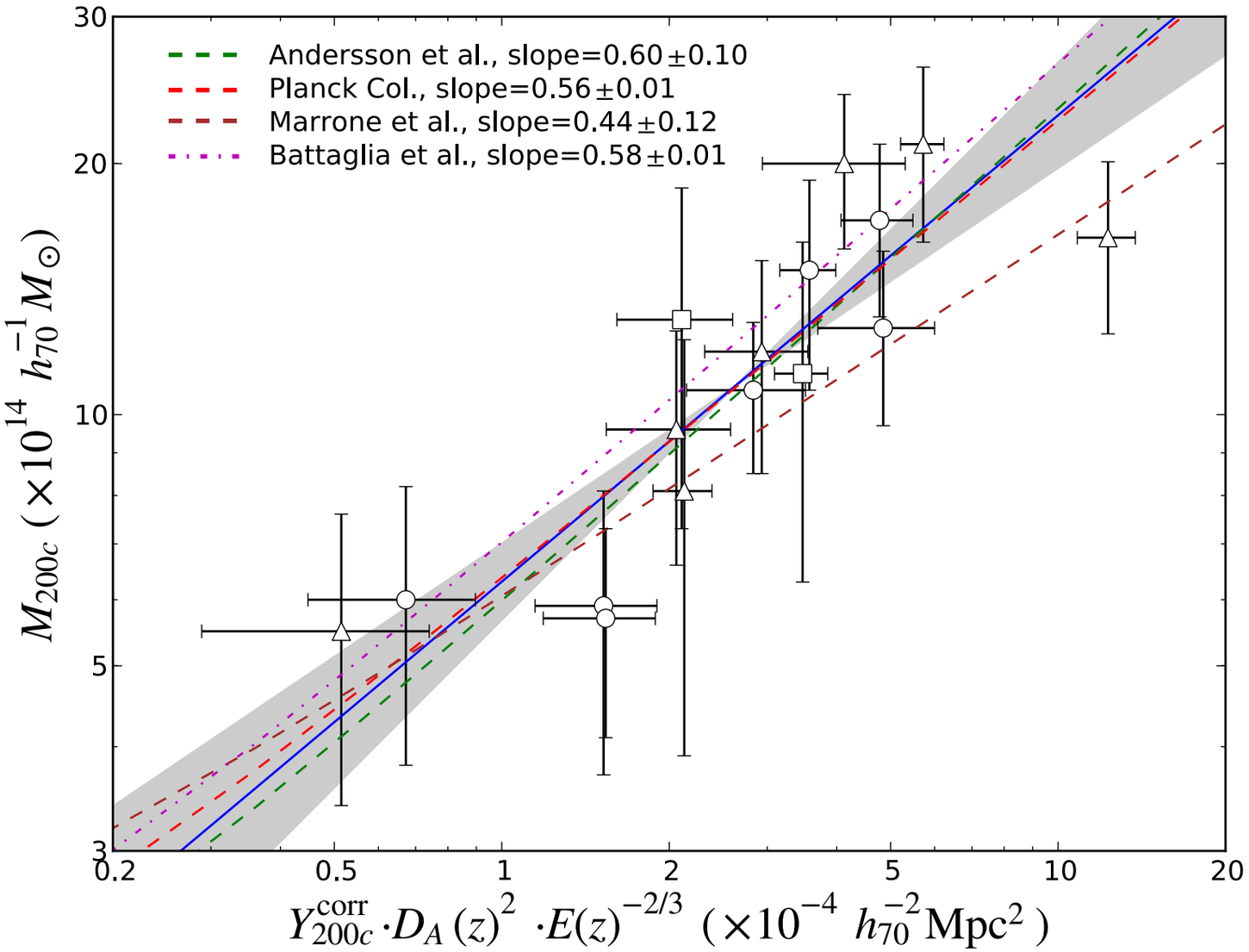

Sifón, Menanteau et al. (2012, arXiv:1201.0991)

Gemini-S/GMOS
Dec, 2010

VLT/FORS2
Jan 2011

ACT Equatorial Observations

2009-2010 seasons [Menanteau et al. 2012, arXiv soon]

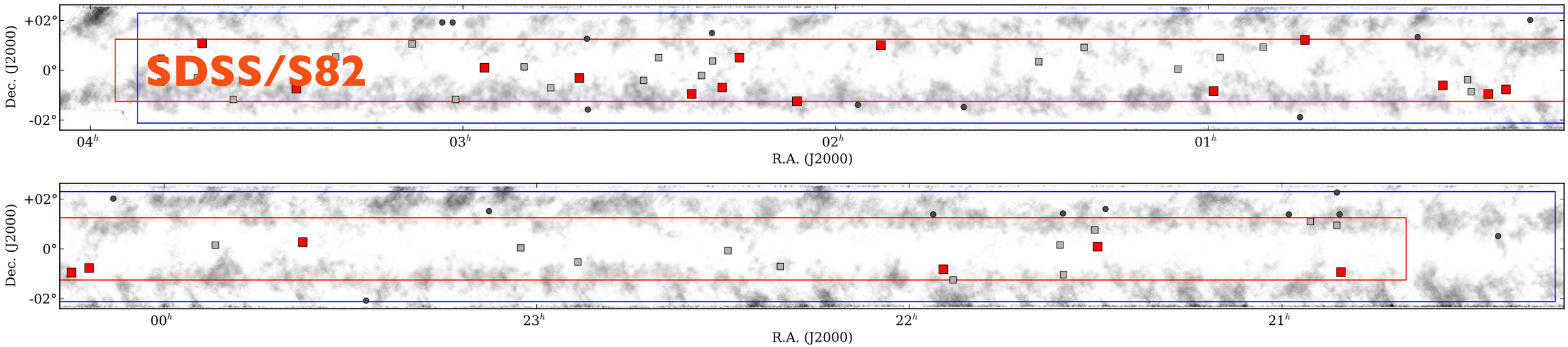

- Total area covered by ACT maps 502 deg^2 over the celestial equator
- Ovelap with SDSS/S82 270.25 deg^2
- Beyond S82, about extra ~190 deg^2
- 49 optical/NIR-confirmed on S82 alone. (2x density to Southern Strip)
- 19 clusters at z<0.5 confirmed using DR8.
- SOAR 4.1-m (2012B) for optical confirmation beyond DR8.
- 68+23 so far combined (Equator + South)

Purity of ACT Equatorial Sample (S82)

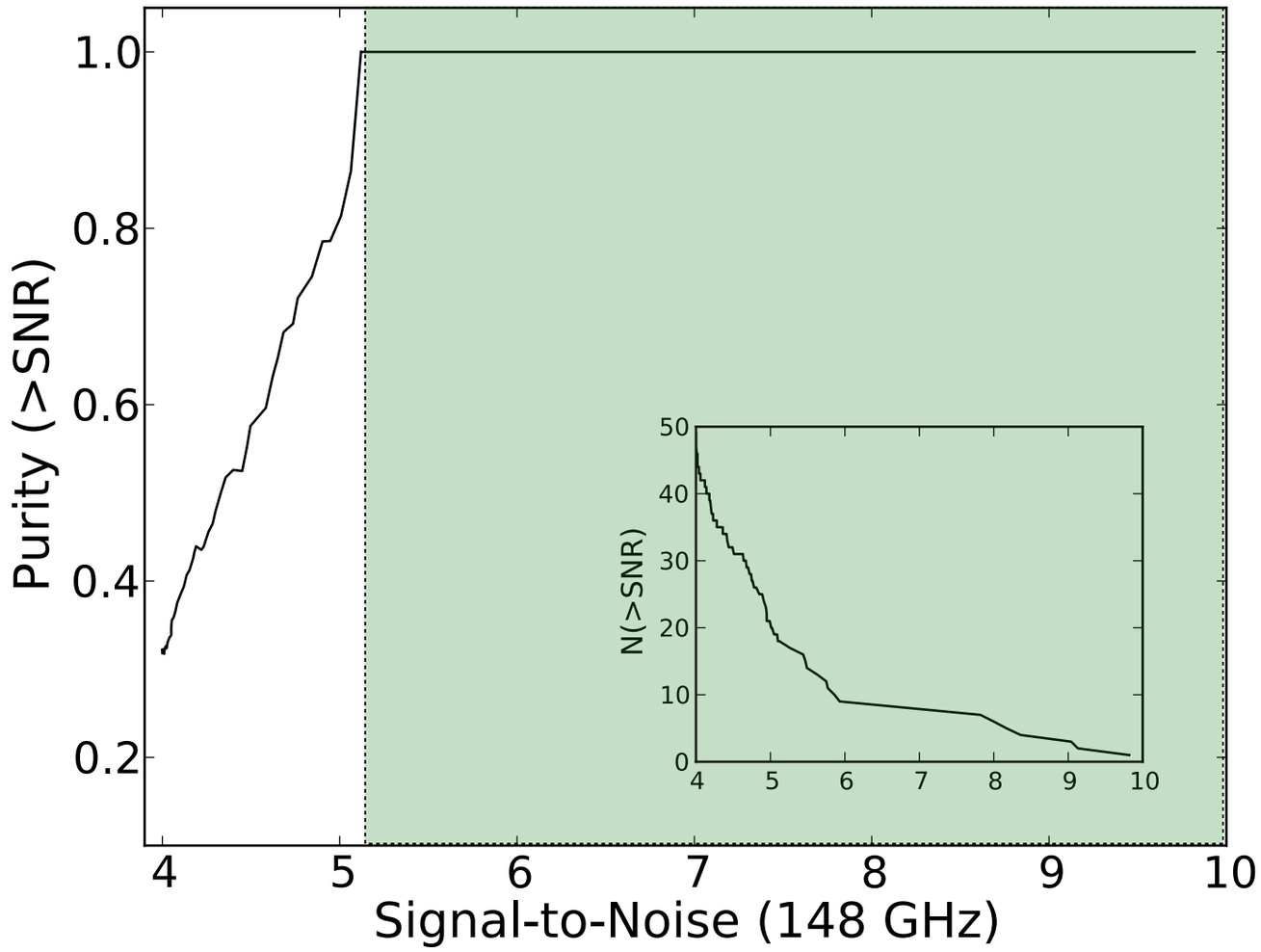

- Purity = $N_{real}/N_{observed}$
- 100% purity for S/N>5.0 (17/18 clusters)
- 60% purity at S/N>4.5

A new SZ-discovered z~1 cluster

[Menanteau et al. 2012, arXiv soon]

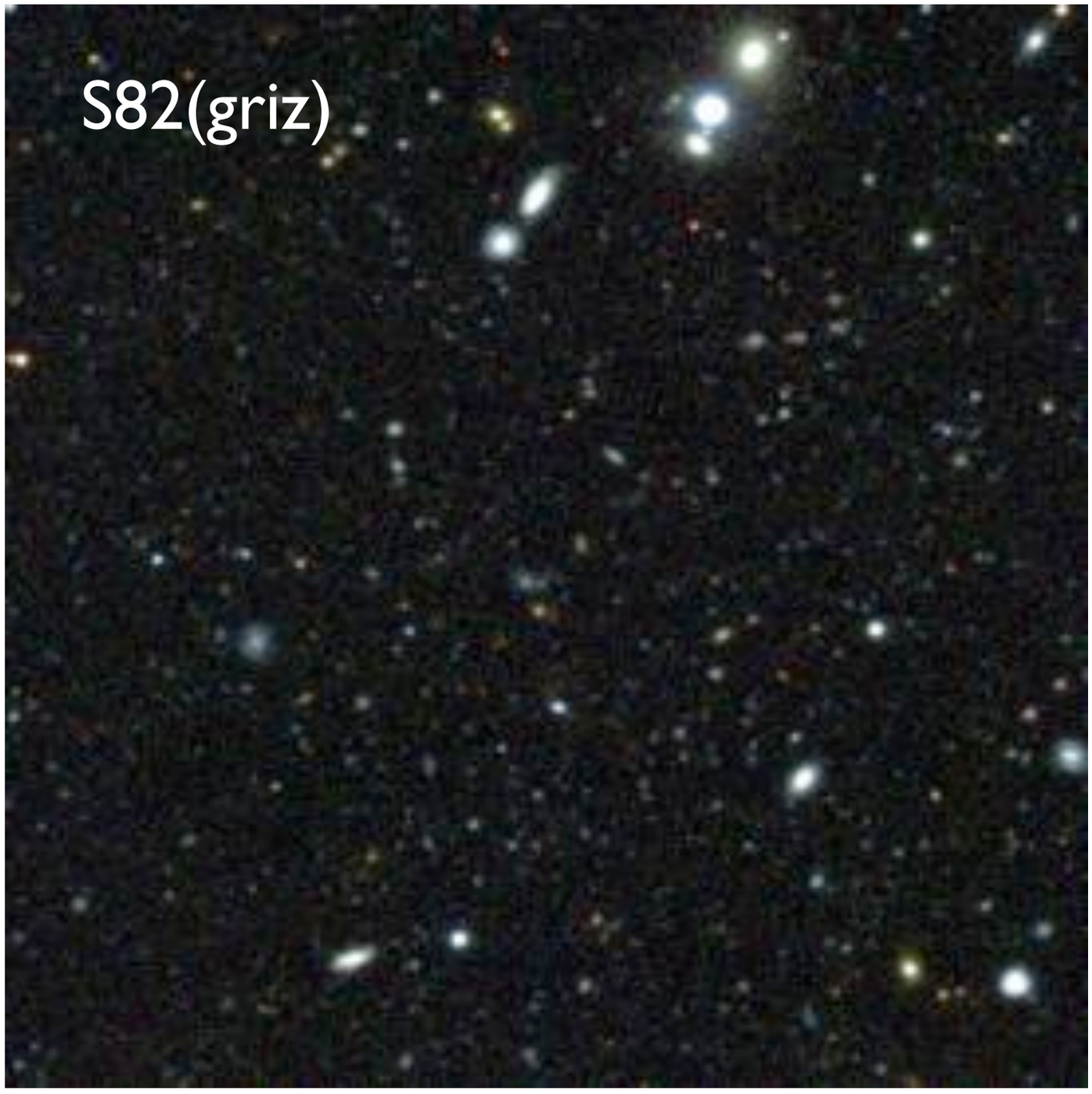

A new SZ-discovered z~1 cluster

[Menanteau et al. 2012, arXiv soon]

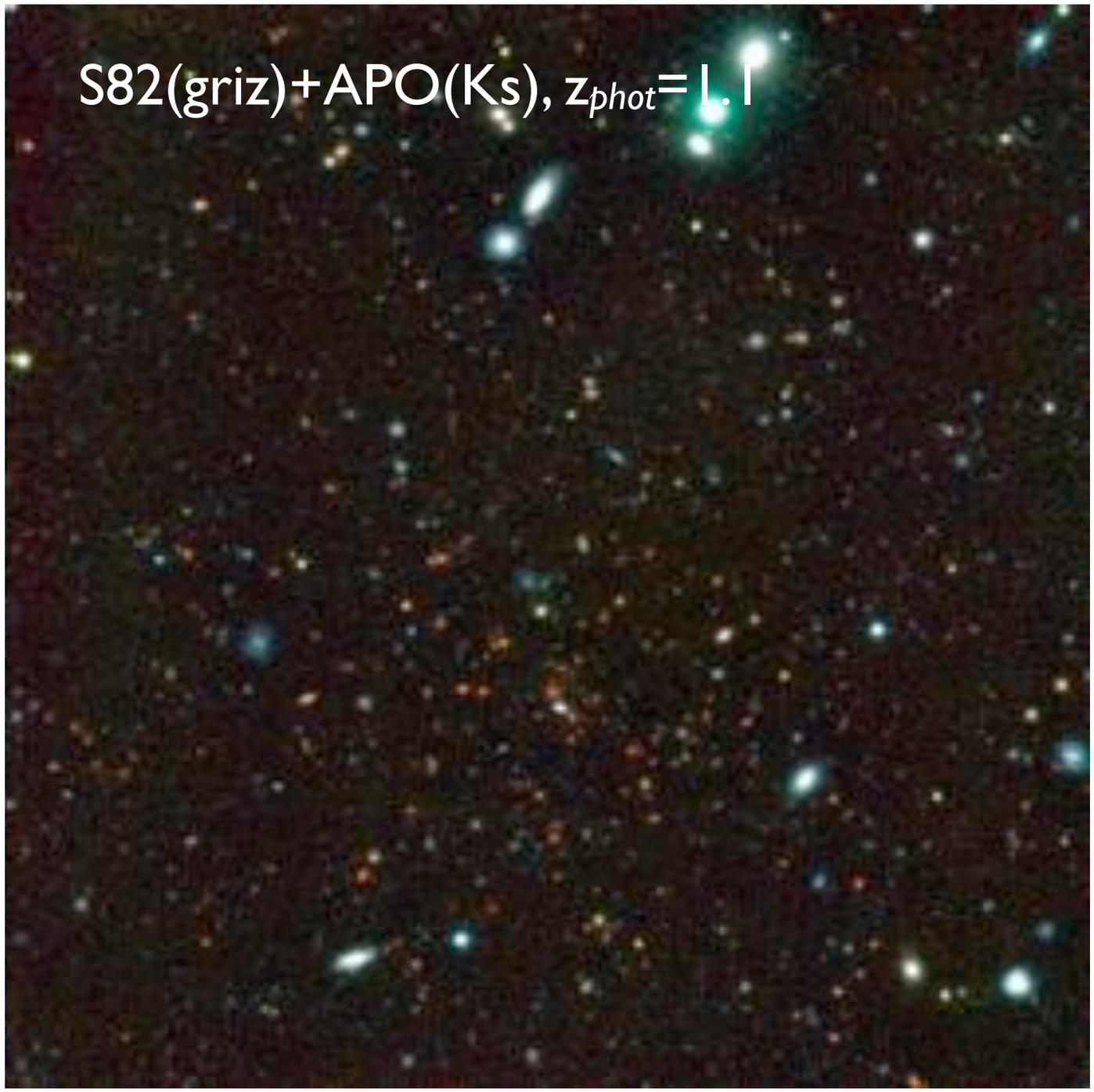

A new SZ-discovered z~1 cluster

[Menanteau et al. 2012, arXiv soon]

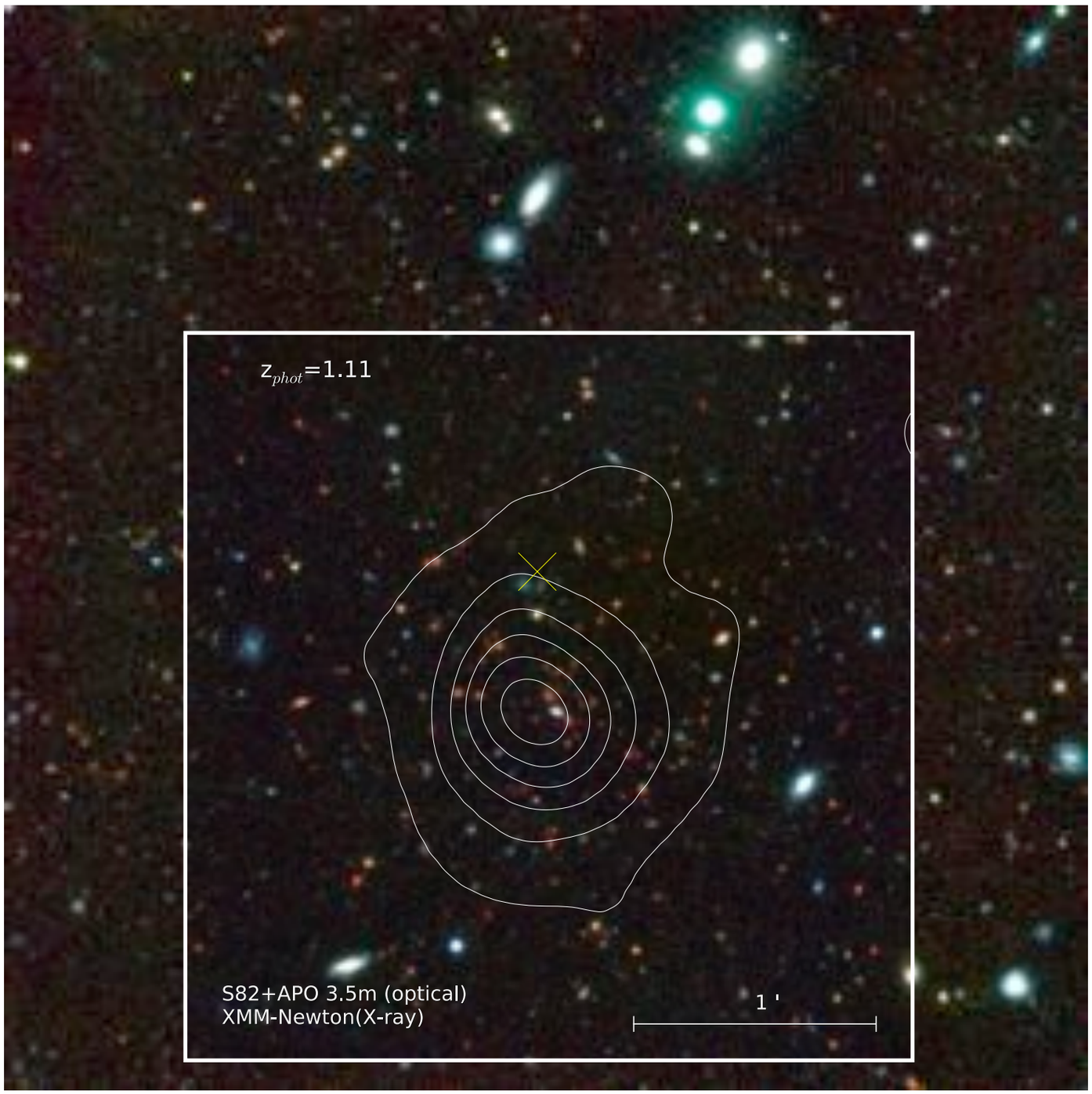

A new SZ-discovered z~1 cluster

[Menanteau et al. 2012, arXiv soon]

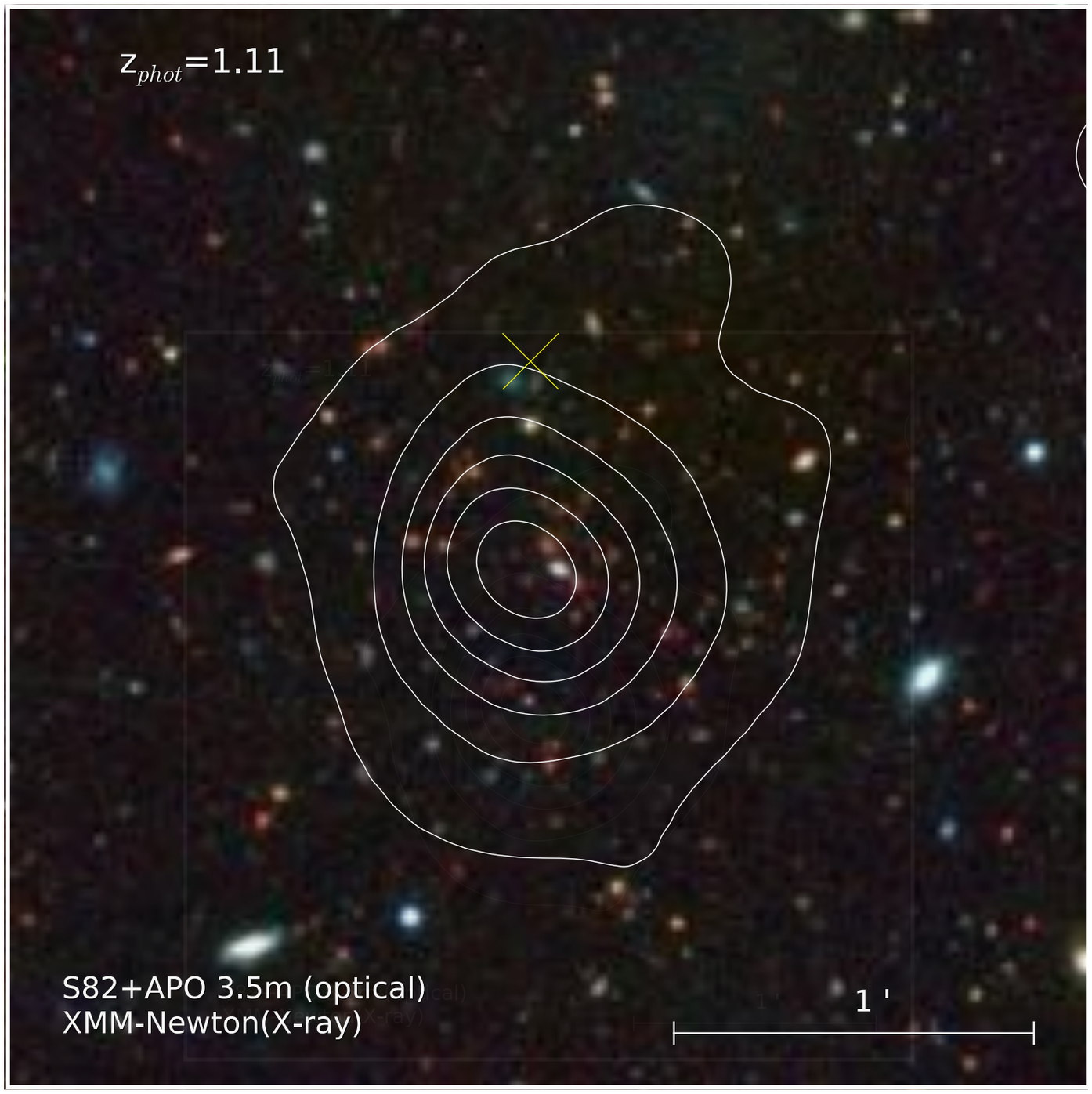

A new SZ-discovered z~1 cluster

[Menanteau et al. 2012, arXiv soon]

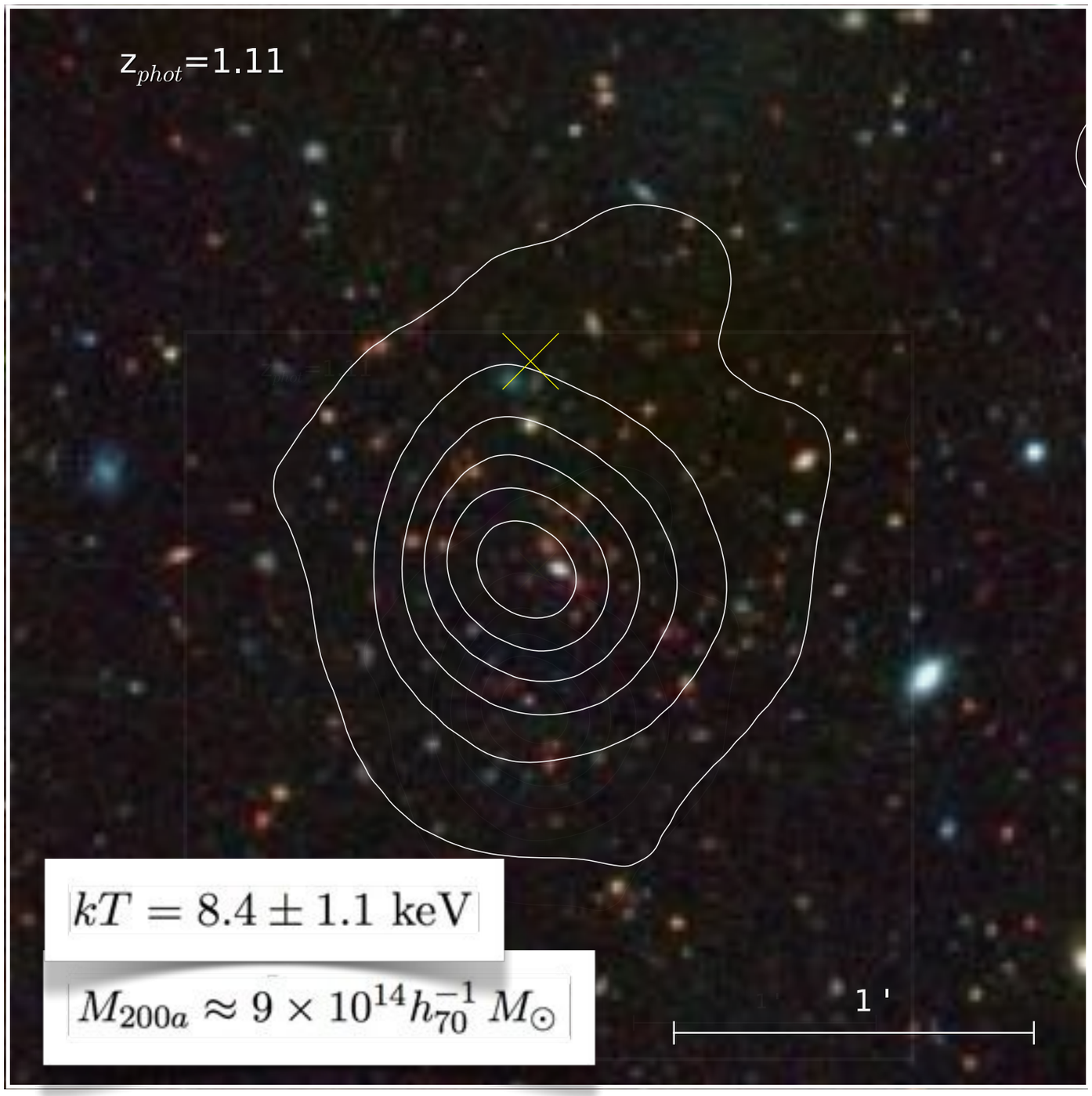

M_{200a} Masses for Equatorial Sample and rarity of the clusters

Sifón et al. (2012)

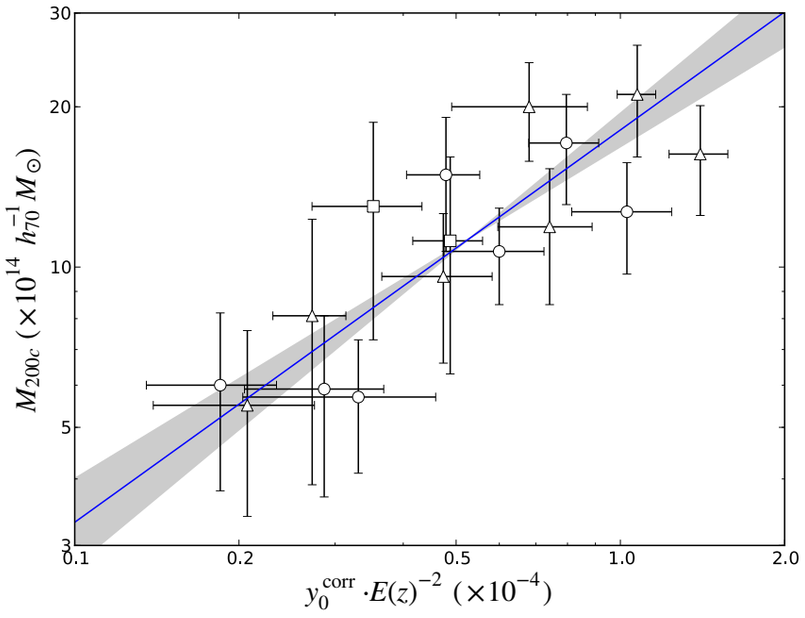

Mass

SZ

M_{200a} Masses for Equatorial Sample and rarity of the clusters

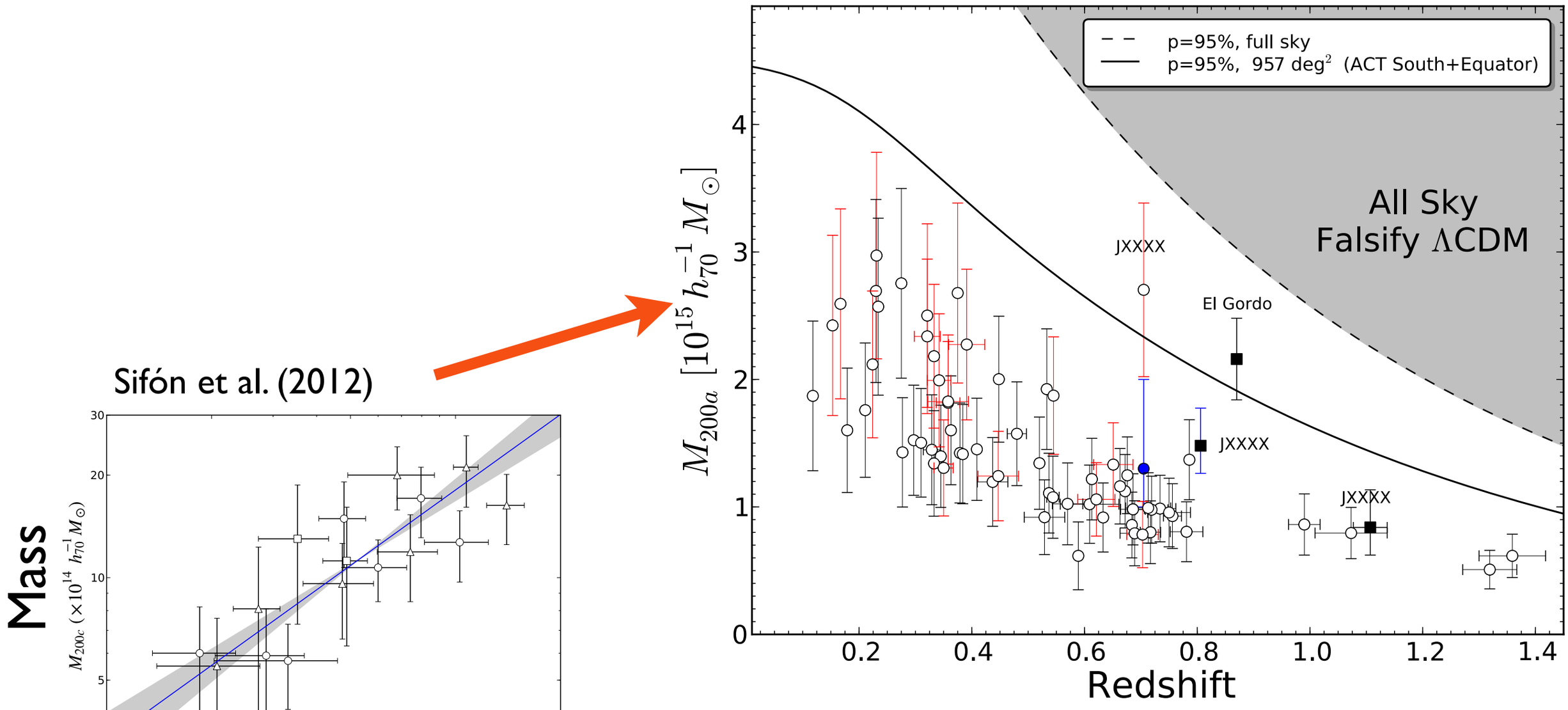

Evidence of "mis-centering"?

Offset Between BCG and SZ?

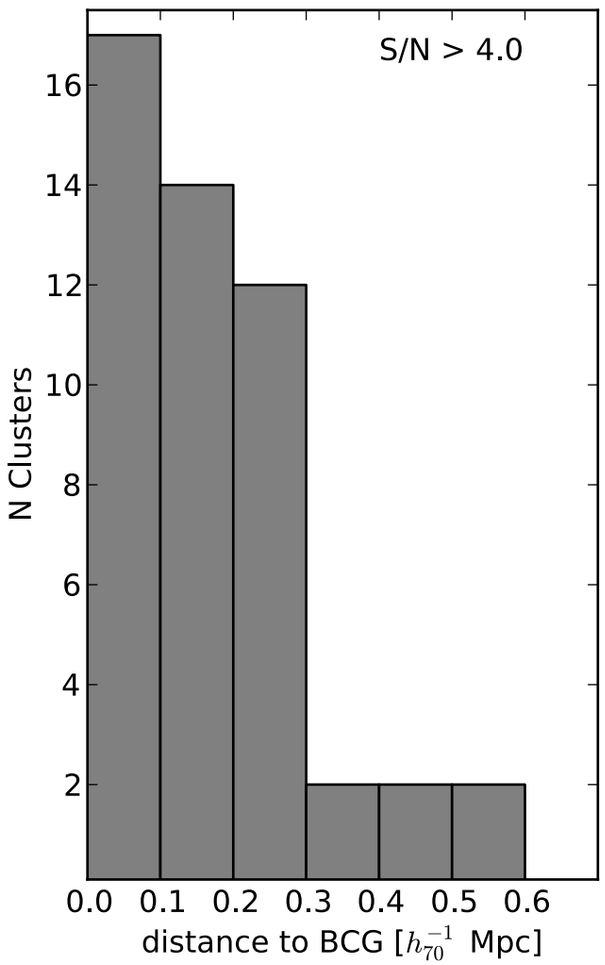

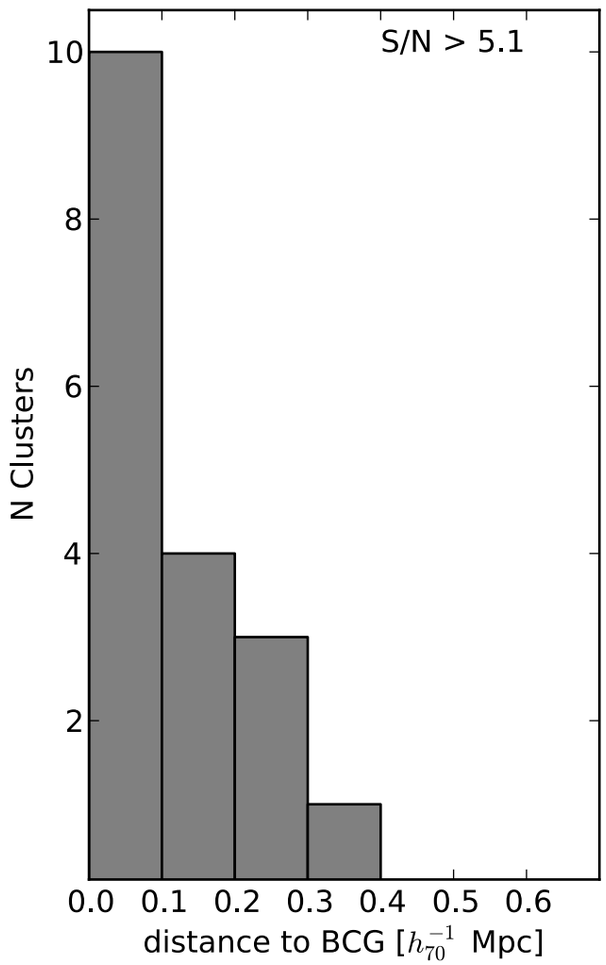

- Mean separation 0.12 Mpc/h_{70} and 0.17 Mpc/h_{70}

- ACT SZ centroid uncertainty ~ 0.15 Mpc/h_{70}

- No significant evidence of offset between SZ/BCG

SZ/Richness Relation on the ACT Equatorial sample

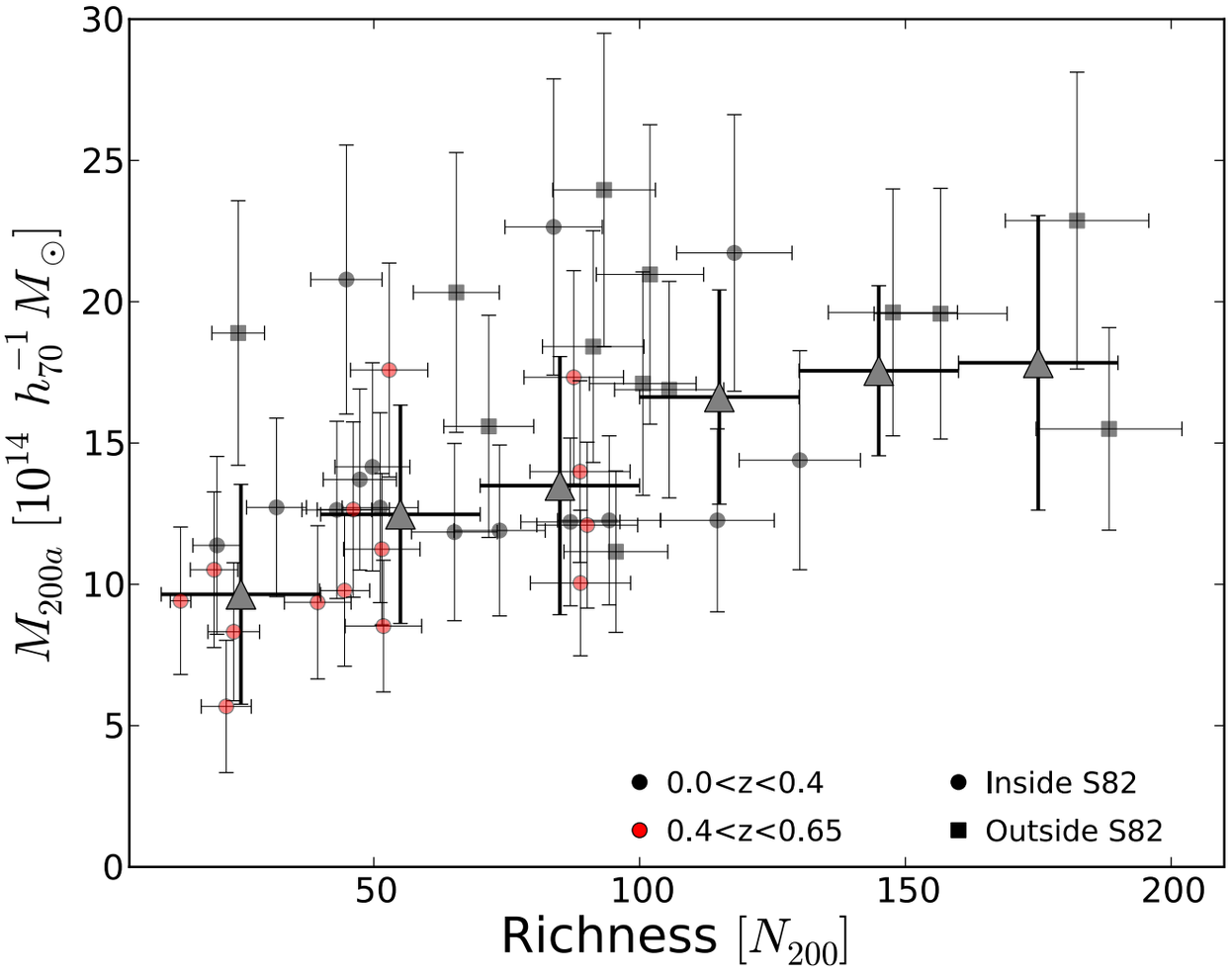

- Compare SZ-Mass with optical richness (N_{200}), own values.
- Clusters to z<0.65 (in S82)
- Clusters to z<0.40 (out S82)
- Weak correlation with N_{200}
- Large scatter in M_{200a} vs N_{200}

Summary

- ~90 confirmed clusters (BCG and red sequence) from >952 deg^2, between 0.1<z<1.3
- We have one of the first redshift-independent samples of galaxy clusters selected via the SZ effect, used to constrain σ_8 and *w*.
- We have the next bullet cluster at z~0.9
- ATCA observations confirms hightest-z ***Double Radio Relic***.
- Scaling relations from 2010-2012: Gemini/GMOS + VLT/FORS
- 100 warm Spitzer/IRAC (3.6*u*m and 4.5*u*m) stellar content.
- HST(6 orbits)+Chandra (300ks) for "El Gordo" confirm DM/gas offset.
- Chandra and XMM observations of new systems
- **ACTPol to start observation in 2013.**

Thank you